CANADIAN JOURNAL OF RESEARCH

VOLUME 13 SEPTEMBER, 1935 NUMBER 3

CONTENTS

SEC. A.—PHYSICAL SCIENCES

SEC. B.—CHEMICAL SCIENCES

NATIONAL RESEARCH COUNCIL
OTTAWA, CANADA

Publications and Subscriptions

The Canadian Journal of Research is issued monthly in four sections, as follows:

A. Physical Sciences
B. Chemical Sciences
C. Botanical Sciences
D. Zoological Sciences

For the present, Sections A and B are issued under a single cover, as also are Sections C and D, with separate pagination of the four sections, to permit separate binding, if desired.

Subscription rates, postage paid to any part of the world (effective 1 April, 1939), are as follows:

	Annual	*Single Copy*
A and B	$ 2.50	$ 0.50
C and D	2.50	0.50
Four sections, complete	4.00	—

The Canadian Journal of Research is published by the National Research Council of Canada under authority of the Chairman of the Committee of the Privy Council on Scientific and Industrial Research. All correspondence should be addressed:

National Research Council, Ottawa, Canada.

Canadian Journal of Research

Issued by THE NATIONAL RESEARCH COUNCIL OF CANADA

VOL. 13, SEC. A. SEPTEMBER, 1935 NUMBER 3

OSCILLATIONS IN THE SPARK FROM INDUCTION OR IGNITION COILS AND THEIR SUPPRESSION[1]

BY R. RUEDY[2]

Abstract

In the low-voltage stage of the spark, the current depends on the solution of a cubic equation, and has therefore in general one strong aperiodic and two alternating components. When the ratios $\alpha_1 = R_1/L_1$ of the primary and $\alpha_2 = R_2/L_2$ of the secondary are kept small compared with the natural angular frequency ω_1 of the primary, damped electrical oscillations of frequency $\omega_1(1 - \kappa^2)^{-\frac{1}{2}}$ are set up in the windings, even when the voltage at the spark gap is constant. With larger values of α_2 and if necessary higher coupling factors, κ, the frequency of the oscillations decreases and near the point at which $(\alpha_1 + \alpha_2)^2/3(1 - \kappa^2)\omega_1^2$ becomes smaller than unity, the discharge becomes aperiodic, or under certain conditions, intermittent. Rapid changes of short duration cause the wires leading from the spark to the coil and portions of the coil to oscillate, the leads acting as antennas rather than as circuit elements with uniform distribution of the current. In the aperiodic stage the current behaves as if it were independent of the primary.

Introduction

It is difficult to investigate the current in the spark discharge because in less than a microsecond it may change from the dark stage, or from a brush dicharge, to a glow or an arc. Since ionization takes place along a narrow path, space charges accumulate in such a way that the resistance of the gap rapidly falls from infinity to a low value. Finally the drop in the discharge voltage stops, however, at the potential of the glow or the arc.

The difference between the early, high voltage, and the later, low voltage, stage of the discharge across a short gap becomes enhanced in the case of the ignition coil. When the strong primary current, a few amperes, is suddenly interrupted, or more accurately reduced in strength, the high voltage in the secondary—about 6000 volts for 0.3 mm. gaps—causes breakdown of the air. The rate at which the voltage across the secondary rises from zero to the sparking potential is governed by the intensity of the primary current and the constants of the coil. As a rule, the primary current is so chosen that the voltage produced is much higher than the potential required to break down the gap, since a higher tension sharply reduces the lag between

[1] *Manuscript received June 7, 1935.*

Contribution from the Division of Research Information, National Research Laboratories, Ottawa, Canada.

[2] *Research Investigator, National Research Laboratories.*

the time of applying the voltage and the passage of the discharge. The work dissipated by the spark proper is relatively small; with an average potential of a few thousand volts, a current not greater than a few milliamperes and of a duration of one microsecond, it may amount to not much more than one microjoule or 0.24 microcalorie, whereas the energy stored in the coil is 0.01 joule, even if the primary inductance be only about 0.01 henry and the current one ampere (1, 4). The discharge of the large amount of energy stored in the coil is then completed in the path remaining conductive after the passage of this initial or capacitive stage of the spark, for which the curve obtained by plotting voltage against current drops sharply. In the second, the so-called inductive stage of the spark, the voltage may on the contrary, as many tests have shown, remain perfectly constant, at a few hundred volts, or change only slightly, despite increasing or fluctuating currents. This behavior reveals the fact that the initial spark which fires the combustible mixture in an ignition engine is followed by a true glow discharge (or in some cases, an arc), at atmospheric or higher pressure. The low-voltage stage presents all the components of the glow discharge as they are known from experience with neon tubes; for instance, the negative glow, the dark space (0.3 mm. wide) the positive column and, in air, a bright reddish anode glow (4, 8).

Since the primary possesses capacity and self-induction in parallel, the sudden break of the current causes electrical oscillations to be set up which are transferred to the secondary circuit. Experience leaves no doubt that the operation of an ignition or an induction coil interferes in general with the reception of radio waves in three very wide regions: (*a*) in the range of short waves higher than 10 Mc. (less than 30 metres wave-length), (*b*) in the entire band from 1500 kc. (broadcasting frequencies) to about 100 kc., and (*c*) in the higher range of audio frequencies.

In order to be able to suppress the vibrations, it is necessary to know where they have their source. Interference in the short-wave region is due simply to oscillations set up at the breakdown of the gap owing to the agreement between the duration of the breakdown proper and the natural period of that portion of the circuit that consists of the spark and the wires, 30 to 100 cm. long, leading from the spark to the ends of the secondary. The current is strongest near the spark and decreases toward the coil, the wires oscillating as half-wave dipoles, so that a small change in their length affects the frequency that is radiated (5). A glance at the constants of the coils used furthermore suggests that the period of the oscillations in the audible range is determined by the coil oscillating as a system of two coupled circuits (1). It remains to examine in more detail the influence of resistance often introduced in the secondary in order to damp the oscillations. The origin of the broadcast frequencies, finally, which in practice are of particular interest, has remained obscure and requires a more complete analysis of the circuit than has hitherto been attempted.

Theory of Audio Frequencies Produced by the Coils

The conditions to be studied are those that follow the extremely brief opening stage during which the voltage drops to a virtually constant value, E_2. At this moment the primary current, i_1, is equal to i_p at a voltage e_p; the

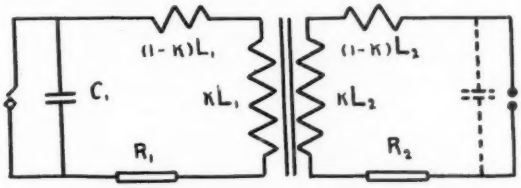

FIG. 1. *Circuit of induction coil.*

secondary current, i_2, is equal to i_s. When L_1, L_2, C_1 and C_2 are the primary and secondary inductances and capacities (Fig. 1), and M the coefficient of mutual induction, the circuit equations are:

$$L_1 \frac{d^2q_1}{dt^2} + M_2 \frac{d^2q_2}{dt^2} + R_1 \frac{dq_1}{dt} + \frac{q_1}{C_1} = 0$$

$$L_2 \frac{d^2q_2}{dt^2} + M_1 \frac{d^2q_1}{dt^2} + R_2 \frac{dq_2}{dt} + E_2\left(\frac{dq_2}{dt}\right) = 0.$$

Providing that the potential across the spark, in the general case a function of the current $i_2 = dq_2/dt$, is virtually constant, the equations may be written in the form.

$$(L_1D^2 + R_1D + 1/C_1)q_1 + MD^2q_2 = 0$$
$$(L_2D^2 + R_2D)q_2 + MD^2q_1 + E = 0.$$

Eliminating q_1 and putting $M^2 = \kappa^2 L_1 L_2$, an equation for q_2 is obtained:

$$\left(D^4(1 - \kappa^2) + \left(\frac{R_1}{L_1} + \frac{R_2}{L_2}\right) D^3 + \left(\frac{R_1R_2}{L_1L_2} + \frac{1}{C_1L_1}\right) D^2 + \frac{R_2D}{L_1C_1}\right) q_2 = -\frac{E_2}{C_1L_1L_2},$$

or writing α_1 for R_1/L_1 and ω_1^2 for $1/L_1C_1$,

$$D\left(D^3 + \frac{\alpha_1 + \alpha_2}{1 - \kappa^2} D^2 + \frac{\omega_1^2 + \alpha_1\alpha_2}{1 - \kappa^2} D + \frac{\alpha_2\omega_1^2}{1-\kappa^2}\right) q_2 = -\frac{E_2\omega_1^2}{L_2(1 - \kappa^2)}$$

or

$$\left(D^3 + \frac{\alpha_1 + \alpha_2}{1 - \kappa^2} D^2 + \frac{\omega_1^2 + \alpha_1\alpha_2}{1 - \kappa^2} D + \frac{\alpha_2\omega_1^2}{1 - \kappa^2}\right) i_2 = \frac{-E_2\omega_1^2}{L_2(1 - \kappa^2)}.$$

Except when R_2 vanishes, the solution of this equation can be obtained in the usual way from the formula

$$q_2 = \int \epsilon^{m_3 t} dt \int \epsilon^{(m_2 - m_3)t} dt \int \epsilon^{(m_1 - m_2)t} dt \int \frac{-E_2}{R_2} \epsilon^{m_1 t} dt,$$

as

$$q_2 = A_1\epsilon^{m_1 t} + A_2\epsilon^{m_2 t} + A_3\epsilon^{m_3 t} + A_4 - \frac{E_2}{R_2} t,$$

where 0, m_1, m_2 and m_3 are the solutions of the equation, with D considered as the unknown and E_2 equal to zero.

Elimination of q_2 from the differential equations leads to the same relation for q_1, but with the right-hand side equal to zero, so that

$$q_1 = B_1\epsilon^{m_1 t} + B_2\epsilon^{m_2 t} + B_3\epsilon^{m_3 t} + B_4.$$

Hence, in that stage of the discharge in which the voltage at the electrodes remains virtually at the value E_2, the primary and secondary current, i_1 and i_2, are given by

$$i_1 = m_1B_1\epsilon^{m_1t} + m_2B_2\epsilon^{m_2t} + m_3B_3\epsilon^{m_3t}$$

$$i_2 = m_1A_1\epsilon^{m_1t} + m_2A_2\epsilon^{m_2t} + m_3A_3\epsilon^{m_3t} - \frac{E_2}{R_2}.$$

The seven constants of integration are determined from the conditions existing at the beginning of the second stage of the spark, while the values of m are given by the solutions of the equation

$$m^3 + \frac{\alpha_1 + \alpha_2}{1 - \kappa^2} m^2 + \frac{\omega_1^2 + \alpha_1\alpha_2}{1 - \kappa^2} m + \frac{\alpha_2\omega_1^2}{1 - \kappa^2} = 0,$$

or

$$m^3 + am^2 + bm + c = 0,$$

an equation that has at least one real root with a sign opposite to that of its last term. The character of the solution depends on the values of p, q and q^2/p^3, where

$$p = \frac{1}{9}\left(\left(\frac{\alpha_1 + \alpha_2}{1 - \kappa^2}\right)^2 - 3\,\frac{\omega_1^2 + \alpha_1\alpha_2}{1 - \kappa^2}\right) = \frac{1}{9}(a^2 - 3b)$$

$$q = \frac{1}{54}\left(9\,\frac{\alpha_1 + \alpha_2}{1 - \kappa^2}\,\frac{\omega_1^2 + \alpha_1\alpha_2}{1 - \kappa^2} - 2\left(\frac{\alpha_1 + \alpha_2}{1 - \kappa^2}\right)^3 - 27\,\frac{\alpha_2\,\omega_1^2}{1 - \kappa^2}\right) = \frac{1}{54}(9\,ab - 2a^3 - 27c).$$

In building ignition coils, α_1 and α_2 are kept small, at least, less than about 500, whereas $\omega_1^2 = 1/L_1C_1$ is very large, usually greater than 10^8. The coupling between primary and secondary is such that $\kappa \geqslant 0.95$, or $\kappa^2 = M/L_1L_2$, about 0.9. Under these conditions p is negative and nearly equal to $-\omega_1^2/3(1 - \kappa^2) = -\omega^2/3$. Whenever p is negative

$$m_1 = -\sqrt{-p}\,\sinh\frac{u}{3} - \frac{\alpha_1 + \alpha_2}{3(1 - \kappa^2)} + i\sqrt{-3p}\,\cosh\frac{u}{3} = \mu + i\omega$$

$$m_2 = -\sqrt{-p}\,\sinh\frac{u}{3} - \frac{\alpha_1 + \alpha_2}{3(1 - \kappa^2)} - i\sqrt{-3p}\,\cosh\frac{u}{3} = \mu - i\omega$$

$$m_3 = 2\sqrt{-p}\,\sinh\frac{u}{3} - \frac{\alpha_1 + \alpha_2}{3(1 - \kappa^2)}$$

$$\frac{q}{\sqrt{-p^3}} = \sinh u.$$

A negative root and two complex roots, the latter corresponding to electrical oscillations, are obtained. Since in the expression for q the first term tends to be largest,

$$\frac{q}{\sqrt{-p^3}} \doteq \frac{\sqrt{3}}{2}\,\frac{\alpha_1 + \alpha_2}{\omega(1 - \kappa^2)} = \sinh u < 1;$$

when ω_1 is very high, $\sinh u$ becomes quite small, and for coils of moderate size the relations

$$m_1 = -\frac{\alpha_1 + \alpha_2}{3(1 - \kappa^2)} + i\omega = m_3 + i\sqrt{-3p}$$

$$m_2 = -\frac{\alpha_1 + \alpha_2}{3(1 - \kappa^2)} - i\omega = m_3 - i\sqrt{-3p},$$

hold for most practical purposes.

as though these roots were simply the solutions of a quadratic differential equation, namely of

$$(D^2 - 2m_3D + (m_3^2 + \omega^2))i_2 = 0.$$

The third root becomes

$$m_3 = -\frac{\alpha_1 + \alpha_2}{3(1 - \kappa^2)} = -\frac{a}{3}.$$

The angular frequency ω is given by $\sqrt{-3p}$, or

$$\omega = \frac{\omega_1}{\sqrt{1 - \kappa^2}},$$

as in ordinary tuned and coupled circuits. This formula is in good agreement with the experimental values. For a coil having $L_1 = 0.005$ $h.$ and $C_1 = 0.46$ $\mu f.$, $\kappa = 0.95$, $L_2 = 11.6$ $h.$, the computed frequency is 10,640 cycles per sec., the measured frequency 10,750 (Finch). For a coil with $L_1 = 0.02$ $h.$, $C_1 = 0.041$ $\mu f.$, $\kappa = 0.97$, the corresponding frequency is 22,300 cycles per sec.

In the second stage of the discharge the current is therefore in general oscillating despite the constant voltage E_2. Its complete equation is

$$i_2 = m_3A_3\epsilon^{m_3t} - \frac{E_2}{R_2} + m_1A_1\epsilon^{(\mu+i\omega)t} + m_2A_2\epsilon^{(\mu-i\omega)t}$$

or

$$i_2 = m_3A_3\epsilon^{m_3t} - \frac{E_2}{R_2} + \epsilon^{\mu t}\Big((m_1A_1 + m_2A_2)\cos\omega t + i(m_1A_1 - m_2A_2)\sin\omega t\Big)$$

$$i_1 = m_3B_3\epsilon^{m_3t} - \frac{E_2}{R_2} + \epsilon^{\mu t}\Big((m_1B_1 + m_2B_2)\cos\omega t + i(m_1B_1 - m_2B_2)\sin\omega t\Big).$$

The constants A and B are obtained, first by computing q_1 and q_2 for $t = 0$, at which time $q_1 = C_1e_p$ and $q_2 = 0$, or C_2 virtually discharged, and second, by substituting the expressions obtained for q in the two differential equations determining q_2. This leads to the following seven equations for the seven unknowns, with $n = M/L_2$

$$\begin{aligned}
A_1 + A_2 + A_3 + A_4 &= 0\\
B_1 + B_2 + B_3 - C_1e_p &= 0\\
m_1B_1 + m_2B_2 + m_3B_3 - i_p &= 0\\
m_1A_1 + m_2A_2 + m_3A_3 - \frac{E_2}{R_2} - i_s &= 0\\
(m_1 + \alpha_2)A_1 + m_1nB_1 &= 0\\
(m_2 + \alpha_2)A_2 + m_2nB_2 &= 0\\
(m_3 + \alpha_2)A_3 + m_3nB_3 &= 0
\end{aligned}$$

The system has the following exact solutions, in which (E) stands for $\left(\frac{E_2}{R_2} + i_s\right)$:

$$A_1 = (m_2 - m_3)\frac{\alpha_2\omega^2nC_1e_p + ni_p\Big(m_1(m_2 + m_3) - \omega^2\Big) + (E)\Big(m_1\alpha_2 + m_1(m_2 + m_3) - \omega^2\Big)}{\alpha_2\Big(m_1m_3(m_3 - m_1) + m_2m_1(m_1 - m_2) + m_3m_2(m_2 - m_3)\Big)}$$

$$A_2 = (m_3 - m_1)\frac{\alpha_2\omega^2nC_1e_p + ni_p\Big(m_2(m_3 + m_1) - \omega^2\Big) + (E)\Big(m_2\alpha_2 + m_2(m_3 + m_1) - \omega^2\Big)}{\alpha_2\Big(m_1m_3(m_3 - m_1) + m_2m_1(m_1 - m_2) + m_3m_2(m_2 - m_3)\Big)}.$$

A similar expression is obtained for A_3 by cyclic increases in the subscripts of the m's. Moreover,

$$A_4 = \frac{n}{\alpha_2} i_p + \frac{1}{\alpha_2}\left(\frac{E_2}{R_2} + i_s\right) = \frac{M}{R_2} i_p + \frac{L_2}{R_2}\left(\frac{E_2}{R_2} + i_s\right)$$

while

$$B_1 = -A_1 \frac{m_1 + \alpha_2}{m_1 n}$$

$$B_2 = -A_2 \frac{m_2 + \alpha_2}{m_2 n}$$

$$B_3 = -A_3 \frac{m_3 + \alpha_2}{m_3 n} .$$

The solutions m_1, m_2 and m_3 being of the form

$$m_1 = -s - \frac{a}{3} + i\omega = \mu + i\omega$$

$$m_2 = -s - \frac{a}{3} - i\omega = \mu - i\omega$$

$$m_3 = 2s - \frac{a}{3} ,$$

the denominator of the A's becomes equal to $2\alpha_2 i\omega(\omega^2 - d)$ or $2i\omega\alpha_2(\omega^2 + (\mu - m_3)^2)$. Grouping together the terms in ω^2 the expression for the aperiodic component of the current i_2 becomes

$$m_3 A_3 = \frac{m_3}{\alpha_2(\omega^2 + d)}\left(\alpha_2\omega^2 n C_1 e_p - n i_p \omega^2 - (E)\omega^2 + 2\mu m_3 n i_p + (E)m_3(\alpha_2 + 2\mu)\right).$$

The sine wave forming part of i_2 is represented by $i(m_1A_1 - m_2A_2)$ sin ωt, its initial amplitude being therefore $i\mu(A_1 - A_2) - \omega(A_1 + A_2)$ or $i\mu Im (A_1 - A_2) - \omega Re(A_1 + A_2)$, where Im and Re are the imaginary and the real part of the expressions which follow them.

$$\begin{aligned} i(m_1A_1 - m_2A_2) &= \frac{\alpha_2 n C_1 e_p}{\alpha_2(\omega^2 + d)}\,\omega\left(\omega^2 + \mu(\mu - m_3)\right) \\ &+ \frac{n i_p + (E)}{\omega\alpha_2(\omega^2 + d)}\left(\omega^2(m_3^2 + \mu^2 + m_3\mu) + \mu^2(m_3^2 - \mu^2)\right) \\ &+ \frac{(E)\alpha_2}{\alpha_2\omega(\omega^2 + d)}\left(\omega^2(\mu + m_3) + \mu^2(\mu - m_3)\right). \end{aligned}$$

The amplitude of the cosine wave becomes in the same way

$$\mu Re(A_1 + A_2) + i\omega Im(A_1 - A_2) = (m_1A_1 + m_2A_2)$$

$$= -m_3 \frac{\alpha_2 n C_1 e_p \omega^2}{\alpha_2(\omega^2 + d)} + m_3 \frac{(E) + n i_p}{\alpha_2(\omega^2 + d)}(\omega^2 - 2\mu m_3) + \frac{(E)}{\omega^2 + d}(\omega^2 + \mu^2 - 2\mu m_3) .$$

These are the exact amplitudes.

With the much simpler expressions that in many practical applications are valid for m, namely, $s = 0$ and

$$m_1 = \mu + i\omega = -\frac{a}{3} + i\omega$$

$$m_2 = \mu - i\omega = -\frac{a}{3} - i\omega$$

$$m_3 = -\frac{\alpha_1 + \alpha_2}{3(1 - \kappa^2)} = -\frac{a}{3} = \mu,$$

the denominator of the constants A becomes equal to $2i\omega\alpha_2\omega^2$, and moreover the real part of

$$m_1A_1 + m_2A_2 = m_3 \frac{2m_3^2ni_p + (E)(2m_3^2 + \alpha_2m_3)}{-\alpha_2\omega^2} + \frac{(E)(m_3 + \alpha_2) + m_3ni_p - \alpha_2m_3nC_1e_p}{\alpha_2},$$

while

$$Im(m_1A_1 - m_2A_2) = i\,\frac{(E)(3m_3^2 + 2m_3\alpha_2) + 3m_3^2ni_p + \omega^2\alpha_2nC_1e_p}{\alpha_2\omega}$$

$$m_3A_3 = m_3 \frac{2m_3^2ni_p + (E)m_3(2m_3 + \alpha_2)}{\alpha_2\omega^2} + m_3 \frac{\alpha_2nC_1e_p - ni_p - (E)}{\alpha_2}.$$

Taking into account the fact that in this case ω is very large, the expression for the discharge current in the low voltage stage becomes

$$i_2 = \frac{a}{3}\,\epsilon^{-\frac{a}{3}t}\left(\frac{ni_p + E_2/R_2 + i_s}{\alpha_2} - nC_1e_p\right) - \frac{E_2}{R_2}$$

$$i_2 = -\frac{E_2}{R_2} + \frac{a}{3}\,\epsilon^{-\frac{a}{3}t}\left(\frac{ni_p + E_2/R_2 + i_s}{\alpha_2} - nC_1e_p\right)(1 - \cos\omega t)$$

$$+ \epsilon^{-\frac{a}{3}t}\left(\frac{E_2}{R_2} + i_s\right)\cos\omega t + \epsilon^{-\frac{a}{3}t}\,\omega nC_1e_p \sin\omega t.$$

The terms involving C_1 are generally small compared to the others, and since

$$-\frac{m_3}{\alpha_2} = \frac{\frac{\alpha_1}{\alpha_2} + 1}{3(1 - \kappa^2)}$$

may become large when α_2 is kept small, the expression for i_2 reduces in practice approximately to

$$i_2 = -\frac{E_2}{R_2} + \frac{\alpha_1 + \alpha_2}{3(1 - \kappa^2)\alpha_2}\,\epsilon^{-\frac{a}{3}t}\left(\frac{M}{L_2}\,i_p + \frac{E_2}{R_2} + i_s\right)(1 - \cos\omega t).$$

If the secondary is shorted ($E_2 = 0$), the current becomes

$$i_2 = \frac{\alpha_1 + \alpha_2}{3(1 - \kappa^2)\alpha_2}\,\epsilon^{-\frac{a}{3}}\left(\frac{M}{L_2}\,i_p + i_s\right)(1 - \cos\omega t).$$

Hence, in agreement with the experiment, in the region of constant voltage across the secondary, the discharge current consists in the simplest case of an exponentially decreasing electrical oscillation of audible frequency ω superimposed upon an aperiodic component that decreases according to the same law. The sum of the two components keeps the same sign. The current vanishes finally at the time t_f for which

$$\frac{1 + \alpha_1/\alpha_2}{3(1 - \kappa^2)}\,\epsilon^{-\frac{a}{3}t_f}\left(\frac{Mi_p}{L_2} + \frac{E_2}{R_2} + i_s\right) = E_2/R_2.$$

When E_2/R_2 is fairly large and the decay so rapid that $-at_f/3$ is smaller than unity,

$$t_f = \frac{3(1 - \kappa^2)}{\alpha_1 + \alpha_2},$$

that is, the secondary current has even then a duration that is larger than that corresponding to the natural period, ω, of the transformer.

For larger coils the value of $\sinh \frac{u}{3}$ is not necessarily negligible, but follows roughly from the relation

$$4 \sinh^3 \frac{\mu}{3} + 3 \sinh \frac{\mu}{3} = \sinh \mu$$

as

$$-2 \sinh \frac{\mu}{3} = \sqrt[3]{-\sinh \mu + \sqrt{1 + \sinh^2 \mu}} + \sqrt[3]{-\sinh \mu - \sqrt{1 + \sinh^2 \mu}}$$

or

$$\sinh \frac{u}{3} \doteqdot \sinh \frac{u}{3} .$$

Therefore

$$m_1 = \frac{\alpha_2}{2} - \frac{\alpha_1 + \alpha_2}{2(1 - \kappa_2)} + i\omega \doteqdot -\frac{\alpha_1 + \alpha_2}{2(1 - \kappa_2)} + i\omega$$

$$m_2 = \frac{\alpha_2}{2} - \frac{\alpha_1 + \alpha_2}{2(1 - \kappa^2)} - i\omega \doteqdot -\frac{\alpha_1 + \alpha_2}{2(1 - \kappa^2)} - i\omega$$

$$m_3 = -\alpha_2.$$

In this case the decay of the aperiodic component can be slowed down at will by keeping $\alpha_2 = R_2/L_2$ sufficiently small. Since $1 - \kappa^2$ is small, the oscillations will have died out long before the aperiodic portion of the current has decreased a great deal. Taking into account the fact that ω^2 is quite large and C_1 very small, the current is obtained by putting in the general formulas $\mu = -a/2$ and $m_3 = -\alpha_2$:

$$i_2 = -\frac{E_2}{R_2} + \left(\frac{Mi_p}{L_2} + \frac{E_2}{R_2}\right)\left(\epsilon^{-\alpha_2 t} - \epsilon^{\left(\frac{\alpha_2}{2} - \frac{\alpha_1 + \alpha_2}{2(1-\kappa^2)}\right)t} \cos \omega t\right) .$$

With $i_0 = Mi_p/L_2$ as its initial strength, the aperiodic component is the same as it would be were a current i_0 set up and allowed to decay in the secondary in the absence of the primary windings; such a current corresponds to the complete sharing of the magnetic flux by the primary and the secondary:

$$Mi_p = L_2 i_0.$$

In the later stage of the discharge the current becomes simply

$$i_2 = -\frac{E_2}{R_2} + \left(i_0 + \frac{E_2}{R_2}\right)\epsilon^{-\frac{R_2}{L_2}t} .$$

and the time required for the current to drop from i_0 to i_2 is

$$t = \frac{L_2}{R_2} ln \frac{i_0 R_2 + E_2}{i_2 R_2 + E_2} .$$

This duration determines the extent to which the coil is discharged.

For large coils this formula is in agreement with observation (McFarlane).

In dealing with the course which the aperiodic component takes, the constants of only the secondary windings need be considered, the circuit equations reducing to

$$\frac{di_2}{dt} + \frac{R_2}{L_2} i_2 + \frac{E_2}{L_2} = 0 .$$

In view of the simple laws obeyed by E_2, for instance $E_2 = C - ci_2$, this equation is the same as that valid for ordinary discharge tube circuits, so that the glow may present all the types found at lower pressures (Kock).

For a small coil, the following constants may be used (Finch):

$L_1 = 0.005$ h. $\quad \kappa = 0.95$ $\quad E_2 = 360$–380 v.
$R_1 = 3$ ohms $\quad M = \kappa\sqrt{L_1 L_2} = 0.229$ $\quad i_p = 2$ A.
$\alpha_1 = 600$ $\quad n = M/L_2 = 0.02$ A. per A. $\quad e_p < 5$ v.
$L_2 = 11.6$ h. $\quad 1 - \kappa^2 = 0.0975$
$R_2 \doteq 300$ ohms
$\alpha_2 \doteq 26$

$C_1 = 0.46\ \mu$f.
$\omega = 66{,}816$
$f = 10{,}640$
$nC_1e_p < 10^{-7}$
$C_2 = 10^{-10}$ f.
$a = 6.66$ $\quad E_2/R_2 \doteq 0.050$

and therefore,

$$i_2 = 0.22\ \epsilon^{-6.66t}\ (1 - \cos 66{,}816t)$$

For a large coil the following constants are appropriate (McFarlane):

$L_1 = 0.1$ h. $\quad \kappa = 0.94$ $\quad E_2 = 380$ v.
$R_1 = 39$ ohms $\quad M = 11.2$ $\quad i_p = 2$ A.
$\alpha_1 = 400$ $\quad n = M/L_2 = 0.0075$ $\quad e_p = 12$ v.
$L_2 = 1500$ h. $\quad 1 - \kappa^2 = 0.12$
$R_2 = 28{,}000$ ohms
$\alpha_2 = 19$

$C_1 = 2.67\ \mu$f.
$\omega = 5600$
$C_2 = 10^{-10}$ f.

$a = \dfrac{\alpha_1 + \alpha_2}{1 - \kappa^2} = 158$ $\quad E_2/R_2 = 0.014$

and therefore,

$$i_2 = -\frac{E_2}{R_2} + \left(\frac{Mi_p}{L_2} + \frac{E_2}{R_2}\right)\left(\epsilon^{-\alpha_2 t} - \epsilon^{\left(\alpha_2 - \frac{\alpha_1 + \alpha_2}{1-\kappa^2}\right)\frac{t}{2}} \cos \omega t\right)$$

$$= -0.013 - 0.028\ \epsilon^{-1750t} \cos \omega t + 0.028\ \epsilon^{-19t}.$$

Curve of Sloping Voltage against Current

So long as the electrodes are separated by a gap barely allowing the negative glow to develop, which involves a distance of about 0.008 mm. at atmospheric pressure, the drop of potential reduces to the normal cathode fall, about 375 volts in air between copper discs and 277 volts between zinc plates, regardless of the pressure. When the distance is increased, the potential gradient across the positive column must be added. This gradient increases with increasing pressure p, measuring about $0.3\ p$ volts per mm. in nitrogen and four times this amount in oxygen, when the pressure is measured in millimetres of mercury. Lower currents require a higher gradient, usually represented by $g + h/i$, where h is not far from unity. The voltage across the spark is therefore

$$E_2 = c + l\ (g + h/i)\ .$$

In air, C is about 380 volts for copper electrodes, g equal to 108 and $h = 0.8$ (McFarlane). The curvature introduced by the term h/i in the curve of voltage against current is so small as a rule that over wide ranges of current the voltage may be represented by a straight line.

The only change that a slightly sloping, or rising, but straight curve of voltage against current causes in the mathematical equations of the problem is the addition of $\mp\alpha_3$ to all the terms containing α_2. In view of the small currents involved, less than 50 ma., and the rather large values of L_2, the existence of the slope $\mp R_3$ in the characteristic curve, beginning in sparks at about 500 volts and several milliamperes current, would probably not be revealed by ordinary measurements with the cathode ray tube even if $-\alpha_3 = R_3/L_2$ were as large as 500 or 600. When appreciable capacity is present in parallel with the gap, however, it absorbs a current, i_c, given by

$$i_c - i_2 = C_2 dE_2/dt = \pm C_2 R_3 .$$

The case where $-\alpha_3$ just neutralizes α_2 deserves special mention. Under these conditions, most favorable to an experimental study, the ignition coil behaves as if there were no resistance in the secondary, whereas, in practice, R_2 cannot be neglected, not at least if, as is sometimes the case, a resistance of several thousand ohms is included in order to record the current changes with the cathode ray. When $(\alpha_2 - \alpha_3)$ vanishes, as seems sometimes to be the case, the differential equation reduces to a quadratic relation.

$$D^2\left(D^2 + \frac{\alpha_1}{1-\kappa^2} D + \frac{\omega_1^2}{1-\kappa^2}\right) q_2 = -\frac{\omega_1}{(1-\kappa^2)L_2} E_2 .$$

The frequency of oscillation is the same as before; the damping has been decreased, and the current is given by the simple formula

$$i_2 = \frac{M}{L_2} i_p (1 - \epsilon^{-\frac{a}{2}t} \cos \omega t) + i_s \epsilon^{-\frac{a}{2}t} - \frac{E_2}{L_2} t ,$$

where

$$a = R_1/L_1(1-\kappa^2)$$

and

$$M/L_2 = \kappa\sqrt{L_1/L_2} .$$

The current consists of a damped oscillation about the straight line $(Mi_p - E_2 t)/L_2$. Once the oscillations have vanished, the secondary current continues to decay to zero along the time axis, giving a total duration of this second, and by far the longest, stage of the spark of

$$t_f = Mi_p/E_2 \text{ sec.}$$

It lasts at least a few milliseconds, whereas the breakdown proper takes less than a microsecond (McFarlane, Finch).

With a slightly more negative value of $-\alpha_3$ a stage is reached where the sum $(\alpha_1 + \alpha_2 - \alpha_3)$ disappears. This change again scarcely affects the frequency which remains at the value given by $\omega_1/\sqrt{1-\kappa^2}$, but it removes all damping. The equation for the current is

$$\left(D^3 - \omega^2 D - (\alpha_3 - \alpha_2)\omega^2\right) i_2 = E_2\omega^2/L_2$$

with the solutions, since

$$\frac{(\alpha_3 - \alpha_2)\omega_1^2}{2(1-\kappa^2)} \ll \sqrt{\frac{\omega_1^6}{27(1-\kappa^2)^3}} ,$$

$$m_{1 \text{ or } 2} = \pm i \frac{\omega_1}{\sqrt{1-\kappa^2}} , \qquad m_3 = 0,$$

solutions which might have been obtained directly from the previous simplified quadratic equation for m_3 and ω. They correspond to oscillations of constant amplitude

$$i_2 = \left(\frac{E}{R_2} + i_s\right) \cos \omega t - \frac{E_2}{R_2} - \frac{M}{L_2} C_1 e_p \sin \omega t ,$$

where the last term is most often negligible.

Beyond this point the discharge enters the stage where the amplitudes instead of being damped increase with each period and finally, owing to the rapidly increasing cathode drop, the oscillations degenerate into slow relaxation currents. At the same time, for large fluctuations in the current, the value of M is no longer constant.

The Aperiodic Discharge

When, on the other hand, as a result of the introduction of a large condenser in the primary, or a large resistance in the secondary, circuit, the value of $R_2/\omega_1 L_2$ increases, the sign of p changes from negative to positive, so that

$$p > 0 \qquad q > 0 \qquad q^2 > p^3 \qquad \cosh u = \frac{+q}{\sqrt{p^3}} .$$

The solutions m_1, m_2 and m_3 now depend on

$$m_1 = -\sqrt{p} \cosh \frac{u}{3} - \frac{a}{3} + i\sqrt{3p} \sinh \frac{u}{3} = \mu + i\omega$$

$$m_2 = -\sqrt{p} \cosh \frac{u}{3} - \frac{a}{3} - i\sqrt{3p} \sinh \frac{u}{3} = \mu - i\omega$$

$$m_3 = +2\sqrt{p} \cosh \frac{u}{3} - \frac{a}{3} = -2\mu + \frac{a}{3} ,$$

where p and q are conveniently written as

$$p = \frac{\omega_1^2}{9}\left(\left(\frac{\alpha_1 + \alpha_2}{\omega_1(1 - \kappa^2)}\right)^2 - 3\,\frac{1 + \frac{\alpha_1\alpha_2}{\omega_1^2}}{1 - \kappa^2}\right)$$

$$q = \frac{\omega_1^3}{54}\left(\frac{9}{\omega_1}\,\frac{\alpha_1 + \alpha_2}{1 - \kappa^2}\,\frac{1 + \frac{\alpha_1\alpha_2}{\omega_1^2}}{1 - \kappa^2} - \frac{2}{\omega_1^3}\left(\frac{\alpha_1 + \alpha_2}{1 - \kappa^2}\right)^3 - \frac{27}{\omega_1}\,\frac{\alpha_2}{1 - \kappa^2}\right),$$

in order to illustrate the importance of the factor $\alpha_2/\omega_1(1 - \kappa^2)$. When α_1 is small, the expression for p changes from negative to positive near the frequency for which

$$\frac{\alpha_1 + \alpha_2}{\sqrt{3}(1 - \kappa^2)} \gtrless \omega_1$$

whilst q keeps its sign. For $\kappa = 0.95$ the equation becomes, for small α_1's, $\alpha_2 = 0.55\omega_1$; for $\kappa = 0.98$ it is $\alpha_2 = 0.35\ \omega_1$.

As α_2 increases, the natural frequency of oscillation given by $\omega = \sqrt{3p}$ $\sinh \frac{u}{3}$ decreases (Table I). The last simple form the discharge may assume is the aperiodic stage, which is obtained when $p > 0$, but $q^2 \leqslant p^3$, or

$$0 < \frac{q^2}{p^3} < 1 .$$

This condition is satisfied when $(\alpha_1 + \alpha_2)$ is rather large, the coupling tight ($\kappa > 0.95$), and when q is nearly zero or negative. By starting with a coil having a small value of α_1 and a large ratio $R_2/L_2 = \alpha_2$, the values of α_2 and κ may always be so chosen that q becomes slightly smaller than the square root of p^3. In this case, which may obtain over a portion only, or over the entire duration of the discharge

$$\cos u = \frac{q}{\sqrt{p^3}}$$

$$m_1 = -\sqrt{p}\cos\frac{u}{3} - \frac{a}{3} + \sqrt{3p}\sin\frac{u}{3}$$

$$m_2 = -\sqrt{p}\cos\frac{u}{3} - \frac{a}{3} - \sqrt{3p}\sin\frac{u}{3}$$

$$m_3 = 2\sqrt{p}\cos\frac{u}{3} - \frac{a}{3}$$

TABLE I

INFLUENCE OF INCREASING RESISTANCE IN THE SECONDARY UPON THE ANGULAR FREQUENCY OF OSCILLATION, $\omega = \sqrt{3p}\sinh u/3$

$\alpha_1 \doteqdot 0$; $\omega_1 = 2000$; $1-\kappa^2 = 0.04$

α_2	p/ω_1^2	$\sqrt{p}/\omega_1$	$\sqrt{p^3}/\omega_1^3$	q/ω_1^3	$\cosh u$	$\cosh\frac{u}{3}$	$\sinh\frac{u}{3}$	$\sqrt{3p}$	$\frac{a}{3}$
Oscillating stage									
690	<0								
695	0.052	0.228	0.0118	7.63	647	5.56	5.46	790	1917
700	0.118	0.344	0.045	7.28	162	3.48	3.34	1190	1944
750	1.423	1.19	1.7	4	2.4	1.13	0.52	2846	2083
Aperiodic stage									
				0		1	0		
800	2.777	1.667	4.6	−0.37	−0.08	0.82	0.57	2886	2222
900	5.73	2.394	13.7	−11.5	−0.83	0.62	0.79	4147	2500
1000	9.03	3.005	27	−26.5	−0.98	0.55	0.83	5206	2777
∞	a^2/ω_1^2	a/ω_1		a^2/ω_1^2	−1	0.5	0.87		

In the aperiodic stage the ordinary trigonometric functions take the place of sinh and cosh. At the limit the current reduces to

$$i_2 = \left(\frac{E_2}{R_2} + i_s\right)\epsilon^{-\frac{\alpha_1+\alpha_2}{1-\kappa^2}t} - \frac{E_2}{R_2}.$$

The current decreases according to an exponential law until the energy is exhausted (10).

Intermittent Discharges

So far, the discharge has been treated as if any current between 0 and 100 ma. could pass at the constant or nearly constant voltage obtained between the electrodes. In reality, for a discharge to be maintained at the glow voltage the current must exceed a certain smallest value, a few milliamperes in the case of short gaps 1 or 2 mm. wide. If in its variations the

current enters a region where this condition is not fulfilled, the discharge is likely to stop without necessarily having discharged the coil. Provided, however, that the coil is able to recharge the electrodes in the interval without current, the discharge may restart at or near the spark potential, or even near the glow voltage in those cases where the path which the current has followed remains fairly conducting. In this case the current increases suddenly from zero to a high value, only to decrease again, and this cycle is repeated until the energy in the coil has been dissipated. When $R_2 > L_2$ and the aperiodic component of the current, the component which merely depends on the constants of the secondary, disappears at a voltage E_0, which is lower than the starting voltage E_1, and E is the potential which the coil is capable of generating in the absence of a discharge, then as in the case of the flashing neon tubes, the period at which the discharges follow one another is (Schallreuter)

$$t = R_2C_2ln\frac{E - E_0}{E - E_1} + C_2Rln\frac{E_1}{E_0},$$

where the last term refers to the duration of the discharge. The difference between E_0 and E_1 depends on the shape and distance of the electrodes, and for the same value of E_0 and E_1 the ratio $(E - E_0)/(E - E_1)$ is smaller, or more nearly equal to unity, the higher E. With discharge tubes, a value of 2 or 3 is often obtained for this ratio. With these figures and C_2, the capacity associated with the gap, equal to 100×10^{-12} *f.*, R_2 a few thousand ohms, the frequency becomes of the order of 1000 kc., so that it falls in the middle of the broadcast band.

When L_2 is large, the duration of the discharge is increased to such an extent that it may determine the frequency of the intermittence. Instead of rapidly increasing with increasing voltage or primary current, the frequency tends toward a constant value

$$f = \frac{1}{2\pi\sqrt{L_2C_2}},$$

which, in view of the small value of C_2, may still lie in the region of high pitched sound waves (Kock).

A particular case of these recurrent discharges presents itself when the primary current is just barely sufficient to break down the gap without being able to establish a fully developed glow discharge. Under these conditions the discharge starts repeatedly at the sparking voltage, and several sparks follow in rapid succession. A large capacity in parallel with the gap favors this type of multiple spark, the so-called condensed spark (4).

The existence of intermittent or recurrent discharges has been well demonstrated under operating conditions (9). The interval between two flashes varies from one spark to the next one, and even within the same group of partial discharges, between 1 and 30 microseconds, corresponding to the periods of waves of 300–3000 metres. At each cycle the wires leading from the coil to the spark gap are excited to resonance, so that reception of short waves is interfered with at the same time.

Prevention of Oscillations

In the case of internal combustion engines, the oscillations of the various kinds described do not seem to improve the performance of the gap, so far as ignition is concerned, since the firing of the charge, requiring merely a temperature of about 700° C. at some point in the mixture, is well under way when the low voltage stage sets in. The oscillations are, however, liable to produce noises and disturbances in the reception of radio waves.

Since the initial strength of the low voltage stage of the discharge current is nearly directly proportional to the primary current at break, it can be readily weakened by lowering the primary current, but such a reduction is likely to create multiple sparks. A more direct procedure for preventing oscillations, though difficult to apply in practice, is to close the primary circuit as soon as breakdown has occurred. The spark is rapidly extinguished. Grid-controlled discharge tubes would be suitable for this purpose.

There still remains in any case the disturbance created by the spark proper, or the surge traveling along the leads owing to the sudden drop in potential at the moment of the breakdown. Its duration, less than a microsecond, is about the same as the natural period of the lead wires acting as half-wave antennas. Strong oscillations are therefore set up at each passage of the spark. The inductance of two straight parallel wires of radius r cm. spaced a cm. apart is $0.4\ ln\ (a/r)$ microhenry per metre, or about $0.28\ \mu$h. per metre for wires touching each other, and the capacity is 10^{-10} farads per metre, equal to $1.06/ln(a/r)$, or $0.15 \times 10^{-10}\ f.$ per metre for wires in contact, so that the angular resonance frequency of the wires connecting coil and spark,

$$\omega_2^2 = \frac{1}{L_2C_2} - \frac{R_2^2}{4L_2^2},$$

is seen to correspond to waves of less than 40 metres, provided that R_2 is small. This circuit can be rendered aperiodic by increasing R_2 and by decreasing the value of L_2 to that for a single straight wire.

The usual remedy is to insert resistance in the secondary until the noise vanishes. Tests on a wide variety of motors, ranging in output from 1 to 60 hp., have shown that resistances of 5,000-15,000 ohms, preferably wire-wound, long and with little self-inductance, greatly weaken the noises without reducing measurably the power of the engine (5).

The formula for ω_2 shows that the lower the value of L_2 the easier it is to suppress the oscillations, and that, as experience shows, it cannot be accomplished by inserting choke-coils between spark and secondary. The same statement applies to incomplete screening of the spark circuit, which is likely to increase L_2 and to add capacitance. Condensers and filters merely shift the resonance frequency to a different wave band.

It is more difficult to deal with the intermittent discharge. Its strength depends on the difference between starting and stopping voltage. The difference increases, in general, with increasing pressure and decreasing

capacitance of the electrodes. It would be of general interest to study spark discharges from this point of view in the same detail in which discharges at low pressures have been investigated.

Multiple sparks, finally, are avoided when the current at break in the primary is made strong enough to produce more than the lowest breakdown voltage in the secondary.

References

1. FINCH, G. I. and SUTTON, R. W. Proc. Phys. Soc. 45 : 288-306. 1933.
2. JAFFRAY, J. Compt. rend. 198 : 2244-2246. 1934.
3. KOCK, W. E. Z. tech. Physik, 15 : 377-384. 1934.
4. MCFARLANE, W. Phil. Mag. 16 : 865-896. 1933.
5. NEUBAUER, A. H.F. tech. El. Ak. 44 : 109-118. 1934.
6. SCHALLREUTER, W. Schwingungserscheinungen in entladungsröhren. F. Vieweg, Braunschweig. 1923.
7. SMITH, W. B. Can. J. Research, 12 : 508-518. 1935.
8. THOMA, H. and HEER, L. Z. tech. Physik, 13 : 464-470. 1932.
9. VIEHMANN, H. H.F. tech. El. Ak. 43 : 85-87. 1934.
10. WATSON, E. A. J. Inst. El. Eng. 70 : 105-134. 1932.

SOME CALCULATIONS OF FIELD STRENGTH DISTRIBUTION IN THE VERTICAL PLANE OF DOUBLE-TAPERED MASTS[1]

By K. A. MacKinnon[2]

Abstract

The approximate current distribution with height in vertical tower antennae of non-uniform cross section is calculated by assuming that the cross section is that of a cylinder whose diameter changes discontinuously. The field strength distribution in the vertical plane is then calculated for this current distribution and compared with field measurements of Ballantine. This is repeated using the experimentally determined current distribution of Gihring and Brown which results in a much closer check with Ballantine's measurements.

The results were then used to calculate the field strength distribution in the vertical plane of an array comprising a 0.597λ vertical double-tapered tower as radiator, and a 0.250λ vertical tower of the self-supporting type as a fed reflector.

During some studies of adjacent channel interference from high powered broadcasting stations, a mathematical investigation was undertaken to ascertain the radiation characteristics of an array comprising a 0.597 wave vertical tower of the Blaw-Knox guyed cantilever type as radiator, and a quarter-wave vertical tower of the self-supporting type as reflector.

The radiating system thus presented has several features not usually encountered in arrays. In the first place, the towers comprising the array are of unequal heights (0.597λ and 0.25λ). In the second place, the non-uniform cross section of the towers results in a current distribution with height which, especially in the case of the higher tower, departs considerably from the sinusoidal distribution to be expected in a thin wire of uniform cross section.

Available Data

The published information on the dimensions and actual electrical performance of the guyed cantilever type of tower is very meagre. There is the recent paper by Ballantine (1), which shows the results of some measurements of the electric field distribution in the vertical plane about the WABC radiator of this type (see solid curve, Fig. 5). One observes the absence of any minimum in the neighborhood of 45° zenith angle, which minimum would be expected from a sinusoidal current distribution in the tower. A more recent paper by Gihring and Brown (2) gives the current distribution as measured on an experimental model of the guyed cantilever type of tower. This distribution is far from sinusoidal (compare Curves A and C in Fig. 3).

[1] *Manuscript received May 28, 1935.*
Contribution from the Engineering Department, Canadian Radio Broadcasting Commission, Ottawa, Canada. This paper was presented at a joint meeting of the Institute of Radio Engineers and the American Section, U.R.S.I., at Washington, April 26, 1935.

[2] *Transmission Engineer, Canadian Radio Broadcasting Commission.*

NOTE.—*While the author was preparing this manuscript, there appeared in the Proceedings of the Institute of Radio Engineers, a letter to the editor by Hans Roder (4) in which he derives the current distribution in this type of tower by treating it as a concentric transmission line.*

Theoretical Investigation of the Current Distribution

Typical cross sections parallel to the axis of the Blaw-Knox cantilever type towers are shown in Figs. 1 and 3. Although the cross section perpendicular to the axis is square it will be considered circular henceforth. Again, although the cross section perpendicular to the axis varies uniformly throughout its length, it will be considered as changing discontinuously as illustrated in the right-hand sketch of Fig. 3. The effect of such a discontinuity on the current distribution can be readily shown for the ideal case.

Let the discontinuity be revealed only as a change in the capacity and inductance per unit length. Assuming that the top section of length X_1 has capacity C_1 and inductance L_1 per unit length, the next section, C_2 and L_2 per unit length, then, according to the simple theory

$$-\frac{dv}{dx} = jL\omega i \qquad -\frac{di}{dx} = jC\omega v$$

which have the general solution

$$v = A\cos B(x+\theta) \qquad i = \frac{AB}{jL\omega}\sin B(x+\theta)$$

where A and θ are constants and $B = \sqrt{LC\omega^2}$. The boundary conditions are

$$\text{when } x = 0, \quad i_1 = 0, \quad \therefore \theta_1 = 0 \tag{1}$$

$$\text{when } x = \underline{X}_1, \quad v_1 = v_2, \quad i_1 = i_2$$

Thus

$$A_1\cos B_1(\underline{X}_1) = A_2\cos B_2(\underline{X}_1 + \theta_2) \tag{2}$$

and

$$\frac{A_1B_1}{jL_1\omega}\sin B_1(\underline{X}_1) = \frac{A_2B_2}{jL_2\omega}\sin B_2(\underline{X}_1 + \theta_2) \tag{3}$$

Assuming that the velocity in each section is the same as that *in vacuo*

$$B_1 = B_2 = \frac{2\pi}{\lambda}$$

Dividing Equation (3) by Equation (2) the expression

$$\tan\frac{2\pi}{\lambda}(\underline{X}_1 + \theta_2) = \frac{C_1}{C_2}\tan\frac{2\pi}{\lambda}(\underline{X}_1) \tag{4}$$

is obtained.

An approximate relation between the radius of the section of the tower and its capacity per unit length is now necessary. Assume that r is the radius of any section of the tower. Let l be the total height of the tower. Assume constant density of charge (σ) over the surface of a tower of length $2l$ (to include image in earth) and radius r.

$$\text{Potential at any point } P = \frac{2\pi r\,dx\,\sigma}{\sqrt{r^2+x^2}}$$

$$\text{Potential at midpoint} = 2\pi r\sigma\int_{-l}^{+l}\frac{dx}{\sqrt{r^2+x^2}}$$

$$= 4\pi r\sigma\sinh^{-1}\frac{l}{r}$$

$$\text{Capacity} = \frac{\text{Charge}}{\text{Potential}} = \frac{2\pi r(2l)\sigma}{4\pi r\sigma\sinh^{-1}\frac{l}{r}}$$

Thus capacity per unit length

$$\propto \frac{1}{\sinh^{-1}\frac{l}{r}} \tag{5}$$

Substituting Relation (5) in Equation (4) the expression

$$\tan\frac{2\pi}{\lambda}(\overline{X}_1 + \theta_2) = \frac{\sinh^{-1}\frac{l}{r_2}}{\sinh^{-1}\frac{l}{r_1}} \tan\frac{2\pi}{\lambda}(\overline{X}_1) \tag{6}$$

is obtained. As r_2 is greater than r_1, it is seen that θ_2 is negative if $\overline{X}_1$ is less than 90°. Thus, although the current distribution from $x = 0$ to $\overline{X}_1$ is sinusoidal, so that $i_{\overline{X}_1} = \sin\frac{2\pi}{\lambda}(\overline{X}_1)$, yet after the discontinuity the current varies as though at $\overline{X}_1$ the current had attained only the value $\sin\frac{2\pi}{\lambda}(\overline{X}_1 + \theta_2)$, where θ_2 is negative. Similarly at the next discontinuity, which occurs at $x = \overline{X}_1 + \overline{X}_2$, where r changes from r_2 to r_3

$$\tan\frac{2\pi}{\lambda}(\overline{X}_1 + \theta_2 + \overline{X}_2 + \theta_3) = \frac{\sinh^{-1}\frac{l}{r_3}}{\sinh^{-1}\frac{l}{r_2}} \tan\frac{2\pi}{\lambda}(\overline{X}_1 + \theta_2 + \overline{X}_2) \cdot$$

Proceeding in this way an idea is obtained of the current distribution in a tower such as that illustrated in Fig. 1. The data in Table I were calculated by the above method.

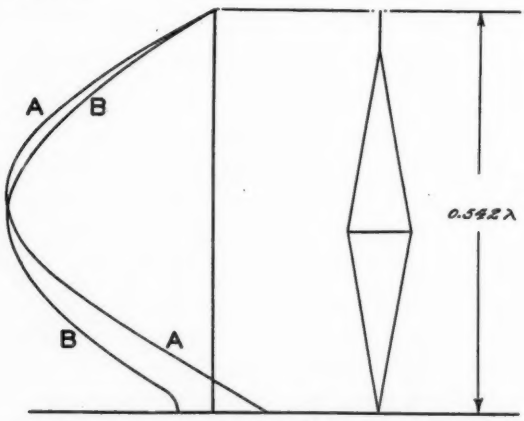

FIG. 1. *Current distribution in 0.542λ mast. A—Sinusoidal distribution. B—Distribution calculated by method presented herein.*

The data in the third and fourth columns are plotted in Fig. 1 as Curve A and Curve B respectively. Thus, Curve A is the current distribution to be expected on a wire of height 0.542λ, and Curve B is the current distribution calculated for the 0.542λ tower illustrated at the right side of Fig. 1.

TABLE I

Distance from top of tower as a fraction of the total height of the tower, x/h	Ratio of capacity, $\sinh^{-1}\frac{l}{r}$	Space angle, $\frac{360^\circ}{\lambda}x$	Current angle $\frac{360^\circ}{\lambda}(x+\Sigma\theta_n)$	Distance from top of tower as a fraction of the total height of the tower, x/h	Ratio of capacity, $\sinh^{-1}\frac{l}{r}$	Space angle, $\frac{360^\circ}{\lambda}x$	Current angle, $\frac{360^\circ}{\lambda}(x+\Sigma\theta_n)$
0	8.29	0	0	0.55	3.43	107.20	94.05
0.05	5.52	9.75	9.75	0.65	3.69	126.80	113.85
0.15	4.71	29.30	26.08	0.75	4.20	146.20	131.68
0.25	4.20	48.80	42.13	0.85	4.89	165.80	147.60
0.35	3.86	68.30	58.40	0.95	7.27	185.50	162.23
0.45	3.60	87.70	75.53	1.00	—	195.00	164.55

Derivation of Field Strength Distribution

There will now be derived the general equation for the root mean square value of the field strength (E_θ) at a zenith angle (θ) to a vertical radiator having the current distribution ($I(x)$) at a given frequency $\left(\frac{c}{\lambda}\right)$, and situated on soil having a given conductivity (σ) and dielectric constant (ϵ).

Consider a vertical radiator with height l. The value of the current at height X from the ground is $I(x)$. At a remote point, P, on the radial through the antenna base making an angle θ with the zenith, the electric field due to the current in dx is (3)

$$de_1 = \frac{\sin\theta}{c^2 r_0} f''\left(t - \frac{r_0 - x\cos\theta}{c}\right)$$

where

$$f''(t) = \frac{\partial i}{\partial t}\,dx$$

or

$$de_1 = \frac{\sin\theta}{c^2 r_0}\left(I(x)\,dx\right)\frac{2\pi c}{\lambda}\cos\left[\frac{2\pi c}{\lambda}\left(t - \frac{r_0 - x\cos\theta}{c}\right)\right]$$

or

$$de_1 = \frac{2\pi}{c r_0 \lambda}\left[I(x)\,dx\sin\theta\cos\frac{2\pi c}{\lambda}\left(t - \frac{r_0 - x\cos\theta}{c}\right)\right].$$

Similarly the field due to the image of dx is

$$de_2 = \frac{2\pi R}{c r_0 \lambda}\left[I(x)\,dx\sin\theta\cos\frac{2\pi c}{\lambda}\left(t - \frac{r_0 + x\cos\theta}{c}\right)\right],$$

where R = reflection coefficient of the earth;

$$= \frac{\cos\theta(\epsilon - j2\sigma T) - \sqrt{\epsilon - \sin^2\theta - j2\sigma T}}{\cos\theta(\epsilon - j2\sigma T) + \sqrt{\epsilon - \sin^2\theta - j2\sigma T}}$$

where ϵ, σ are in *e.s.u.* and T = period.

Then the total field at P due to dx is

$$de = de_1 + de_2$$

$$de = \frac{2\pi}{c r_0 \lambda} I(x)\,dx\sin\theta\left[\cos\frac{2\pi c}{\lambda}\left(t - \frac{r_0 - x\cos\theta}{c}\right) + R\cos\frac{2\pi c}{\lambda}\left(t - \frac{r_0 + x\cos\theta}{c}\right)\right].$$

The bracketed term can be rearranged so that

$$\text{bracket} = (\mathrm{R}+1)\cos\frac{2\pi}{\lambda}(ct-r_0)\cos\frac{2\pi}{\lambda}(x\cos\theta) + (\mathrm{R}-1)\sin\frac{2\pi}{\lambda}(ct-r_0)\sin\frac{2\pi}{\lambda}(x\cos\theta).$$

Thus

$$E_\theta = \frac{2\pi}{cr_0\lambda}\sin\theta\left[\cos\frac{2\pi}{\lambda}(ct-r_0)\,.\,(R+1)\int_0^l I(x)\cos\frac{2\pi}{\lambda}(x\cos\theta)\,dx + \sin\frac{2\pi}{\lambda}(ct-r_0)\,.\,(R-1)\int_0^l I(x)\sin\frac{2\pi}{\lambda}(x\cos\theta)dx\right].$$

The root mean square value of E_θ is then

$$E_{\theta\ r.m.s.} = \frac{\pi}{cr_0\lambda}\sin\theta\sqrt{\left[(\mathrm{R}+1)\int_0^l I(x)\cos\frac{2\pi}{\lambda}(x\cos\theta)dx\right]^2 + \left[(R-1)\int_0^l I(x)\sin\frac{2\pi}{\lambda}(x\cos\theta)dx\right]^2}.$$

Field Strength Distribution for Calculated Current Distribution

For the case represented in Fig. 1 the current distribution can be represented approximately by

$$I(x) = \sin\frac{1.675\pi}{\lambda}(l-x).$$

Assuming New Jersey soil characteristics ($\sigma = 4\times10^{-14}$ *e.m.u.*, $\epsilon\,13$ = *e.s.u.*), a frequency of 860 kilocycles, and this $I(x)$, Curve C of Fig. 2 is obtained for E_θ.

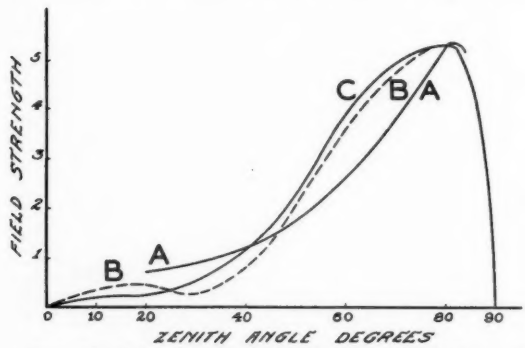

FIG. 2. *Field strength distribution in vertical plane of 0.542λ mast, over New Jersey soil. A—Ballantine's measurement of WABC (eastern side). (See Reference (1), p. 624, Fig. 41.) B—Calculated from sinusoidal distribution and for New Jersey soil. C—Calculated from distribution derived by method presented herein.*

Curve B of Fig. 2 is E_θ for New Jersey soil and a 0.542λ vertical wire, where, of course,

$$I(x) = \sin\frac{2\pi}{\lambda}(l-x).$$

Curve A, Fig. 2 is a graphical representation of Ballantine's measurement of E_θ on the eastern side of WABC (860 kilocycles, Wayne, New Jersey).

It is seen in Fig. 2 that although the calculated distribution (Curve C) has no minimum like the sinusoidal distribution (Curve B), yet it does not check satisfactorily with the experimental values (Curve A).

Field Distribution of Gihring and Brown's Current Distribution

Accordingly, the case of the 0.597λ mast for which there is Gihring and Brown's experimental distribution is next taken. Fig. 3 shows on the right-hand side the shape of the mast assumed for the calculations, and the actual shape. $I(x)$ is found for this mast by the method just outlined, and the current distribution is found to be as shown in Curve B, Fig. 3. Curve A gives the sinusoidal distribution, and Curve C, the experimentally measured distribution of Gihring and Brown.

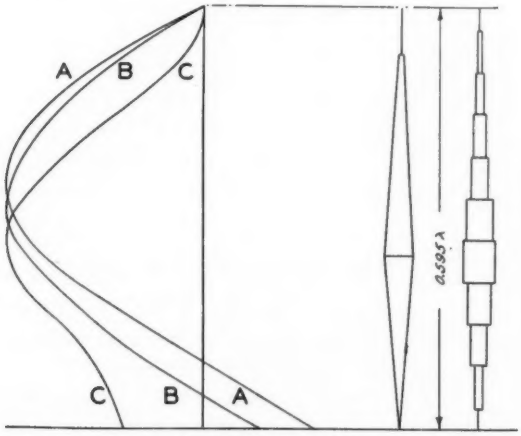

FIG. 3. *Current distribution in 0.597λ mast. A—Sinusoidal distribution. B—Distribution calculated by method presented herein. C—Distribution as experimentally measured by Gihring and Brown (2).*

The calculated distribution fails, as it always must, to indicate the very low current at the top of the mast.

To ascertain how the Gihring and Brown distribution checked with Ballantine's field measurements, an empirical relation was evolved for Curve C of Fig. 3. This is

$$I(x) = \frac{I_{\text{Loop}}}{2}\left[1 + \sin\frac{2\pi}{\lambda_0}\left(x - \frac{\lambda_0}{10}\right)\right],$$

where $\lambda_0 \equiv 0.716\lambda$.

A comparison of this $I(x)$ and the experimental curve it represents is given in Fig. 4. The solid curve, B, is Gihring and Brown's values, whilst the dotted curve, C, is $I(x)$.

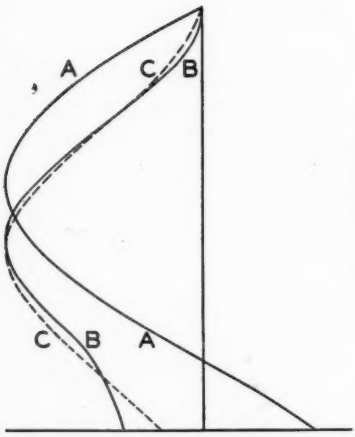

FIG. 4. *Current distribution in 0.597λ mast. A—Sinusoidal distribution. B—Experimentally measured curve of Gihring and Brown. C—Empirical distribution used in later calculations.*

$$I(x) = \frac{I_{\text{Loop}}}{2}\left[1 + \sin\frac{2\pi}{\lambda_0}\left(x - \frac{\lambda_0}{10}\right)\right]$$

where $\lambda_0 = 0.716\lambda$.

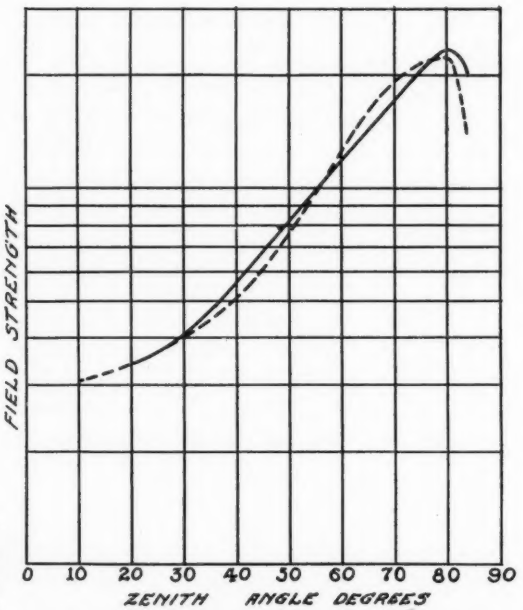

FIG. 5. *Field strength distribution in vertical plane of 0.597λ mast over New Jersey soil. Solid curve—Ballantine's measurement of WABC (eastern side). Dotted curve—Calculated from empirical distribution based on Gihring and Brown's measurements.*

Calculations using this $I(x)$, a frequency of 860 kilocycles, and New Jersey soil characteristics gives E_θ as indicated by the dotted curve of Fig. 5. The solid curve of Fig. 5 is a graphical representation of Ballantine's measurements on the eastern side of WABC. The agreement* is striking, especially when it is found that the assumption of a slightly lower conductivity for the soil will straighten out the dotted curve so that it will not depart so much from the solid curve at 45° and 68°. Fig. 6 shows the same calculated curve and Ballantine's measurements for the western side of WABC. Why there should be such a great difference between the fields on the west and east sides is not apparent. Differences in the soil characteristics (σ, ϵ) on either side cannot explain it.

**In applying this parallel ray method (large r_0) to Ballantine's experiment (measurements made at a constant altitude of 4000 ft.), it can be shown that the error is negligible. Likewise considering the problem in the light of the developments of van der Pol and Niessen (5), it seems that the author's results should be applicable to Ballantine's results up to zenith angles of the order of 70°. In any case, the interest here lies only in the zange of renith angles up to 50°, as this range includes the lobe and minimum in field strength which a sinusoidat antenna current distribution demands, and of which experiment yields no sign.*

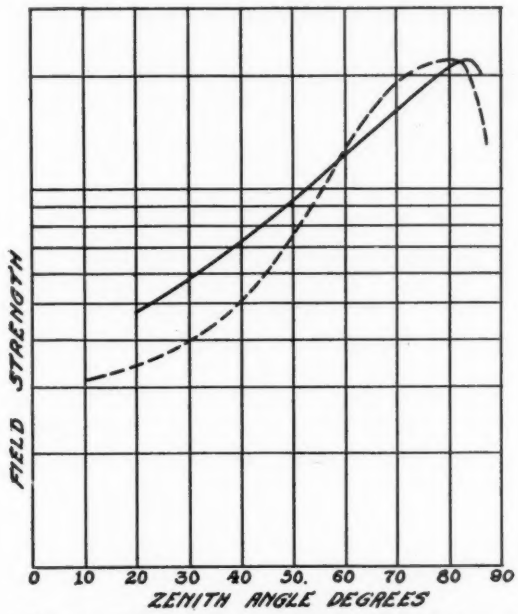

FIG. 6. *Field strength distribution in vertical plane of 0.597λ mast over New Jersey soil. Solid curve—Ballantine's measurement of WABC (western side). Dotted curve—Calculated for empirical distribution based on Gihring and Brown's measurements.*

Current Distribution in the Array Towers

As this current distribution of Gihring and Brown checks so well with Ballantine's measurements, and as it also checked with measurements of Gihring and Brown on another such radiator, it seems safe to assume that this distribution will be valid generally for this type of 0.597λ tower.

As regards the current distribution in the quarter-wave tower used as the reflector, calculations by the above method show that the difference in the shape of the field strength curves of a quarter-wave tower and of a quarter-wave wire is slight. Hence sinusoidal current distribution is assumed in the quarter-wave reflector.

Calculations for the Array

Assume that the 0.25λ reflector with current distribution $I'(x)$, height l', is placed a distance d from the 0.597λ radiator with current distribution $I(x)$, height l : x' is the variable distance up the reflector from the ground; x is the variable distance up the radiator. Assume also that the quarter-wave tower is fed $\phi°$ in phase ahead of the other tower.

Then in the vertical plane containing the array

$$dE_\theta = \frac{2\pi}{cr_0\lambda} I'(x)\,dx' \sin\theta \left[\cos\frac{2\pi}{\lambda}(ct - r_0 + x'\cos\theta + d\sin\theta + \phi) + R\cos\frac{2\pi}{\lambda}(ct - r_0 - x'\cos\theta + d\sin\theta + \phi)\right]$$

$$+ \frac{2\pi}{cr_0\lambda} I(x)\,dx \sin\theta \left[\cos\frac{2\pi}{\lambda}(ct - r_0 + x\cos\theta) + R\cos\frac{2\pi}{\lambda}(ct - r_0 - x\cos\theta)\right].$$

Letting

$$a = \frac{2\pi x}{\lambda}\cos\theta \qquad b = \frac{2\pi}{\lambda}(d\sin\theta) + \phi$$

and rearranging, the following expressions are obtained

$$\frac{dE_\theta}{\sin\theta} \propto \cos\frac{2\pi}{\lambda}(ct - r_0)\left\{\begin{array}{l}(R+1)\,[I(x)\cos a\,dx + \cos b\,I'(x)\cos a'\,dx'] \\ \quad + (R-1)\,[\sin b\,I'(x)\sin a'\,dx']\end{array}\right\}$$

$$+ \sin\frac{2\pi}{\lambda}(ct - r_0)\left\{\begin{array}{l}(R+1)\,[-\sin b\,I'(x)\cos a'\,dx'] \\ \quad +(R-1)\,[\cos b\,I'(x)\sin a'\,dx' + I(x)\sin a\,dx]\end{array}\right\}$$

$$E_{\theta\ r.m.s.} \propto \sin\theta \sqrt{\left\{\begin{array}{l}(R+1)\left[\displaystyle\int_0^l I(x)\cos a\,dx + \cos b\int_0^{l'} I'(x)\cos a'\,dx'\right] \\ \quad + (R-1)\left[\sin b\displaystyle\int_0^{l'} I'(x)\sin a'\,dx'\right]\end{array}\right\}^2 + \left\{\begin{array}{l}(R+1)\left[-\sin b\displaystyle\int_0^{l'} I'(x)\cos a'\,dx'\right] \\ \quad + (R-1)\left[\cos b\displaystyle\int_0^{l} I'(x)\sin a'\,dx' + \int_0^l I(x)\sin a\,dx\right]\end{array}\right\}^2}$$

where $l = 0.597\lambda$ and $l' = 0.25\lambda$

Constants for the Array

For purposes of calculation the following constants were assumed:—frequency, 700 kilocycles; ground conductivity, 10^{-13} e.m.u.; ground dielectric constant, 14 e.s.u.

The current distribution in the 0.597λ mast was taken to be the empirical distribution of Fig. 4 based on the experimental measurements of Gihring and Brown. That is,

$$I(x) = \frac{I_{\text{Loop}}}{2}\left[1 + \sin\frac{2\pi}{\lambda_0}\left(x - \frac{\lambda_0}{10}\right)\right]$$

where $\lambda_0 \equiv 0.716\lambda$.

The sinusoidal distribution assumed in the 0.25λ tower is

$$I'(x) = I'_{\text{Loop}}\left[\sin\frac{2\pi}{\lambda}\left(\frac{\lambda}{4} - x'\right)\right].$$

In order to select the spacing d and phasing ϕ, it is necessary to decide on the zenith angle at which minimum radiation is desired. Assuming that 70° is the angle, then a likely choice of array constants is

$$d = \frac{\lambda}{4}\operatorname{cosec} 70° \qquad \phi = 90°.$$

The remaining array constant, the ratio of the loop currents, is decided after introducing all the above values into the array equation. A good minimum is then seen to be possible for the quarter-wave loop current equal to 1.5 times the 0.597 wave loop current.

Comments on Results of Array Calculations

The relative values of E_θ for the above conditions have been calculated for every 10° zenith angle. The resulting curve is given in Fig. 7. This gives the field strength distribution in the vertical plane passing through the array.

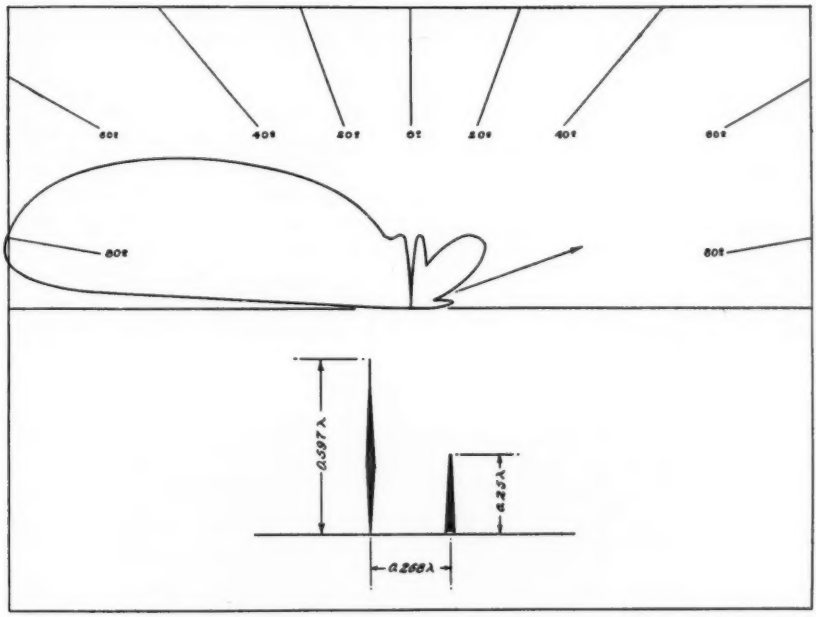

FIG. 7. *Field strength distribution in the vertical plane parallel to an array comprised of a 0.597λ double-tapered tower with a quarter-wave self-supporting tower as a fed reflector.*

CONDITIONS

Frequency: = 700 kc.
Soil constants: $\sigma = 10^{-13}$ e.m.u.
$\epsilon = 14$ e.s.u.
Current distribution in 0.597λ mast:

$$I(x) = \frac{I_{\text{Loop}}}{2}\left[1 + \sin\frac{2\pi}{\lambda_0}\left(x - \frac{\lambda_0}{10}\right)\right]$$

where $\lambda_0 = 0.716\lambda$.
Current distribution in 0.25λ mast:

$$I'(x) = I'_{\text{Loop}}\left[\sin\frac{2\pi}{\lambda}(l - x)\right].$$

ARRAY CONSTANTS

Spacing: $\frac{\lambda}{4}$ sec. 20°

Phasing: 0.25λ mast current 90° ahead of that of 0.597λ mast.

Current ratio: 0.25λ loop current = 1.5 of 0.597λ loop current.

Fig. 8 gives the distribution in the vertical plane perpendicular to the plane of the array. In this case d is zero.

Returning to Fig. 7, it is seen that almost complete extinction has been achieved at 70°, and in fact from 60° to 85° zenith angle the radiated power is very small. This broad minimum is advantageous as it would take care of variations in the height of the Heaviside layer, the average height being used

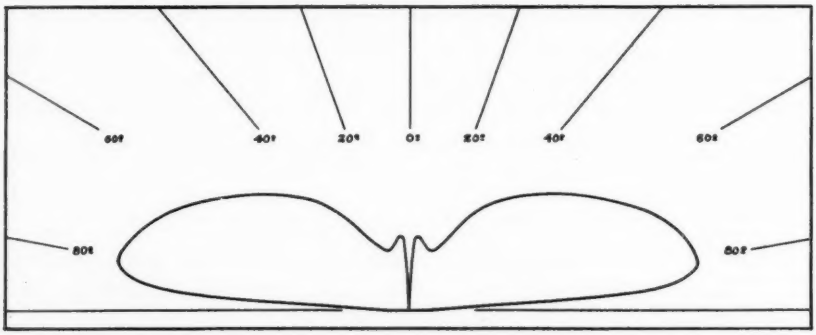

FIG. 8. *Field strength distribution in vertical plane perpendicular to the above array.*

to determine the zenith angle at which minimum radiation should occur. The large lobe at 45° would be expected to intersect the earth's surface about 200 miles away. Severe fading would occur about 100 miles from the high powered station. In the other directions it is seen that the polar pattern differs from that of the single mast in that there is relatively more high angle radiation.

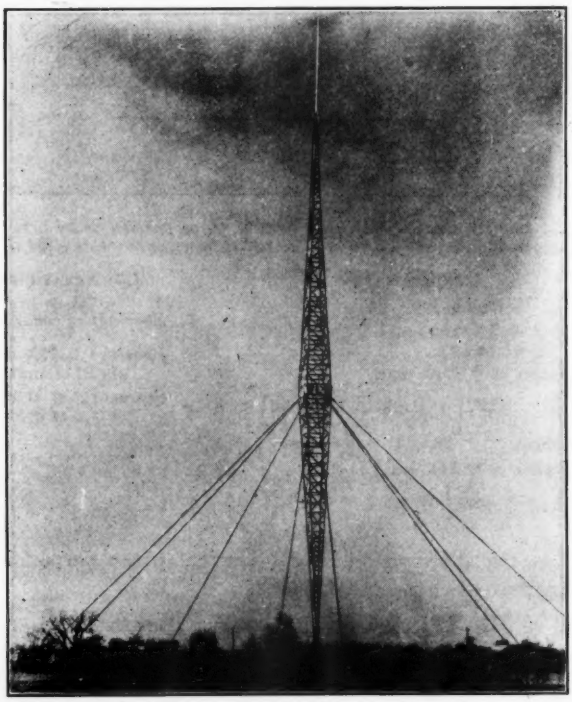

A typical double-tapered mast. The 828 ft. Blaw-Knox mast at WLW, the Crosley Radio Corporation, Cincinnati, Ohio.

Conclusion

The calculations indicate that the array is efficacious in reducing the sky wave at zenith angles between 60° and 85°. The local coverage in the unfavored direction, however, is very unsatisfactory with the array constants chosen. Thus an increase in the ground wave and a decrease in the high angle lobe can be achieved by decreasing the ratio of the quarter-wave tower loop current to the 0.597 wave tower loop current. Other choices of spacing and phasing are also available.

It is concluded, therefore, that by a judicious choice of the three array constants a considerable reduction in the sky wave at remote distances can be achieved, whilst still maintaining fair local coverage in the unfavored direction.

Acknowledgment

The author wishes to acknowledge his indebtedness to Lieut.-Col. W. A. Steel, who suggested the problem, for his continued interest, and to Mr. J. A. Ouimet, for his assistance in some of the computations.

References

1. BALLANTINE, STUART. Proc. Inst. Radio Eng. 22 : 564-629. 1934.
2. GIHRING, H. E. and BROWN, G. H. Broadcast News, No. 13 : 4-9. 1934.
3. PIERCE, G. W. Electric oscillations and electric waves. Chap. IX. Sec. 85. McGraw-Hill Book Co., New York. 1920.
4. RODER, H. Proc. Inst. Radio Eng. 23 : 256-260. 1935.
5. VAN DER POL, BALTH and NIESSEN, K. F. Ann. Physik, 10 : 485-510. 1931.

Canadian Journal of Research

Issued by THE NATIONAL RESEARCH COUNCIL OF CANADA

VOL. 13, SEC. B. SEPTEMBER, 1935 NUMBER 3

THE ELECTROLYTIC PREPARATION OF ANTHRANILIC ACID[1]

BY J. W. SHIPLEY[2] AND J. M. CALHOUN[3]

Abstract

The electrolytic reduction of *o*-nitrobenzoic acid in alcoholic sulphuric acid at a lead cathode was investigated. The effect of various experimental conditions was studied and a maximum yield of 92% of amine obtained under favorable conditions. No evidence of the reduction of the carboxyl group was observed.

Introduction

The electrolytic reduction of *o*-nitrobenzoic acid has been studied only to a very limited extent. It has a theoretical interest because of the two unsaturated groups, the nitro and the carboxyl, since the presence of one, particularly in the ortho position, may influence the reduction of the other. The nitro group is reduced much more readily than the carboxyl and hence it should be possible, by regulation of the cathode potential, to reduce the nitro group while the carboxyl group is left intact, and so produce anthranilic acid. There is an additional interest in this reduction because of the commercial importance of anthranilic acid in the synthesis of indigo.

Löb (7) in 1896 reduced a solution of *o*-nitrobenzoic acid in sodium hydroxide solution, using platinum electrodes, and obtained a mixture of 50% of *o*-azoxybenzoic acid and 5–10% of *o*-hydrazobenzoic acid. A few years later Mettler (8) reported the reduction of both anthranilic acid and *o*-nitrobenzoic acid to *o*-aminobenzyl alcohol in 20–30% alcoholic sulphuric acid at a lead cathode at 20–30°C. with a current density of 6–12 amp. per sq. dm. Apparently both the nitro and carboxyl groups yielded to reduction.

The most recent work is due to Alvarez (1) who reported the preparation of anthranilic acid in 1928 by the electrolytic reduction of *o*-nitrobenzoic acid. Alvarez used as catholyte a solution of 60 gm. of *o*-nitrobenzoic acid in 20 cc. of alcohol and 100 cc. of sulphuric acid (20° Baumé). The anolyte was sulphuric acid (100 cc.) of the same concentration. Lead electrodes were used, the cathode being purified by electrolysis. A current of 8 amp. was passed for 7.5 hr. at a current density of 0.1 amp. per sq. dm. This corresponds to an excess of 4% of the quantity of electricity theoretically required.

[1] *Manuscript received April 9, 1935.*
Contribution from the Department of Chemistry, University of Alberta, Edmonton, Alberta, Canada.

[2] *Professor of Chemistry, University of Alberta.*
[3] *Honors Student, University of Alberta.*

It is difficult to understand how so low a current density could be used successfully since a cathode 40 sq. dm. in area would be required, which is much too large for the volume of solution. The solubility of *o*-nitrobenzoic acid in a solution of the same volume and composition was found to be less than 15 gm. even at 90° C., so that most of the depolarizer must have been in suspension, a condition notably inefficient. Alvarez does not mention the temperature used, whether the catholyte was stirred, or the yields obtained.

Since both Mettler and Alvarez used virtually the same experimental conditions, other than current density and temperature, with such widely different results, it was thought that a more thorough investigation of the reduction would be of value.

Experimental

It was decided to conduct the reduction with lead electrodes in acid solution. This procedure tends to favor amine formation, since lead is a metal of high hydrogen overvoltage, thus making complete reduction of the nitro group possible. The use of an acid, rather than an alkaline, electrolyte necessitates the addition of alcohol to dissolve the *o*-nitrobenzoic acid, but the formation of any azoxy and azo derivatives in the reduction is reduced to a minimum.

The apparatus in which the reduction was carried out consisted of a 600 cc. Pyrex beaker in which was placed a porous cup 10 by 5 cm. to serve as the cathode chamber. The cathode was a cylinder made of 1 mm. sheet lead which just fitted inside the porous cup and was rotated by a small motor. Electrical connection was made through a mercury seal.

The anode was a second lead cylinder which fitted inside the annular space between the porous cup and the walls of the beaker. A thermometer was suspended in the anode compartment. The beaker was insulated with asbestos and heat was applied by means of a controlled Bunsen burner. A d-c. generator supplied current at 5 amp. and 120 volts.

Before each reduction the cathode was specially treated according to the method of Tafel (10). After washing in 20% sodium hydroxide solution it was electrolyzed as the anode in 20% sulphuric acid for 30 min. at a current density of 2 amp. per sq. dm. It was then washed with water, immersed in boiling water for several minutes, dipped in alcohol and air dried. The effect of this treatment was to free the cathode from traces of metallic impurities which would lower the hydrogen overvoltage and render it useless for a vigorous reduction. In addition the cathode surface was covered with a layer of oxide which in the first few minutes of the run was reduced to a thin membrane of spongy lead. According to Brockman (4), the spongy lead has a catalytic effect on the reduction.

The *o*-nitrobenzoic acid was obtained from two sources: One, a c.p. commercial product, melted at 146–146.5° C. (corr.) and the second, prepared in the laboratory by the oxidation of *o*-nitrotoluene with potassium perman-

ganate by the method of Reimer and Gatewood (9), melted at 146.5–147° C. (corr.). The melting point of *o*-nitrobenzoic acid reported in the literature (6) is 147.5° C.

Analytical

The amount of amine produced in the reductions was determined by the titration of an aliquot portion of the reduction product with 0.05 *M* sodium nitrite solution, using potassium iodide-starch paper as indicator. The sodium nitrite solution was standardized against potassium permanganate and checked against pure anthranilic acid. It was found, in agreement with Bradt and Frost (2), that the permanganate method gave a value slightly too high.

The diazotization was carried out at 5–10° C. A 25 cc. aliquot was diluted to 50 cc. with water and 3 cc. of hydrochloric acid added. Standard sodium nitrite was then run in until a drop of the solution touched to the potassium iodide-starch paper indicated the end point. It was necessary to add the sodium nitrite slowly because of a slight lag in the establishment of the end point. Later it was found that the use of 0.1 *M* sodium nitrite and a larger aliquot gave a more satisfactory end point.

Effect of Temperature

The procedure followed was similar to that described by Bradt and Hart (3) for the electrolytic preparation of 3-amino-4-hydroxytoluene. The effect of different experimental conditions on the yield of amine was determined by making series of reductions, varying only one condition at a time.

The effect of temperature is shown in Table I and Fig. 1. It will be noted that the yield of amine increases with the temperature to a maximum of 88% at 80° C. At higher temperatures the yield drops off slightly owing to the proximity of the boiling point (92° C., 700 mm.) and the fact that *o*-nitrobenzoic acid is slightly volatile.

At temperatures between 40° and 80° C. the curve obtained (Fig. 1) is virtually a straight line, indicating that the yield of amine is directly proportional to the temperature. This is analogous to purely chemical reactions. At temperatures progressively lower than 40° C. the yield of amine rapidly drops off, owing to the fact that the *o*-nitrobenzoic acid was not completely soluble, a portion of it remaining in suspension.

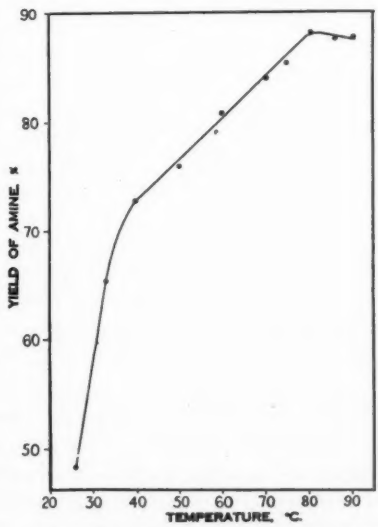

FIG. 1. *Effect of temperature on yield of anthranilic acid.*

TABLE I

EFFECT OF TEMPERATURE

Temp., °C.	E.m.f. across cell after 10 min., volts	Av. time during which H_2 was evolved, %	Yield of amine, %	Av. yield of amine, %
26	4.1	100	48.3	48.3
33	3.2	73	65.5	65.5
40	3.0 3.1	51	72.6 73.0	72.8
50	3.2 3.4	30	75.8 76.4	76.1
60	3.0 2.8	30	81.6 80.5	81.0
70	3.1 3.1	28	84.4 84.0	84.2
75	3.0 3.2 3.0	25	85.3 85.1 85.5	85.3
80	2.8 2.6 3.0 3.0 2.9	24	88.9 88.8 87.5 87.5 88.2	88.2
86	3.2 3.0	24	87.3 87.9	87.6
90	3.0 2.9	23	88.3 87.1	87.7

Cathode, lead cylinder 2.5 by 6 cm. Anode, same, 6 by 3 cm. Catholyte, 2.000 gm. o-nitrobenzoic acid, 40 cc. of 96% ethanol, 80 cc. of 25% sulphuric acid. Anolyte, 300 cc. of 25% sulphuric acid. Rate of stirring, about 150 r.p.m. Quantity of electricity, 1.926 amp.-hour (theoretical quantity of electricity calculated for the complete reduction of NO_2 to NH_2 in 2 gm. of o-nitrobenzoic acid). Cathodic current density, 2.0 amp. per sq. dm. (both sides).

The evolution of hydrogen represents a loss in current efficiency (current efficiency and yield of amine are equivalent when the theoretical quantity of electricity, in this case, 1·926 amp.-hr., is passed through the solution). Column 3, Table I, shows that the time during which hydrogen is evolved decreases as the temperature and efficiency rise. At 26° C. hydrogen is evolved during the entire reduction period, while at 80° C. evolution occurred only during the last quarter of the period. At the lower temperatures the velocity of reduction is not sufficiently great to absorb all the hydrogen as rapidly as it is produced. This results in greater evolution of hydrogen and lowered current efficiency. It is therefore probable that in the experiments at lower temperatures, the material unaccounted for in the analysis is unreduced *o*-nitrobenzoic acid and not products of secondary reactions.

Effect of Current Density

Table II and Fig. 2 show the effect of cathodic current density on yield of amine. At current densities greater than 5 amp. per sq. dm. it was necessary to use a smaller cathode, since the maximum current available was 5 amp.

TABLE II

EFFECT OF CURRENT DENSITY

Cathodic current density, amp./dm.²	E.m.f. across cell after 10 min., volts	Av. time during which H_2 was evolved, %	Yield of amine, %	Av. yield of amine, %
0.5	2.3	9	88.3	88.3
	2.6		89.8	
	3.6		90.3	
1.0	3.4	13	87.6	88.9
	2.5		88.5	
	2.6		88.8	
	2.6		88.9	
1.5	2.6	18	87.7	88.5
	2.7		88.9	
*2.0		24		88.2
	2.6		89.6	
2.25	2.8	26	88.2	88.1
	2.8		86.6	
	2.9		88.3	
2.5	3.0	26	86.4	88.2
	3.0		90.0	
3.0	3.7	25	87.2	87.3
	3.0		87.3	
4.0	4.0	35	86.0	86.1
	3.9		86.2	
5.0	3.9	61	85.4	85.4
	3.0		85.4	
**6.0	3.4	28	84.0	84.2
	3.9		84.3	
**8.0	4.1	42	81.1	80.5
	3.6		79.8	
**10.0	4.8	57	77.6	77.6

Temp., 80°C. Other conditions as given in Table I.
**See Table I for details. **Cathode 2.5 by 3 cm.*

A maximum yield of 89% was obtained at a current density of 1 amp. per sq. dm. At a lower current density a smaller yield resulted, probably owing to the longer time required for the reduction, which would permit loss of *o*-nitrobenzoic acid by diffusion to the anode chamber. Increase in current density resulted in an increase in the amount of hydrogen evolved and a corresponding decrease in efficiency.

It should be pointed out that current density measurements are only approximate at best. This is because the effective area depends on the condition of the surface of the metal, which is impossible to measure or duplicate exactly. However, for a given current the apparent surface area is a useful measure of the current density.

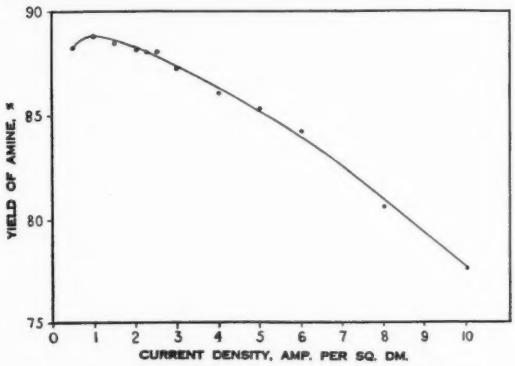

FIG. 2. *Effect of current density on yield of anthranilic acid.*

Effect of Electrolyte Composition

The data showing the effect of electrolyte composition on yield of amine are given in Table III. In each case the anolyte consisted of sulphuric acid of the same concentration as that used in the catholyte. It was found that one

TABLE III

EFFECT OF ELECTROLYTE COMPOSITION

Catholyte composition	E.m.f. across cell after 10 min., volts	Av. time during which H_2 was evolved, %	Yield of amine, %	Av. yield of amine, %
25 cc. alcohol; 100 cc. 25% H_2SO_4	2.9	17	86.8	86.8
*80 cc. alcohol; 40 cc. 25% H_2SO_4	3.0	31	83.8	83.8
40 cc. alcohol; 80 cc. 2% H_2SO_4	3.3	23	85.4	85.4
40 cc. alcohol; 80 cc. 5% H_2SO_4	2.9	15	90.2	90.0
	3.0		89.8	
40 cc. alcohol; 80 cc. 10% H_2SO_4	2.7	16	89.8	89.6
	2.7		89.3	
40 cc. alcohol; 80 cc. 15% H_2SO_4	3.0	16	88.8	88.8
40 cc. alcohol; 80 cc. 25% H_2SO_4		24		88.2
40 cc. alcohol; 80 cc. 35% H_2SO_4	2.9	33	85.1	85.1

Temp., 80°C. (except where otherwise stated). Other conditions as given in Table I.
**Temp., 75° C.*

part of 96% alcohol in the catholyte to two parts of sulphuric acid solution gave the best results. A decrease in the amount of alcohol lowered the solubility of *o*-nitrobenzoic acid, and an increase lowered the boiling point of the solution, necessitating the use of a lower temperature.

The optimum concentration of the sulphuric acid solution was between 5 and 10%, and resulted in a yield of 90% of amine. A lower concentration of acid resulted in a marked decrease in yield, owing to the increased resistance of the electrolyte. At higher concentrations of acid the lowered efficiency was considered to be due to an increase in side reactions, such as condensations or rearrangements favored by the high acidity. This was borne out by the fact that the reduction product was colored a bright red, indicating the presence of azoxy or azo compounds.

Effect of Concentration of o-Nitrobenzoic Acid

Table IV shows the effect of the concentration of *o*-nitrobenzoic acid on the yield of amine. The optimum concentration was found to be 2 gm. in 120 cc. of solution (about 0.1 *M*). At lower concentrations, diffusion of

TABLE IV

EFFECT OF CONCENTRATION OF *o*-NITROBENZOIC ACID

Weight of *o*-nitrobenzoic acid, gm.	E.m.f. across cell after 10 min., volts	Av. time during which H_2 was evolved, %	Yield of amine, %	Av. yield of amine, %
1.000	3.0 3.0	31	85.2 84.8	85.0
2.000	2.7 2.7	16	89.8 89.3	89.6
4.000	3.3 3.1	13	87.0 89.1	88.1
6.000	2.8	10	87.3	87.3

Temp., 80°C. Catholyte: 40 cc. of 96% alcohol, 80 cc. of 10% sulphuric acid. Anolyte: 300 cc. of 10% sulphuric acid. Other conditions as given in Table I.

o-nitrobenzoic acid to the cathode surface was not rapid enough, and hydrogen was evolved for 30% of the total time, resulting in a lowered efficiency. The efficiency probably could be increased by stirring the solution more rapidly.

Increasing the concentration of *o*-nitrobenzoic acid decreased the amount of hydrogen evolved, but there was not a corresponding increase in material yield when concentrations greater than 2 gm. were used. This may be due to the longer time required for reduction, which permits loss of *o*-nitrobenzoic acid by diffusion or volatilization.

Effect of Quantity of Current Passed Through the Solution

Since yield of amine is more important than current efficiency it was desirable to determine whether an excess of the theoretical quantity of electricity (1.926 amp.-hr.) would increase the yield of amine. The results are given in Table V.

TABLE V

EFFECT OF QUANTITY OF CURRENT PASSED THROUGH THE SOLUTION

Per cent theoretical current (1.926 amp.-hr.)	E.m.f. across cell after 10 min., volts	Time during which H_2 was evolved, %	Yield of amine, %	Av. yield of amine, %	Av. current efficiency, %
85	2.7 2.7	5	78.1 78.7	78.4	92.2
100	2.7 2.7	16	89.8 89.3	89.6	89.6
125	2.8 2.8	34	90.3 92.3	91.3	73.0

Temp., 80°C. Catholyte: 2.000 gm. of o-nitrobenzoic acid, 40 cc. of 96% alcohol, 80 cc. of 10% sulphuric acid. Anolyte: 300 cc. of 10% sulphuric acid. Other conditions as given in Table I.

When 85% of the theoretical quantity of electricity had been passed through the solution, very little hydrogen evolution had taken place. This resulted in high current efficiency but low material yields. After 100% of the theoretical quantity of electricity had been passed through, the material yield had considerably increased, indicating that reduction continued after hydrogen evolution began. When an excess of 25% had been passed through, the yield of amine had increased only slightly, and at the expense of a large decrease in current efficiency.

Effect of Cathode Surface

The velocity of reduction, and hence the yield of amine, depends to a large extent on the nature of the cathode surface. In an attempt to increase the yield, a coating of sponge lead was deposited on the cathode according to the directions of Bradt and Hart (3).

Lead monoxide (20 gm.) and sodium hydroxide (100 gm.) were dissolved in water to give a 300 cc. solution and the lead cylinder electrolyzed as cathode for about five minutes at a current density of 5 amp. per sq. dm. It was then washed with water, dilute sulphuric acid, and again with water. This procedure gave a very rough spongy surface.

TABLE VI

EFFECT OF CATHODE SURFACE

Cathode surface	E.m.f. across cell after 10 min., volts	Av. per cent time during which H_2 evolved	Yield of amine, %	Av. yield of amine, %
Smooth	2.7	16	89.8 89.3	89.6
Spongy	2.6	9	91.4 92.5	92.0

Temp., 80°C. Catholyte: 2.000 gm. of o-nitrobenzoic acid, 40 cc. of 96% alcohol, 80 cc. of 10% sulphuric acid. Anolyte: 300 cc. 10% sulphuric acid. Other conditions as given in Table I.

The results are shown in Table VI. The smooth cathode was prepared by anodic electrolysis as previously described. It is evident that an increase in yield of more than 2% is obtained with a spongy lead cathode, and at the same time the amount of hydrogen evolved is less. The effect of a spongy surface is in reality to lower the effective current density by increasing the surface area available to the depolarizer. The use of a spongy surface is more effective than decreasing the current strength, since the spongy surface does not require a longer time for the reduction, as would be the case with a plain cathode and a low current strength.

Separation of Reduction Products

Anthranilic acid was separated when desired from the combined products of a number of reductions. The solution was neutralized with an excess of sodium carbonate and the alcohol distilled off. It was then made slightly acid with acetic acid, filtered, and the filtrate extracted with ether.

The residue from the ether extraction was recrystallized from hot water, using animal charcoal for decolorizing. A white crystalline product which melted at 146° C. (corr.) was obtained, the acetyl derivative of which melted at 184.5° C. (corr.). The melting points reported in the literature (6) are: anthranilic acid, 145° C. and *o*-acetylaminobenzoic acid, 185° C.

An attempt was made to identify any *o*-aminobenzyl alcohol by the method of Mettler (8). The alkaline residue from the distillation of the alcohol was saturated with ammonium sulphate and extracted with ether. The ether layer yielded nothing but a trace of resinous material, indicating the absence of *o*-aminobenzyl alcohol. Ether extractions in acid solution yielded nothing but small amounts of unchanged *o*-nitrobenzoic acid.

The results of analysis show that anthranilic acid represented the major portion of the reduction product. However, the color of the solutions, which varied from pale yellow to cherry red, indicated the presence of other compounds, probably azoxy or azo derivatives, but in quantities too small to separate and indentify.

Discussion

The electrolytic reduction of *o*-nitrobenzoic acid in dilute alcoholic sulphuric acid at a lead cathode, under favorable conditions, has been shown to yield anthranilic acid in yields of more than 90%. The reaction may be represented by the equation:

$$NO_2.C_6H_4.COOH + 6H^+ + 6e = NH_2.C_6H_4.COOH + 2H_2O$$

It is assumed that the mechanism is analogous to that suggested by Haber (5) for the electrolytic reduction of nitrobenzene.

It is evident that under the foregoing experimental conditions the intensity of reduction was not sufficiently great to reduce appreciably the carboxyl group. It is possible that at a higher current density and lower temperature the formation of *o*-aminobenzyl alcohol as reported by Mettler (8) would be

favored. However, the vigorous evolution of hydrogen at the completion of the reduction of the nitro group in the authors' experiments indicates that little, if any, additional reduction is taking place.

The maximum yield of amine obtained was 92%. The remaining 8% of material may be accounted for in loss by volatilization and diffusion to the anode chamber, by the fact that a small amount of *o*-nitrobenzoic acid remained unchanged and by the formation of products of various side reactions, such as azoxy and azo derivatives. It is not impossible that even higher yields of amine might be obtained. The addition of *o*-nitrobenzoic acid in successive portions as the reduction progresses and a decrease in the current density towards the end of the reduction, with perhaps the use of a small excess of current, would be expected to cause an increase in the amount of *o*-nitrobenzoic acid reduced. The use of addition agents or hydrogen carriers might also increase the yield. More rapid stirring might be advantageous, although, when the depolarizer is in solution, the effect of stirring at a rate greater than a certain minimum is small. Bradt and Hart (3) found that, in the electrolytic reduction of 3-nitro-4-hydroxytoluene, an increase of only 0·8% in the yield of amine was obtained when the rate of stirring was varied between 0 and 2000 r.p.m. after complete solution of the nitrocresol.

The limitations of the experimental results are considered to be chiefly analytical. The standardization of sodium nitrite by potassium permanganate gives values slightly too high, while the lag in the endpoint gives values slightly too low. Manipulative errors are due chiefly to the lack of an automatic temperature control and loss of solvent by vaporization. The use of a closed cell, fitted with a return condenser, and an automatic electrical heating device would be more satisfactory. The fact that more than 100 reductions were satisfactorily carried out shows that the process is highly successful if sufficient care is taken in the preparation of the cathode.

References

1. Alvarez, L. B. Mon. farm. therap. 34 : 121-122. 1928.
2. Bradt, W. E. and Frost. Dissertation. Univ. of Cincinnati. 1928.
3. Bradt, W. E. and Hart, E. J. Trans. Am. Electrochem. Soc. 60 : 205-216. 1931.
4. Brockman, C. J. Electro-organic chemistry. John Wiley and Sons. New York. 1926.
5. Haber, E. Z. Elektrochem. 4 : 506-514. 1898.
6. International Critical Tables. Vol. I. Pp. 207, 210, 226. 1st ed. McGraw-Hill Book Company. New York. 1926.
7. Löb, W. Z. Elektrochem. 2 : 529-534. 1896.
8. Mettler, C. Ber. 38 : 1745-1753. 1905.
9. Reimer, M. and Gatewood, E. S. J. Am. Chem. Soc. 42 : 1475-1478. 1920.
10. Tafel, J. Ber. 33 : 2209-2224. 1900.

THE SORPTION OF DIMETHYL ETHER ON ALUMINA[1]

By J. Edwards[2] and O. Maass[3]

Abstract

The sorption of dimethyl ether on alumina has been investigated at pressures from 0.5 to 52 atm., the critical pressure, over the temperature range 25–135° C. The results are comparable to those for the propylene–alumina system. No discontinuity in the sorption accompanies the transition of sorbate from vapor to gas at the critical temperature; this differs from the previous results for the liquid-to-gas change. The initial stages of the sorption involve the formation of a monomolecular layer followed, with increasing pressure, by a multimolecular layer of increasing depth. It is unlikely that condensation to liquid occurs in the pores except at high relative pressures. The increase in critical temperature of such a liquid must be exceedingly great to account for the continuous form of the isobars up to 135° C.

Introduction

Although there has been a great deal of experimental work done on the adsorption of vapors and gases by solids, relatively little has been carried out at pressures greater than atmospheric. Since the leading hypotheses regarding the nature of this phenomenon differ mainly in their predictions of the extent of adsorption in this region, data for a number of systems are highly desirable.

A recent contribution by Morris and Maass (9) on the adsorption of propylene by alumina contained data for a wide range of pressures including the critical one, and for a temperature range of 20–100° C. The interesting behavior of the system accompanying the transition of sorbate from liquid to gas led to further work in the critical region, and the results for the system dimethyl ether–alumina were recently published (5). These results dealt with the sorption of the liquid phase (below the critical temperature), and of the "persistent liquid phase" (above the critical temperature).

In the present paper the results obtained for the sorption of dimethyl ether on alumina from 0.5 to 52 atm., the critical pressure, are given for the temperature range 25–135° C. The sorption was measured throughout with the sorbate definitely in the vapor or gaseous state. While the previous paper (5) was of interest primarily for the information given regarding the critical phenomena, the present paper deals with the nature of the sorption process over a pressure range including high pressures.

Experimental

Alumina, prepared according to the method of Munro and Johnson (10), was selected as sorbent on account of its high porosity and rigid structure. In view of the well known physical properties of dimethyl ether at high pressures, and of its suitable critical constants which permit the use of glass

[1] *Manuscript received March 16, 1935.*
Contribution from the Physical Chemistry Laboratory, McGill University, Montreal, Canada.

[2] *Demonstrator in Chemistry, McGill University.*
[3] *Macdonald Professor of Physical Chemistry, McGill University.*

apparatus, this substance was chosen as sorbate. The sample used throughout the present investigation was prepared and purified as described by Tapp, Steacie and Maass (16).

The apparatus employed was similar to that used by Morris and Maass (9), differing only in dimensions and thermostatic control, modified on account of the higher temperatures employed.

The McBain-Bakr balance had a sensitivity of 0.00376 gm. per mm. extension, a normal length of 57.66 mm.; the maximum load was 0.45 gm. The cathetometer used permitted weight measurements to within ± 0.0004 gm.

The calculation of the sorption has been fully described elsewhere (5, 9). No correction was made for the buoyant effect of the quartz spiral itself, since under the conditions of the experiments this factor seldom exceeded 0.0001 gm., the greatest error being 0.00017 gm.

Results

Sorption is given in the usual form, x/m, where x is the number of grams sorbed per m grams of sorbent.

Although the sorption at low relative pressures appeared to reach an equilibrium value within the time necessary for the gel to attain thermal equilibrium with the container, longer times were often necessary at high relative pressures before no further extension of the spiral could be detected. In such cases there appeared to be no systematic behavior that could be used as a measure of the rate of sorption in its final stages. The nature of the apparatus does not permit mesaurements of sorption rates to be made throughout the whole course of the process.

The density of the vapor surrounding the sorbent was obtained from the data of Cardoso and Coppola (3). The determination of the densities at relative humidities less than 100% was made by assuming a linear relation between density and temperature at constant pressure. The error involved in this assumption was negligible at low pressures, and at high pressures was not serious, since in these cases the temperature range over which the calculations were made was small. In the region approaching the critical, the more recently obtained density values of Tapp, Steacie and Maass (16) were used. Pressure values were taken from the vapor pressure curve for dimethyl ether obtained by Cardoso and Bruno (2).

The values in Table I, selected from approximately 250 readings, indicate the manner in which the sorption varied with the temperature and pressure. The corresponding isobars and isotherms are illustrated graphically in Figs. 1, 2 and 3. In Fig. 3, in which the sorption has been plotted against the relative pressure, P/P_s, there is some uncertainty in the form of the curves near the saturation value. In the cases where the extrapolation was short it was considered justifiable to indicate the probable endpoint, though a

TABLE I

SORPTION OF DIMETHYL ETHER (x/m) ON ALUMINA AT VARIOUS TEMPERATURES AND PRESSURES

Gel temp., °C.	Pressure, atm.					
	0.45	3.9	19.0	27.5	38.5	45.6
30	0.0192	0.0338				
40	0.0176	0.0287				
50	0.0142	0.0244				
60	0.0123	0.0209				
70	0.0106	0.0182				
80	0.0084	0.0156				
90	0.0053	0.0127	0.0242			
100	0.0036	0.0098	0.0192	0.0292		
110	0.0023	0.0078	0.0159	0.0228		
115	0.0020	0.0072	0.0140	0.0203	0.0320	
120	0.0017	0.0066	0.0120	0.0184	0.0266	
124	0.0015	0.0063	0.0110	0.0167	0.0243	0.0310
126	0.0015	0.0062	0.0106	0.0158	0.0235	0.0290
128	0.0015	0.0061	0.0102	0.0132	0.0229	0.0277
130	0.0014	0.0060	0.0096	0.0145	0.0220	0.0268
135	0.0013	0.0058	0.0080	0.0136	0.0207	0.0252

sharper increase in $d(x/m)/d(P/P_s)$ has been found in some cases for other systems (1). However, the general form of the isotherms closely resembles that of the cellulose–water-vapor system curves (6) and of the active-silica –water,–benzene and –alcohol isotherms (13), in which cases the saturation value was approached in a manner similar to that indicated in Fig. 3. The point is of interest in that an estimation of the saturation value of the adsorption may yield important information regarding the pore volume of the sorbent. These data were utilized previously (5) in an attempt to consider the possibility that liquid might exist in the pores of the sorbent above the critical temperature of the sorbate in the bulk phase.

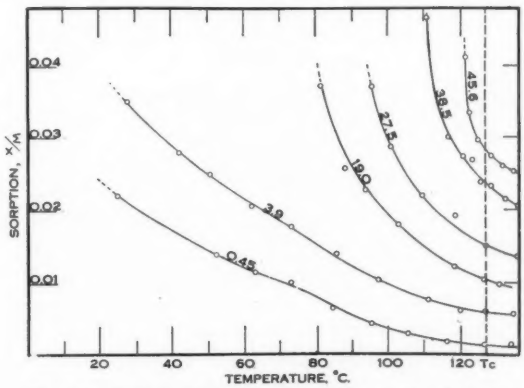

FIG. 1. *Isobars showing the sorption of dimethyl ether vapor and gas on alumina. Pressures in atmospheres.*

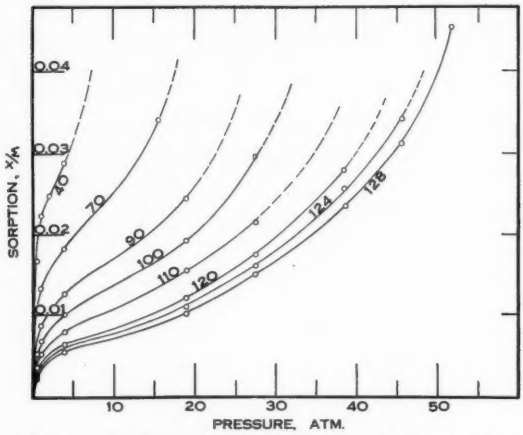

FIG. 2. *Isotherms showing the sorption of dimethyl ether on alumina. Temperatures in °C.*

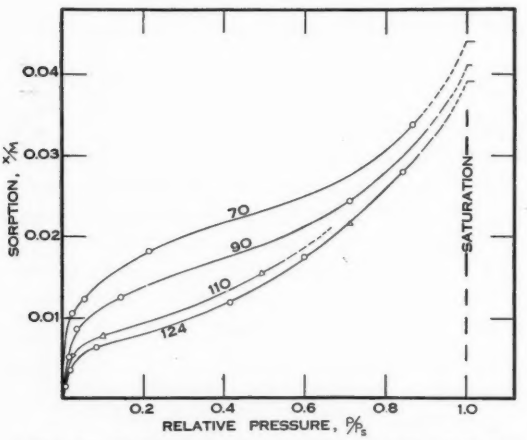

FIG. 3. *Isotherms showing the sorption of dimethyl ether on alumina. Temperatures in °C.*

Discussion

The form of the isobars and isotherms is similar in most respects to the forms of those of the propylene–alumina system. There is, however, a difference in the low-pressure region of the high-temperature isotherms: for the system propylene–alumina it is apparent that the first stage of the adsorption corresponds to the existence of a monomolecular layer forming a surface complex which is stable at high pressures throughout the temperature range studied, but which for low pressures breaks down at the higher temperatures. In the present system the slight inflections in the 0.45 and 3.9 isobars in the neighborhood of 80–100° C. indicate

a tendency toward destruction of the surface layer, but the extent of this decomposition appears insufficient to be particularly noticeable in the high-temperature isotherms. The isobars indicate however that, for lower pressures, the surface complex would probably be unstable within the temperature range studied. Although this difference in behavior might be attributed to a higher heat of adsorption of dimethyl ether than that of propylene, the slope of the isosteres plotted semilogarithmically does not indicate this to be so, and it is very probable that the difference can be attributed to a difference in the alumina gels used in the two investigations.

In general the S-shaped isotherms may be interpreted according to the method of Rideal (15), whereby the first part of the curve corresponds to a monomolecular layer followed by a multimolecular one which has been regarded by Polanyi (14) as a thick, compressed film, and by others (11) as condensation to liquid in the capillary tubes of the sorbent. It can be readily demonstrated that the first stages of the sorption process are characterized by the formation of a monomolecular layer, by testing the results according to the Williams-Henry formula (7, 17). The equation for the isostere is $(\log x/mP) = k_1/T + k_2$, and in Fig. 4 the results have been

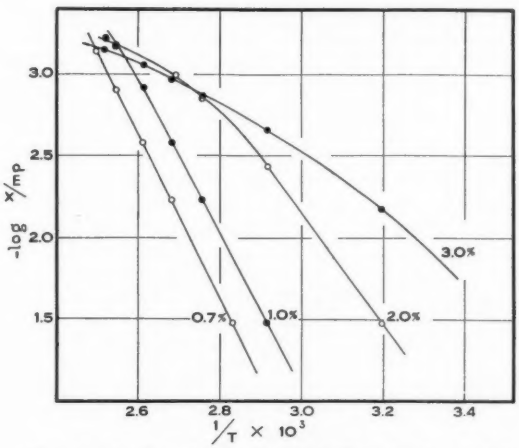

FIG. 4. *Isosteres for the dimethyl-ether–alumina system, plotted according to the Williams-Henry formula.*

represented for 0.7 to 3% sorption. The straight lines obtained in the 0.7% and 1% isosteres indicate that the sorption is exactly monomolecular, but for higher values of the sorption this is no longer true.

Following the region in which a monomolecular layer is formed, is the characteristic region of smaller slope, followed by the final region of increasing slope corresponding to a sorption tending toward saturation. From the point of view of the theory of capillary condensation, the isotherms of Fig. 3 indicate

that the sorption tends to become independent of temperature at the higher relative pressures, a condition predicted by the hypothesis. (When the volume, rather than the weight of sorbate, is taken into consideration, still better agreement is obtained, except in the case of those isotherms very near the critical temperature.) Thus at high relative pressures it appears probable that condensation of the sorbate to a liquid of density approximately that of the normal liquid does occur.

It will be noticed (Fig. 3) that the inflection in the curve, following which the sorption tends to saturation, occurs at relative pressures as low as 0.2. McBain has shown conclusively that the theory of capillary condensation must break down under these conditions, for the Kelvin equation for the lowering of the vapor pressure requires that the radius of the capillaries be of the order of molecular dimensions (8, pp. 436-442). It is singularly forced to regard molecules as in the liquid state when they are in immediate contact with the wall.

Further evidence not in complete agreement with Patrick's hypothesis may be obtained from Fig. 2. The isotherms above and below the critical temperature are identical in form, and indeed an isotherm at 136° C. shows no break in sorption. Similar results with the carbon-dioxide–charcoal system led Patrick *et al.* (12) to the belief that the surface tension of the liquid in the capillaries was considerably greater than that of the normal liquid, resulting in an increased critical temperature of the capillary liquid. While the partial pressures studied by Patrick were so small that capillary condensation would not be expected to occur, the study of the present system has been made over all possible pressures, and it is interesting to consider the results in the light of this hypothesis. On the basis of an increase in the critical temperature of liquid in the pores, the magnitude of this effect would depend on the pore size, so that the form of the sorption isobar at temperatures higher than the normal critical temperature would be dependent upon the frequency distribution of pore sizes in the gel. When the critical temperature of the liquid in the smallest capillaries had eventually been reached, the density of the sorbed material would become equal to that of the material in the normal bulk phase. Since this is a gravimetric method and corresponds exactly to the definition of sorption, in that the excess of material in the vicinity of the sorbent over that present in an equal volume of bulk phase is considered as the amount sorbed, then under the final temperature conditions mentioned above, sorption would become zero. The fact that, at temperatures higher than the normal critical temperature, the sorption isobars (Fig. 1) show no decrease in sorption in excess of that given by the normal temperature coefficient, indicates that the Patrick conception cannot hold. There appears then to be no adequate interpretation of the similarity in form of the isotherms at temperatures higher than, and lower than, the critical temperature, and it becomes evident that the theory of capillary condensation cannot account for the experimental results. Since the relative pressure isotherms, taken at temperatures lower than the critical temperature, gave

evidence at high values of the relative pressure that closely fits the requirements demanded by the theory, the possibility that the familiar S-shaped isotherms do not represent capillary condensation becomes apparent.

Substantiation of these results has been obtained by Morris and Maass (9), who demonstrated that even at a temperature of 15° C. higher than the critical temperature no change in the form of the isotherms took place. Coolidge (4) has recently extended the study of the carbon-dioxide–charcoal system to a high pressure range, and concluded that no break in the isotherm was apparent when the density of the sorbed phase itself was taken into account. A quantitative agreement with the Polanyi theory was obtained.

An interpretation of these results will await more complete data, and it is hoped that the study of other systems will be shortly carried out, and the behavior of these systems in the neighborhood of the critical temperature be compared with these and earlier results.

References

1. Bray, W. C. and Draper, H. D. Proc. Nat. Acad. Sci. 12 : 295-299. 1926.
2. Cardoso, E. and Bruno, A. J. chim. phys. 20 : 347-351. 1923.
3. Cardoso, E. and Coppola, A. A. J. chim. phys. 20 : 337-346. 1923.
4. Coolidge, A. S. and Fornwalt, H. J. J. Am. Chem. Soc. 56 : 561-568. 1934.
5. Edwards, J. and Maass, O. Can. J. Research, 12 : 357-371. 1935.
6. Filby, E. Ph.D. Thesis, McGill University. 1933.
7. Henry, D. C. Phil. Mag. 44 : 689-705. 1922.
8. McBain, J. W. The sorption of gases and vapours by solids. G. Routledge and Sons. London. 1932.
9. Morris, H. E. and Maass, O. Can. J. Research, 9 : 240-251. 1933.
10. Munro, L. A. and Johnson, F. M. G. J. Phys. Chem. 30 : 172-188. 1925.
11. Patrick, W. A. and McGavack, J., Jr. J. Am. Chem. Soc. 42 : 946-978. 1920.
12. Patrick, W. A., Preston, W. C. and Owens, A. E. J. Phys. Chem. 29 : 421-434. 1925.
13. Pidgeon, L. M. Can. J. Research, 12 : 41-56. 1935.
14. Polanyi, M. Trans. Faraday Soc. 28 : 316-333. 1932.
15. Rideal, E. K. An introduction to surface chemistry, 2nd ed. University Press, Cambridge. 1930.
16. Tapp, J. S., Steacie, E. W. R. and Maass, O. Can. J. Research, 9 : 217-239. 1933.
17. Williams, A. M. Proc. Roy. Soc. A 96 : 287-297. 1920.

THE VARIATION OF THE VISCOSITY OF GASES WITH TEMPERATURE OVER A LARGE TEMPERATURE RANGE[1]

By A. B. Van Cleave[2] and O. Maass[3]

Abstract

The coefficients of viscosity of ammonia, propylene, ethylene and methyl ether, over the temperature range 23 to −80° C., have been measured. A comparison is made between the present data and those of other authors for temperatures above 0° C. It is estimated that the authors' results are correct to 0.2% and have a relative accuracy of 0.1%. It is claimed that they are the most accurate data for the viscosity of gases at low temperatures to date.

The validity of a number of viscosity–temperature relations has been tested with the present data and those previously published (18, 20). In general, it is found that the equations of Sutherland and Jones hold at high temperatures but fail at low temperatures for substances such as carbon dioxide, sulphur dioxide, ammonia, methyl ether and propylene, which have viscosity–temperature curves that are convex to the temperature axis below room temperature. An empirical equation is suggested which adequately represents the variation of viscosity with temperature for these five gases over the temperature range 23 to −80° C. However, this relation fails at high temperatures for all gases, and even at low temperatures for substances such as hydrogen, air and ethylene.

It is pointed out that the viscosity–temperature curves for carbon dioxide, sulphur dioxide, ammonia, methyl ether and propylene each show a definite inversion or inflexion point. Below this inversion temperature the viscosity curves are convex to the temperature axis; above it they are concave to the temperature axis. In general, it seems that this inversion temperature bears a direct relation to the polarity of the molecule and to the critical temperature.

Introduction

This research is a continuation of the systematic investigation of the viscosity of gases carried out in this laboratory. The object of the work is to obtain sufficiently accurate data to test rigidly certain proposed equations for the variation of the viscosity of gases with temperature, as well as to test the validity of an equation of state which depends on viscosity measurements (6, 12).

Owing to the failure of the classical kinetic theory of gases to represent adequately the variation of viscosity with temperature, a number of modified relations have been suggested. Sutherland (19) was the first to realize that the mean free path of a molecule must vary with the temperature and, in correcting for this factor, he derived his well known relation.

$$\eta = \eta_0 \left(\frac{T}{T_0}\right)^{\frac{3}{2}} \frac{T_0 + C}{T + C} \quad , \tag{1}$$

where η is the coefficient of viscosity of a gas at the temperature T, η_0 is the viscosity of the gas at a standard temperature T_0, and C is a constant known as Sutherland's constant. This equation gave a fairly satisfactory representation of the variation of viscosity with temperature for a number of gases at high temperatures. However, the general failure of Sutherland's equation at low temperatures has been noted and discussed by Schmitt (15), Bestelmeyer (1) and Vogel (26).

[1] *Manuscript received March 22, 1935.*
Contribution from the Department of Chemistry, McGill University, Montreal, Canada.
[2] *Demonstrator, Department of Chemistry, McGill University.*
[3] *Macdonald Professor of Physical Chemistry, McGill University.*

Chapman (4), in a detailed mathematical treatment of the dynamics of an encounter, derived expressions for the viscosity, diffusivity and thermal conductivity of a gas without assuming any property of the molecules save that they be spherically symmetrical. When his formula is applied to molecules acting as attracting spheres, Sutherland's equation is obtained. When molecules are considered as point centres of repulsive or attractive forces varying inversely as the n^{th} power of the distance the relation

$$\frac{\eta}{\eta_0} = \left(\frac{T}{T_0}\right)^n \tag{2}$$

results. Kamerlingh Onnes and Weber (11) found that Equation (2) gave a much better representation of the variation of the viscosity of helium over a large temperature range than did Equation (1).

Jones (10) developed a relation between viscosity and temperature on the basis that molecules repel according to an inverse n^{th} power law and attract according to an inverse third power law. His formula may be written

$$\eta = \eta_0 \left(\frac{T}{T_0}\right)^{\frac{1}{2}} \frac{T_0^{\frac{n-5}{n-1}} + S}{T^{\frac{n-5}{n-1}} + S} \quad , \tag{3}$$

where S is a constant depending on the index n of the repulsive field. For Maxwellian molecules n becomes infinite and Equation (3) reduces to Equation (1). For molecules acting as point centres of force the constant S becomes zero and Jones' equation reduces to the form of Equation (2). Hence, Jones' equation is more general than any yet given. This equation contains two adjustable constants, and hence it is not possible to determine either uniquely, as was noted by Jones (10). In general, he finds Equation (3) to conform to the experimental results better than Sutherland's equation.

Cooper and Maass (6) found that an empirical equation of the type

$$\frac{\eta}{\sqrt{T}} = a + bT \, , \tag{4}$$

(where a and b are constants), represented the data of Sutherland and Maass (20) for the viscosity of carbon dioxide over a low temperature range. Stewart (17) found Equation (4) to fit his results for the viscosity of sulphur dioxide at low temperatures. It is to be noted that Equation (4) could be considered as the expanded form of the exponential equation

$$\frac{\eta}{\sqrt{T}} = Ae^{BT} \, , \tag{5}$$

in which all but the first two terms in the converging series have been neglected.

The application of the above formulas to the data obtained in this work will be discussed later. It may be mentioned here, however, that up to the present there has been no wholly satisfactory, universally accepted formula for expressing the observed relation of viscosity and temperature—particularly at low temperatures. It is therefore desirable to extend accurate data in this direction.

Experimental

The apparatus was essentially the same as that used by Stewart and Maass (18) and described in detail by Sutherland and Maass (20). Since the publication of the results of the viscosity of sulphur dioxide by Stewart and Maass (18), an entirely new viscosity apparatus has been assembled and found to give results consistent with the previous determinations (18, 20). The only change that has been made in the original apparatus is the addition of two 4 in. reading lenses to facilitate the reading of the oscillating image. The lenses have been arranged so that they may easily be moved in a horizontal direction between the observer and the scale. They are set at the extreme ends of the scale at the beginning of an experiment and gradually moved towards the centre as the magnitude of the oscillations decreases. This arrangement makes the moving image much clearer and is a great aid to the eyes of the observer.

Preparation and Purification of Materials

Ammonia, propylene, ethylene and methyl ether were selected for this work on account of the ease with which they may be prepared and purified, and also because accurate data for their viscosities at low temperatures have not previously been given.

Ammonia was condensed from a tank of very pure anhydrous material and then fractionated twice at low temperatures before being distilled into the apparatus. The purity of the ammonia was indicated by the fact that it could easily be frozen when surrounded by a bath of solid carbon dioxide and acetone.

Propylene was prepared by the dehydration of isopropyl alcohol over alumina at 365° C., and was purified by low temperature fractionation as described by Maass and Wright (13). The fractionations were repeated until the vapor pressure was constant.

Ethylene was condensed from a tank of 99.9% pure material and then subjected to a series of low temperature fractionations in the apparatus used in the purification of propylene.

Methyl ether from a tank of 99.9% pure material was fractionated twice at low temperatures and then distilled into the viscosity apparatus. Magnetic stirring was used during fractionations.

The apparatus was filled with gas at room temperature after it had been thoroughly flushed several times with the pure material. At least half an hour was allowed for the gas to come to the temperature of the bath before any measurements were made. At temperatures below the normal boiling point of the gas used, the pressure was reduced so as to be well below the known vapor pressure at that temperature. Since it is known that the viscosity of a gas is independent of its pressure (20), the results obtained at low pressures are comparable with those obtained at atmospheric pressure.

The apparatus was calibrated with dry air free from carbon dioxide, as previously described (18, 20), both before and after a series of experiments in order to ensure that no change in the apparatus had taken place either during the course of the flushing with the pure gas or while the experiments were being made. The value of the wire constant used was that determined experimentally be Stewart (17).

Results

Table I shows the results obtained for the coefficient of viscosity of ammonia, methyl ether, ethylene and propylene. Each value is the mean of three or four independent experiments. These results are shown graphically in Fig. 1.

TABLE I

RESULTS OF MEASUREMENTS OF THE VISCOSITY OF AMMONIA, PROPYLENE, ETHYLENE, AND METHYL ETHER

Temp., °C.	$\eta \times 10^7$	Temp., °C.	$\eta \times 10^7$	Temp., °C.	$\eta \times 10^7$	Temp., °C.	$\eta \times 10^7$
Ammonia				*Propylene*			
24.27	1022.8	−26.70	825.6	24.16	858.3	−38.75	670.4
10.85	967.7	−47.02	755.5	18.69	840.6	−55.63	623.6
4.75	944.1	−57.65	719.4	9.36	813.3	−60.70	611.9
0.43	928.9	−71.25	675.2	0.00	784.1	−70.89	582.6
−12.30	878.7			− 0.15	783.9	−75.70	572.4
				−11.79	750.0	−79.72	561.5
				−25.84	709.3		
Ethylene				*Methyl ether*			
23.35	1010.6	−38.00	802.5	22.90	899.4	− 8.67	797.4
17.18	990.7	−52.50	752.3	18.11	883.0	−23.39	755.2
11.23	969.6	−60.38	724.2	11.71	862.4	−41.16	703.0
− 0.07	932.2	−68.52	697.2	−0.13	824.7	−56.91	658.4
− 9.02	900.8	−80.86	652.1				
−22.59	856.0						

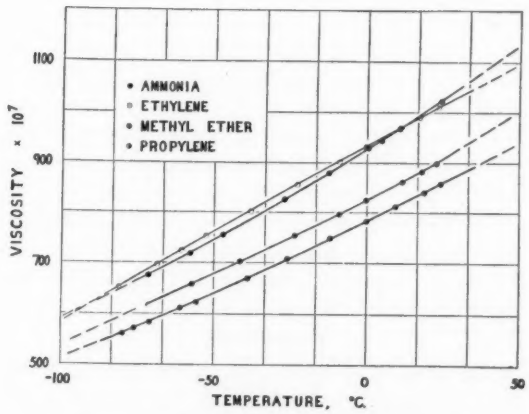

FIG. 1. *Variation of viscosity with temperature.*

Since measurements of the viscosity of gases at low temperatures are rare, comparisons between the present results and those of other authors can usually be made only at room temperature. Such comparisons are shown in Table II.

TABLE II

COMPARISON OF PRESENT RESULTS WITH THOSE OF PREVIOUS INVESTIGATORS

Gas	Temp., °C.	$\eta \times 10^7$		
		Observed in present work	Published previously	
Ammonia	25.1	1026	1002 Trautz and Heberling (22)	(1931)
	20.3	1007	982 Braune and Linke (2)	(1930)
	15.0	989	1005 Edwards and Worswick (7)	(1925)
	0.0	926	957 Graham (8)	(1849)
			918 Vogel (27)	(1914)
			950 Stackelbeck (16)	(1933)
	−77.1	656	680 Vogel (27)	(1914)
Propylene	20.0	845	835 Titani (21)	(1933)
	0.0	784	783 Titani (21)	(1933)
Ethylene	20.0	1000	1008 Trautz and Heberling (22)	(1931)
	0.0	932	966 Graham (8)	(1849)
			922 Obermayer (14)	(1875)
			961 Breitenbach (3)	(1901)
			907 Zimmer (29)	(1912)
			907 Titani (21)	(1933)
	−75.72	670	699 Zimmer (29)	(1912)
Methyl ether	20.0	889	1020 Graham (8)	(1849)
			910 Titani (21)	(1933)
	0.0	825	905 Graham (8)	(1849)
			850 Titani (21)	(1933)

Where there was no experimental value of viscosity for the temperature given by other authors, the observed values for the present work have been estimated from the curves in Fig. 1. Except for a few cases the agreement between the present results and those previously given is not good. The more recent data of Titani (21) and Trautz and Heberling (22) seem to be the most accurate. The present data for propylene and methyl ether check fairly well with those of Titani at room temperature. There is also good agreement between the authors' values and those of Trautz and Heberling (22) for ethylene. In the case of ammonia, however, agreement with these authors is not found. No doubt some of the discrepancies between the authors' values and those of the early workers in the field are due to the erroneous value for the viscosity of air assumed by them in their calculations. In Table II the results of Vogel (27) for the viscosity of ammonia have been corrected for this error.

Discussion

The present data, as well as those previously given (18, 20), will now be employed to test the validity of equations which represent the variation of viscosity with temperature.

It is interesting to make a comparison of Equations (1), (2), (4) and (5) for each of the gases for which low temperature data are available. The comparison over the approximate temperature range −80° to 30° C. has been made in the following manner. Experimental values of viscosity near the limits of the above-mentioned temperature range were selected and substituted in each of the four equations to obtain the values of the constants. With the constants thus determined the viscosity corresponding to some intermediate temperature, approximately in the centre of the temperature range, was calculated and compared with the experimental value. The results of these comparisons are summarized in Table III.

TABLE III

COMPARISON OF CALCULATED AND EXPERIMENTAL VALUES

Gas	Deviation of equation, %			
	(1)	(2)	(4)	(5)
Carbon dioxide	2.57	1.43	0.88	0.18
Sulphur dioxide	1.67	0.94	0.30	0.21
Ammonia	1.77	1.35	0.82	0.21
Methyl ether	1.14	0.87	0.60	0.35
Propylene	1.48	0.94	0.32	0.20
Mean deviation	1.72	1.10	0.58	0.23
Ethylene	0.19	0.39	0.97	1.55
Hydrogen	0.33	0.21	0.60	0.72
Air	0.30	0.45	1.28	1.73
Mean deviation	0.27	0.35	0.95	1.33

This summary shows that Equation (5) accurately represents the variation of viscosity with temperature in the temperature region in which the viscosity–temperature curve is convex to the temperature axis. In general, this seems to occur in the region well below the critical temperature. When the temperature–viscosity curve is concave to the temperature axis, Equation (5) fails entirely, whereas Equation (1) (Sutherland's equation) holds well over the temperature range selected. However, if a larger temperature range is selected Equation (1) also fails. In some cases Equation (2) might fit the results more accurately than Equation (1), *e.g.*, hydrogen in Table III.

In testing Jones' relation (Equation (3)), very good agreement between calculated and observed values is obtained in temperature regions where the viscosity curve is concave to the temperature axis. However, this equation, like Sutherland's, fails completely at low temperatures for gases like carbon dioxide, sulphur dioxide, ammonia, methyl ether and propylene. From Table III it may be noted that Equation (5) gives much the best representation of the variation of viscosity with temperature for these gases over the low temperature range considered. Equation (5) may be written in the form:

$$\log\left(\frac{\eta}{\sqrt{T}}\right) = aT + b \ . \qquad (6)$$

Thus, if $\log(\eta/\sqrt{T})$ is plotted against the temperature, a straight line of slope a and intercept b should be obtained. This has been done for each of the above-mentioned five gases, and all the experimental points fell on a straight line for temperatures between 20° and −80° C. Table IV shows the values of the constants a and b determined in this manner.

A comparison of the observed results and those calculated by means of Equation (6) with the constants given in Table IV, shows agreement to within 0.2%, over the temperature range 30° to −80° C. However, this relation fails at the higher temperatures at which the relations of Sutherland and Jones have been found to hold. In general, Equation (5) or (6) seems adequate in temperature regions where the viscosity curve is convex to the temperature axis, as has been found for some gases at low temperatures.

TABLE IV
VALUES OF THE CONSTANTS OF EQUATION (6)

Gas	a	b
Carbon dioxide	0.000865	−5.32187
Sulphur dioxide	0.000855	−5.38600
Ammonia	0.001010	−5.52737
Methyl ether	0.000842	−5.53129
Propylene	0.000876	−5.56332

Since the viscosity of a gas does not vary directly as the square root of the temperature, owing to variation of the mean free path with temperature, Fig. 2, in which the quantity $\eta/\sqrt{T}$ for several gases is plotted against the temperature, graphically represents the variation of mean free path with

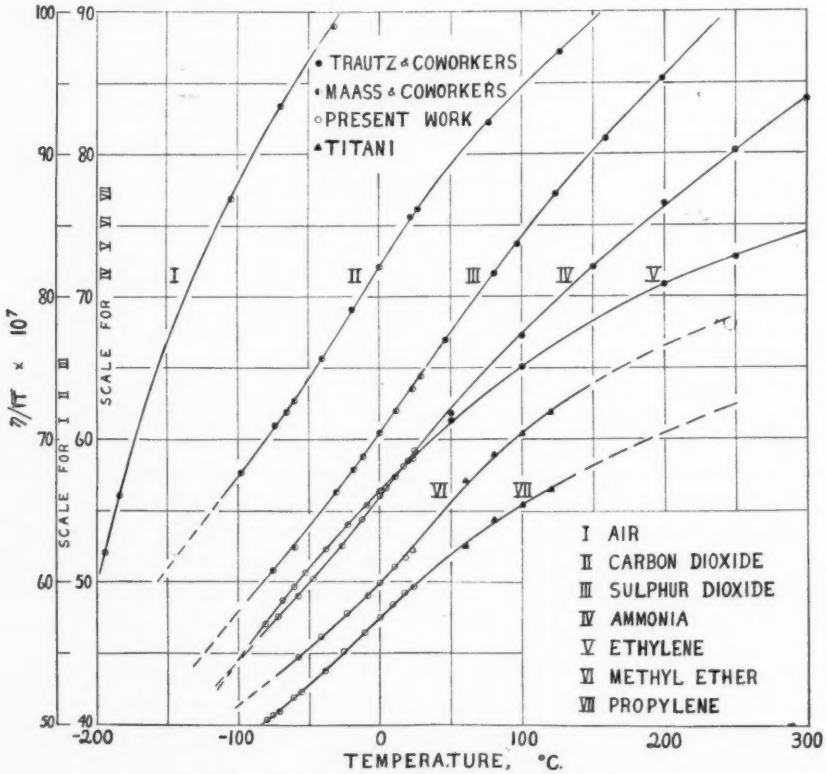

FIG. 2. *Variation of mean free path with temperature.*

temperature. For points above room temperature the data of Trautz and co-workers (22–25) for carbon dioxide, sulphur dioxide, ammonia and ethylene were used. The high-temperature values for methyl ether and propylene are those given by Titani (21). The low-temperature data for air and carbon dioxide are those given by Sutherland and Maass (20), for sulphur dioxide, those of Stewart and Maass (18). The low-temperature values for ammonia, ethylene, methyl ether and propylene are from the present work. Since the authors' values for the viscosity of ammonia at room temperature do not check with those of Trautz and Heberling (22), the whole high-temperature portion of the ammonia curve has been given a vertical displacement to make it continuous.

The curves for carbon dioxide, sulphur dioxide, ammonia, methyl ether and propylene in Fig. 2 each show a point of inflection or an inversion point. Below these points the viscosity–temperature curves are convex to the temperature axis, while above they are concave. Below this inversion point the authors have found Equation (5) to represent the variation of viscosity with temperature adequately. Other authors have found Sutherland's equation to hold well for the higher temperatures.

Fig. 2 shows that the temperature–viscosity curves for air and ethylene are always concave to the temperature axis over the temperature range considered. Hydrogen gives a similar curve (20). The data for the viscosity of helium (9, p. 286) give a curve which is concave to the temperature axis over the entire range -258 to 100° C.

So far as the authors know, the inversion from concave to convex at low temperatures in the viscosity–temperature curves has not been previously pointed out. The suggestion is made that this is the general form of the curve, and that if measurements could be made at low enough temperatures, air, hydrogen and ethylene would show similar inflections.

In general, it seems that the inversion point in the viscosity curves may be related to the critical temperature and the dipole moment of the gas. The approximate inversion temperatures for five gases in Fig. 2 have been found in the following manner. Starting with a temperature of $-80°$ C., the value of $\eta/\sqrt{T}$ corresponding to every 10 degree rise in temperature was read off from the graphs for each gas. The increase in the value of $\eta/\sqrt{T}$ for every 30 degree interval, *e.g.*, $-80°$ to $-50°$ C., $-70°$ to $-40°$ C., etc., was found by subtraction. These differences were then plotted against the mean tempera-

TABLE V

COMPARISON OF DIPOLE MOMENTS, CRITICAL TEMPERATURES AND INVERSION TEMPERATURES

Gas	Dipole moment $\mu \times 10^{18}$	Critical temp., °C.	Inversion temp., °C.
Hydrogen	0.00	−239.9	—
Air	0.00	−140.7	—
Ethylene	0.00	9.7	—
Carbon dioxide	0.13	31.1	12
Propylene	0.34	92.3	30
Methyl ether	1.32	126.9	42
Ammonia	1.48	132.4	35
Sulphur dioxide	1.66	157.2	65

ture of the interval. All the curves thus obtained showed a well defined maximum which corresponds to the point of inflection of the $\eta/\sqrt{T}$ *versus* temperature curves. These results, together with the values for the critical temperature and dipole moment of each gas, are given in Table V.

The dipole moments of hydrogen, air, ethylene, carbon dioxide, ammonia and sulphur dioxide are the mean of several values given in Table IV, p. 40 of Debye's "Polar Molecules". The value for methyl ether is that given in Table II, p. 8 of Debye's "Dipole Moment and Chemical Structure"; that of propylene is given by Watson, Rao and Ramaswamy (28).

The critical temperature values are those given in International Critical Tables, Vol. 3, p. 248.

Table V shows that the dipole moments, critical temperatures and the inversion temperatures of the viscosity curves are roughly parallel. The values of the inversion temperatures given are estimated to be correct to $\pm 10°$ C. The only misplacement seems to be ammonia, but, when it is remembered that the data of Trautz and Heberling (22) had to be changed to check with the present data for ammonia, it may be suggested that this is perhaps due to experimental error.

The fundamental analysis of Jones (10) was based on an equal attraction or repulsion in all directions. Though this condition is approached at high temperatures for polar molecules, it is conceivable that at a sufficiently low temperature this postulate ceases to express the facts. The more polar the molecule, the higher the temperature at which this would occur. It may be possible to extend the theory to take this into account.

References

1. Bestelmeyer, A. Munich Dissertation. 1903.
2. Braune, H. and Linke, R. Z. physik. Chem. A148 : 195-215. 1930.
3. Breitenbach, P. Ann. Physik, 5 : 166-169. 1901.
4. Chapman, S. Phil. Trans. Roy. Soc. A211 : 433-483. 1911.
5. Chapman, S. Phil. Trans. Roy. Soc. A216 : 279-348. 1916.
6. Cooper, D. LeB. and Maass, O. Can. J. Research, 6 : 596-604. 1932.
7. Edwards, R. S. and Worswick, B. Proc. Phys. Soc. Lon. 38 : 16-23. 1925.
8. Graham, T. Phil. Trans. Roy. Soc. 139 : 349-392. 1849.
9. Jeans, J. Dynamical theory of gases. 4th. ed. Cambridge University Press. 1925.
10. Jones, J. E. Proc. Roy. Soc. A106 : 441-462. 1924.
11. Kamerlingh Onnes, H. and Weber, S. Commun. Leiden Phys. Lab. No. 134b. 1913.
12. Maass, O. and Mennie, J. H. Proc. Roy. Soc. A110 : 198-232. 1926.
13. Maass, O. and Wright, C. H. J. Am. Chem. Soc. 43 : 1098-1111. 1921.
14. Obermayer, A. V. Sitzb. Wien. Akad. 71 : 281-308. 1875.
15. Schmitt, K. Ann. Physik, 30 : 393-410. 1909.
16. Stackelbeck, H. Z. ges. Kälte-Ind. 40 : 33-40. 1933.
17. Stewart, W. W. Ph. D. Thesis, McGill University. 1933.
18. Stewart, W. W. and Maass, O. Can. J. Research, 6 : 453-457. 1932.
19. Sutherland, W. Phil. Mag. 36 : 507-531. 1893.
20. Sutherland, B. P. and Maass, O. Can. J. Research, 6 : 428-443. 1932.
21. Titani, T. Bull. Chem. Soc. Japan, 8 : 255-276. 1933.
22. Trautz, M. and Heberling, R. Ann. Physik, 10 : 155-177. 1931.
23. Trautz, M. and Kurz, F. Ann. Physik, 9 : 981-1003. 1931.
24. Trautz, M. and Weizel, W. Ann. Physik, 78 : 305-369. 1925.
25. Trautz, M. and Zink, R. Ann. Physik, 7 : 427-452. 1930.
26. Vogel, H. Berlin Dissertation. 1914.
27. Vogel, H. Ann. Physik, 43 : 1235-1272. 1914.
28. Watson, H. E., Rao, G. G. and Ramaswamy, K. L. Proc. Roy. Soc. A143 : 558-588. 1934.
29. Zimmer, O. Verhandl. deut. physik. Ges. 14 : 471-492. 1912.

THE INFLUENCE OF THE PREHEATING OF WOOD IN WATER ON THE RATE OF DELIGNIFICATION BY SULPHITE LIQUOR[1]

By A. J. Corey[2] and O. Maass[3]

Abstract

The rate of delignification of wood chips has been measured and found to conform to the monomolecular relation, provided that the standard method of penetration developed in this laboratory is used(3). Pretreatment of the wood chips by heating in liquid water at 130° C. decreases the rate of delignification by subsequent cooking in sulphite liquor, and the rate no longer conforms to the monomolecular relation. Preheating of the wood to 130° C. in the absence of water does not influence the rate of subsequent delignification. The results indicate the advantage of reducing the time of cooking, and a tentative explanation has been offered regarding the mechanism involved.

A study has been made of the delignification rate in calcium bisulphite liquor of sprucewood chips which have been subjected to three different types of heat pretreatment:—(i) In an atmosphere of nitrogen; (ii) in distilled water; (iii) in toluene. Black spruce heartwood of density 0.33 was used, and the chip size was 3 × 10 × 20 mm. The wood contained 30.5% of lignin, as determined by the method of Potter and Ross.

Method 1. The wood sample was dried in an oven at 105° C. for 24 hr. and weighed in a closed receptacle. It was then transferred immediately to a distilling flask fitted with a rubber stopper, through which a glass tube extended to the bottom of the flask. This tube was connected to a nitrogen cylinder, and the side arm of the flask, to a suction pump. The flask was evacuated and nitrogen introduced, the process being repeated several times to ensure the complete displacement of the air by nitrogen. This precaution was taken to avoid oxidation of the wood. The flask was immersed in an oil bath at a temperature of 130° C., and heated for one to six hours.

Method 2. Wood samples of known weight were placed in a vacuum desiccator, and after the vessel had been evacuated distilled water was run in. Then by alternately evacuating and applying atmospheric pressure the chips were completely impregnated with water. The chips were then removed, placed in a bronze bomb of 200 cc. capacity containing distilled water, and heated in an oil bath at 130° C. for definite periods of time.

Method 3. Pretreatment with toluene was carried out in a similar manner, except that the chips were thoroughly dried at 105° C. before impregnation with toluene. After the heat pretreatment was completed, the chips were removed from the liquid, dried at 105°, and evacuated to remove the last traces of toluene.

[1] *Manuscript received May 29, 1935.*
Contribution from the Division of Physical Chemistry, McGill University, Montreal, Canada.

[2] *Holder of an International Paper Company Scholarship in the Graduate Department of Chemistry, McGill University.*

[3] *Macdonald Professor of Physical Chemistry.*

After the heat pretreatment the chips were left in contact with air long enough to ensure that the moisture contents were approximately the same in every case.

The cooking was carried out in a small cell of 60 cc. capacity, so designed that it could be evacuated, and pressures up to 10 atm. could be applied during the cooking period. Wood samples of approximately six grams were used in each experiment. The composition of the calcium bisulphite cooking liquor was as follows:—total SO_2, 5.15; free SO_2, 3.90; combined SO_2, 1.25%.

The cooking procedure was as follows. The chips were placed in the cell which was then subjected to evacuation for 30 min. at a pressure of one centimetre of mercury. The cooking liquor was run in, the cell immersed in the oil bath and the temperature raised to 140° C. in 30 min. The temperature was then held constant for the duration of the experiment by means of a suitable electric thermoregulator, and the pressure in the cell kept at seven atmospheres by means of a cylinder of compressed nitrogen gas and a reducing valve.

The chips were removed from the cell, disintegrated with a small, high speed electric disintegrator, and washed several times with distilled water. The resulting pulp was divided into two portions, one being used to make a test sheet, and the other for analytical determinations.

Experimental Results

In the first series of experiments (Table I, A) wood samples were heated in an atmosphere of nitrogen, as described in Method 1, for varying periods of time, and afterward were cooked at maximum temperature (140° C.) for three hours.

TABLE I

EFFECT ON COOKING PROPERTIES OF WOOD OF PREHEATING TO 130° C. IN *(A)* NITROGEN, AND IN *(B)* WATER

Run no.	Yield of pulp, %	Yield of cellulose, %	Lignin in pulp, %	Residual lignin, %, based on wood used	Mullen strength, %	Time of pretreatment at 130° C., hr.
A. Method 1.—Preheating in an atmosphere of nitrogen						
110	53.2	49.3	7.35	3.9	166.5	No pretreatment
119	53.7	50.2	6.45	3.5	159.5	No pretreatment
122	55.7	52.1	6.42	3.58	157	1
115	54.4	51.1	7.11	3.86	150	2
117	53.0	49.2	7.22	3.92	175	4
121	53.8	50.2	6.74	3.63	164	6
B. Method 2.—Preheating in water						
111	54.8	48.8	11.0	6.2	132	1
113	58.2	51.0	12.4	7.23	109	2
116	65.0	54.6	16.1	10.45	54.0	4
120	67.5	54.0	20.05	13.5	—	6

The yield of cellulose was determined by difference, and so includes all carbohydrates not determined as lignin.

For purposes of comparison two runs were made on untreated wood chips.

Table I, *B*, shows the results obtained when the chips were pretreated by heating in water at 130° C. for varying periods of time, and then cooked for three hours at 140° C.

Table II is a comparison between wood heated in toluene at 130° C. for six hours, and untreated wood. The two samples were cooked for three hours at 140° C.

TABLE II

RESULTS OBTAINED WITH WOOD PRETREATED IN TOLUENE AND WITH WOOD NOT PRETREATED

Run no.	Yield of pulp, %	Yield of cellulose, %	Lignin in pulp, %	Residual lignin, %	Mullen strength, %	Type of treatment
134	52.2	48.8	6.88	3.6	145	Toluene-treated
110	53.2	49.3	7.35	3.9	166.5	Not pretreated

The runs listed in Table III were made on chips which had been pretreated in water for six hours at 130° C. and then cooked at 140° C. for the periods of time indicated.

For purposes of comparison a "burnt cook" was obtained as follows. Untreated chips were placed in the cooking cell and the usual pre-evacuation

TABLE III

RESULTS OBTAINED WITH WOOD PRETREATED FOR SIX HOURS WITH WATER AT 130° C., AND WITH UNTREATED WOOD

Run no.	Yield of pulp, %	Yield of cellulose, %	Lignin in pulp, %	Residual lignin, %	Mullen strength, %	Hours cooked at 140° C.
A. Chips pretreated for six hours in water at 130° C.						
123	43.3	42.4	1.83	0.79	100	8
129	45.2	44.3	2.08	0.94	130	7
127	47.0	45.4	3.35	1.57	130	6
126	50.5	47.2	6.62	3.34	138	5
128	59.3	52.0	12.3	7.3	63.5	4
120	67.5	54.0	20.05	13.6	—	3
132	80.7	60.0	25.2	20.3	—	1.5
B. Untreated wood						
135	46.3	45.0	2.55	1.17	145	5
110	53.2	49.3	7.35	3.9	166.5	3
131	65.3	55.8	14.4	9.4	—	1.5
130	85.9	61.3	28.7	24.7	—	0.5

was omitted. The liquor was introduced and the cell immersed in the oil bath, which had been preheated to 120° C. The temperature of the bath was raised to 140° C. in 15 min.

A three hour test run was made and definite "burning" was obtained. Using the same procedure, Run 125 was "burned" at the beginning and the cooking continued for eight hours.

TABLE IV

RESULTS OBTAINED WITH A BURNT COOK

Run no.	Yield of pulp, %	Yield of cellulose, %	Lignin in pulp, %	Residual lignin, %	Mullen strength, %	Length of cook, hr.
125	43.5	37.5	13.5	5.8	—	8

Discussion

A consideration of Table I, *A*, shows that the cooking properties of wood are not altered by heating to 130° in the absence of liquids. Any variation in the results, particularly in the mullen strength, is to be attributed to variations in the composition of the different samples. Small knots in the dry wood chips are hard to detect and wood containing them will yield a sheet containing shives. Hence the mullen strength value is lowered.

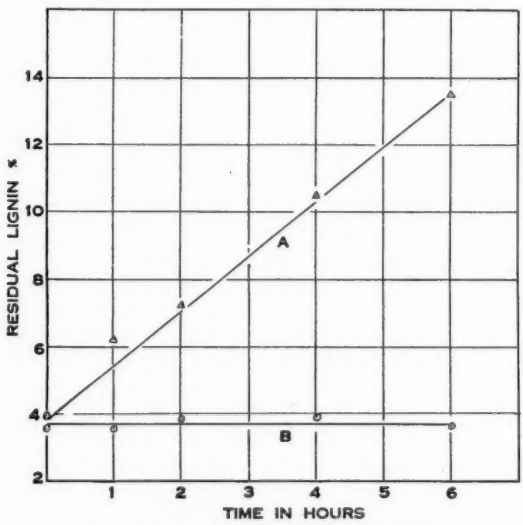

FIG. 1. *Influence of preheating wood at 130° C. on delignification in a 3 hr. standard sulphite cook at 140° C. A, pretreated by Method 2; B, pretreated by Method 1.*

Table I, *B*, indicates that heat treatment of wood in water makes subsequent delignification of the wood in calcium bisulphite liquor very difficult, and this effect increases with the length of the pretreatment. The wood pretreated for six hours was so slightly cooked after three hours at 140° C. that the chips could not be disintegrated.

The difference in the results obtained by the two methods of pretreatment is brought out in Fig. 1, in which the residual lignin, calculated on the basis of the original wood, is plotted against the time of pretreatment.

In order to ascertain whether liquids other than water produced this effect, a wood sample was pretreated in toluene for six hours at 130° and cooked for three hours at 140° C. In Table II the results of this run are compared with those of a cook made on untreated wood, also cooked three hours.

Table III, *A*, shows that wood pretreated in water can be delignified if cooked a sufficient length of time, but owing to this increased period of digestion the cellulose fibres are degraded and low mullen strengths are obtained. The maximum strength is shown after five hours' cooking but with untreated wood (Table III, *B*) the maximum strength is indicated after three hours' digestion.

The results of Run 125 confirm the belief that a "burned cook" cannot be delignified by prolonged cooking. The rate of cellulose degradation was more rapid in this case than the rate of delignification, so that no separation of cellulose from lignin could be obtained. It would then appear that the result of water-heat pretreatment differs in nature from that of "burning".

Investigation has shown that the rate of delignification in the sulphite process approximates that given by a monomolecular reaction (4, 5) *i.e.*,

$$\frac{1}{t}\ln\frac{L_o}{L} = k,$$

where t is the time in hours, L_o the percentage lignin in the wood, L the percentage lignin remaining at time t, and k the velocity constant of the reaction. Thus if the logarithm of the percentage of residual lignin, calculated on the weight of the wood, is plotted against time, a straight line relation should be obtained. This result has been obtained with woodmeal in a thorough investigation carried out by Yorston (5). The authors found that the same result could be obtained with wood chips provided that the perfect penetration procedure outlined by de Montigny and Maass (1) was followed.

In Fig. 2 are plotted values taken from Table III, and though the untreated wood follows the monomolecular relation approximately, the pretreated wood shows a great deviation.

According to Hägglund (2) there are three main reactions leading to the removal of lignin—

1. Sulphite addition to the lignin-carbohydrate compound in the solid phase.

2. Hydrolysis of the lignin sulphonic carbohydrate compound in the solid phase.

3. Hydrolysis of the liberated carbohydrate. Sulphur determinations made in the experiments listed in Table III, *A*, indicated that sufficient sulphonation had taken place, so that the decreased rate of delignification observed with

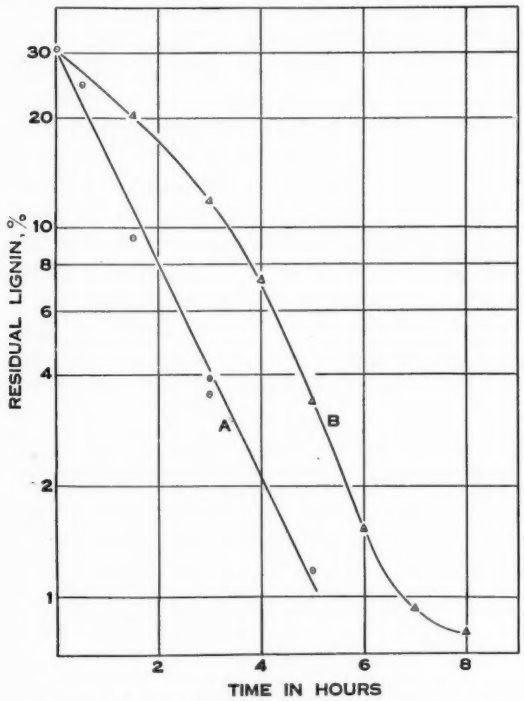

FIG. 2. *Rate of delignification of untreated and of pre-heated wood. A, untreated wood; B, pretreated by Method 2.*

pretreated wood must be attributed to a change in the rate of hydrolysis. A possible explanation is advanced to account for this change, and for the shape of the curves in Fig. 2.

If the lignin is present in the wood as submicroscopic particles, heating in aqueous solutions might tend to cause agglomeration and increase in particle size. On the other hand, the cooking action tends to decrease the particle size, so that in the cooking process two opposite effects are superimposed. If these two effects could be separated, curves would be obtained as shown in Fig. 3, but acting together the two cancel and give the straight line relation required by the monomolecular rate.

When wood is pretreated by heating in water the particle size of the lignin is increased to a maximum, and the rate of delignification greatly decreased in the first stages of the process. Later on, the effect of decreasing particle size, brought about by the cooking action, predominates and the curve falls rapidly.

The inflexion in the curve after seven hours may indicate that some of the lignin is more resistant to removal, but the inaccuracy of lignin determinations in this region of the curve makes it of doubtful significance.

This work was repeated using a wood specimen of different density, and the same results as those described above were obtained. They have been omitted owing to lack of space.

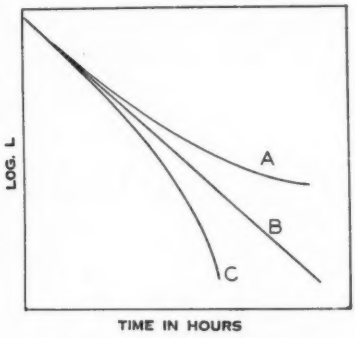

FIG. 3. *Effect of changing particle size on the rate of delignification. A, effect of increasing particle size; B, monomolecular relation; C, effect of decreasing particle size.*

The hypothesis advanced to explain the effect of heat pretreatment in water is of course a tentative one, and other explanations, such as a structural change in the lignin, produced by the pretreatment, suggest themselves. In any case it appears from the experiments described that a decrease in cooking time will benefit the process of delignification, an additional reason for finding means of decreasing the so-called penetration period. Experiments designed to test this out are contemplated. Furthermore work is being undertaken on the pretreatment of wood in aqueous solutions of salts, acids, and bases, but sufficient results have not yet been obtained to warrant the drawing of conclusions.

References

1. DE MONTIGNY, R. and MAASS, O. Forest Service Bull. 87. Dept. of the Interior, Canada. 1935.
2. HÄGGLUND, E. Papierfabr. 24 : 775-780. 1926.
3. SAUNDERSON, H. H. Ph. D. Thesis, McGill University. 1932.
4. SCHMIDT-NIELSEN, S. Paper Trade J. 84 : No. 19. 43-44. 1927.
5. YORSTON, F. H. Project 70 M., Progress Report No. 2. Forest Products Laboratory, December, 1934.

MEASUREMENT OF THE VARIATION OF THE DIELECTRIC CONSTANT OF WATER WITH EXTENT OF ADSORPTION[1]

By G. H. Argue[2] and O. Maass[3]

Abstract

An experimental technique has been devised for the measurement of the dielectric constants of cellulosic materials containing various amounts of adsorbed water. From measurements made with standard cellulose the dielectric constant of the adsorbed water was calculated over the concentration range 0 to 18% of water. The dielectric constant of the water initially adsorbed is less than one-quarter of that of liquid water, but it increases with the amount of water subsequently adsorbed, until the dielectric constant approximates that of liquid water as the water content of the fibre approaches the saturation point. These results are shown to be in agreement with the hypothesis concerning the nature of the system cellulose–water.

Introduction

In a recent paper (1) the nature of the adsorption of water on cellulosic materials was discussed at considerable length. With the hope of finding further evidence in favor of the views set forth, an investigation was started in which the change in the dielectric constant of the adsorbed water with increasing concentration of water was measured. A technique was developed whereby the dielectric constant of bone-dry cellulose could be determined and subsequent measurements made after the addition of a known amount of water.

While no work has been published on the dielectric constant of water adsorbed on cellulose, a paper by Von Tausz and Rumm (5) on the dielectric constant of adsorbed water appeared while this work was in progress. The sorbents used by them were silica, lignite and tobacco. Of these, only the last-named bears any similarity to the system to be described. Their results will be discussed later.

Apparatus

The dielectric constant apparatus that was employed has been in use in this laboratory for some time. With it, small capacities are measured by means of a heterodyne beat method. The set-up was arranged to give a wave-length of 600 metres. The frequency of the two oscillators differed by 1000 cycles per sec., so that a telephone could be used for the null point reading. The precision-measuring condenser was mounted in the centre of a circular platform, 5 ft. in diameter, with a 6 in. vertical scale around the edge. A beam of light was thrown on a small mirror fastened to the central rotor shaft of the condenser so that a spot of light was reflected on to the scale. The sensitivity was such that a change of 0.05 cm. on the scale could be easily detected.

[1] *Manuscript received June 1, 1935.*
Contribution from the Division of Physical Chemistry, McGill Univversity, Montreal, Quebec, Canada.
[2] *Holder of a bursary under the National Research Council of Canada.*
[3] *Macdonald Professor of Physical Chemistry, McGill University.*

The experimental condenser consisted of two concentric brass cylinders 0.07 cm. in thickness. The inner diameter of the larger cylinder was 2.58 cm., and the outer diameter of the smaller plate was 2.05 cm. The outer and the inner condenser plates were respectively 22.95 cm. and 23.6 cm. in length; the entire condenser was enclosed in a glass tube provided with platinum leads and an outlet to the evacuated glass system, as shown in Fig. 1. The outer brass plate fitted snugly into the glass cylinder and three

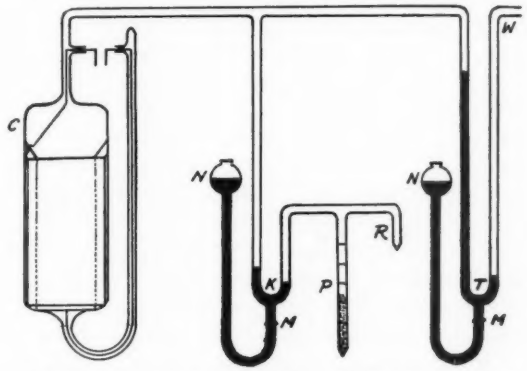

FIG. 1. *Apparatus for measuring dielectric constants of water adsorbed on cellulose.*

small prongs on each plate held the condenser centrally in the glass tube. The dimensions of these projections were: on inner cylinder, 2 by 0.29 by 0.07 cm.; on outer cylinder, 1.02 by 0.4 by 0.07 cm. A direct electrical contact was made between the platinum wires and two of the outer binding posts of a double-throw mercury switch, not shown in the diagram. The central binding posts were connected to the capacity-measuring apparatus. With the switch in one position the capacity of the external leads from the measuring condenser to the mercury switch was measured. With the switch in the other position, the total capacity of the external leads, internal leads from the switch to the condenser plates and the experimental condenser itself was determined. The experimental capacity readings given in this work are the differences in the capacities measured when this switch was in these two positions. That is, the measured capacity was due to the brass condenser and its internal leads only. Further, the repeated measurement of the capacity of the external leads served as a check on the operation of the capacity-measuring apparatus.

All external leads were enclosed in copper tubes which were held in a fixed position and earthed. The various parts of the entire capacity-measuring apparatus were grounded. Further, the oil bath surrounding the experimental condenser was provided with a constant level device, so that no variable capacity effects due to a change in the volume of liquid in the bath were introduced. The metallic parts of the thermostat and the supports for the

glass apparatus were connected to an equipotential, earthed shield. The negative side of the 110 volt d-c. which supplied the power for the motor and heaters was grounded through a 10,000 ohm resistance. It was found that the effect of mutual and earth capacity had been minimized, and since only differential capacity measurements were made, any small variable change in capacity cancelled out, or was negligible compared to the large capacity of the experimental condenser.

The evacuated glass system, shown diagrammatically in Fig. 1, was of simple design. Two mercury traps T and K were used in place of stopcocks. The former served as a manometer by which the pressure in the apparatus was measured; it also formed a seal between the entire apparatus and the atmosphere. The latter isolated the short section forming the pipette, P, by which the amount of water vapor admitted to the chamber containing the cellulose was measured. By adjusting the leveling bulb, N, and the stopcock, M, the required amount of water could thus be admitted. The pressure in the entire system could be reduced to that of 10^{-5} cm. of mercury in a few minutes by means of the two mercury diffusion pumps and a Cenco Hyvac pump, all in series and sealed on at W. In order to ensure that water vapor did not condense in the various parts of the apparatus when the moisture content of the cellulose sample approached the saturation point, two precautions were taken. Fine resistance wire (16 ohms per foot) was wound around the glass tubing connecting the component parts of the system, and a small current was passed through the wire. In this way the temperature of the glass was maintained at from 30 to 35° C. Further, a small Dewar flask filled with ice was placed around the pipette before the water level was measured.

Experimental Procedure

A weighed sample of dry cellulose, purified as previously described (1), was packed into the annular space between the plates of the experimental condenser. The apparatus was assembled in the glass case, C, and the electrical contacts were made.

A small bulb, partly filled with distilled water, was sealed to the system at R, and small traces of gas were removed by alternate freezing and melting of the liquid while the apparatus was kept evacuated. The part of the system forming the pipette was shut off from the remainder of the apparatus by the mercury in the trap K, and the liquid was distilled into the pipette and the bulb was sealed off at R.

In order to remove the water vapor which the cellulose sample sorbed from the atmosphere during its transfer to the condenser, the temperature of the oil bath was raised to 100° C. and maintained at that point for two hours. The entire apparatus was evacuated and at regular intervals dry air was admitted to the system until the pressure was approximately that of 20 cm. of mercury, and allowed to remain in contact with the sample for 10 min. Finally, the bath was cooled to 25° C., the temperature control was regulated and the mercury limb in the manometer T was raised to a height sufficient to withstand atmospheric pressure.

The capacity of the condenser containing dry cellulose was measured. A known volume of water was allowed to evaporate into the evacuated system by lowering the level of the mercury in K. After equilibrium was established, the capacity of the condenser was again determined. This procedure was repeated until the fibre was almost saturated. Furthermore, the difference between the barometric pressure and that indicated by the height of the mercury in the manometer T was the equilibrium pressure of the water vapor in contact with the cellulose. By means of the vapor pressure-adsorption data (5), it was possible to check the amount of water adsorbed on the sample, and also to ensure that equilibrium was established before the capacity was measured.

Capacities could be measured to within 0.1%. For a sample containing up to 2% of adsorbed water the change in the capacity was 2.3 cm. units. At this concentration the probable error in the value deduced for the capacity of water was 1.6%. When the water concentration on the cellulose sample was 10%, the probable error was 0.3%, and with the higher moisture concentrations the errors were smaller.

The largest probable error was introduced by the measurement of the amount of water adsorbed by the cellulose. The volume of water was estimated to within 0.005 cc.; the total volume of water adsorbed by cellulose containing 2% of water was 0.1 cc., hence the probable error was 5%. The error decreases and, with increasing amounts of water, eventually becomes less than 1%.

The Calculation of the Dielectric Constant

The absolute value of the capacity of the condenser was measured and it agreed fairly well with that calculated on the basis of the dimensions of the condenser. The difference between the calculated and the measured capacity of the condenser can be accounted for by certain lead corrections and the capacity due to the projections on the top of the condenser. These corrections were difficult to estimate. Since it was found that the actual capacity of the condenser does not enter into the calculation of the dielectric constant of the absorbed water, this difference will not be considered further.

The capacity of the empty condenser is given by the following relation:

$$L + C = xd_1,$$

where L is the capacity due to the internal lead wires from the condenser plates to the mercury switch, C is the capacity of the condenser, d_1 is the measured deflection on the scale of the measuring condenser, and x is a proportionality factor, which can be calculated from a consideration of the calibration of the measuring condenser by the measurement of the capacity of a standardized fixed capacity.

Similarly, the capacity of the internal leads is

$$L = xd_2.$$

At the conclusion of the experiments the glass tube surrounding the condenser was opened, the two cylindrical plates were removed, and the capacity of the internal leads was measured. The lead wires were in the same position relative to one another as they were in the actual experiments. Hence, d_2 is the deflection on the scale of the measuring condenser due to the capacity of the lead wires. The value of d_2 found experimentally was 8.0 cm. From these two relations, it follows that the capacity of the condenser is given by

$$C = x(d_1 - d_2).$$

Further, the capacity of the condenser filled with dry cellulose, C_m, is

$$C_m = x(d_3 - d_2),$$

where d_3 is the deflection measured by the precision condenser.

The dielectric constant of the cellulose-air mixture, ϵ_m, will be given by

$$\epsilon_m = \frac{(d_3 - d_2)}{(d_1 - d_2)}.$$

From the last equation, the value of ϵ_m was calculated as follows

$$\epsilon_m = \frac{82.96 - 8.0}{68.23 - 8.0} = 1.24.$$

Hence the dielectric constants of the cellulose and of the adsorbed water do not depend on the absolute capacity of the condenser, since they are calculated from the dielectric constants of the cellulose-air and cellulose-air-water mixtures given by the above relation.

Also, it should be pointed out that the method used and the arrangement of the electrical measuring apparatus were such that the electrical conductivity of the adsorbed water had no effect on the results of the capacity measurements. This method was, in part, developed in this laboratory for the measurement of the dielectric constant of water and hydrogen peroxide (4).

It is difficult to estimate the dielectric constant of a dielectric that does not completely fill the space between the plates of the condenser. If the sample is in a regular arrangement in layers parallel to the surface of the plates with air spaces between the layers, it can be shown that

$$\epsilon_m = \frac{1}{\frac{v_1}{V} + \frac{v_2}{V\epsilon}}, \tag{1}$$

where ϵ is the dielectric constant of the substance, ϵ_m is the resultant dielectric constant of the material and the air in the sample, and $\frac{v_1}{V}$ and $\frac{v_2}{V}$ are the volume percentages of air and the substance.

If the dielectric is arranged at right angles to the surface of the plates, that is, if the material forms a continuous conductor across the air gap between the plates with alternate columns of air and material, it can be shown that—

$$\epsilon_m = \frac{v_1}{V} + \frac{v_2}{V}\epsilon. \tag{2}$$

According to Lichtenecker (3), if the dielectric is in the form of very small particles distributed at random in the air space in the condenser, the following empirical relation obtains

$$\log \epsilon_m = \frac{v_2}{V} \log \epsilon \ . \tag{3}$$

The diagrams shown in Fig. 2, clearly define the spatial arrangement of the dielectrics in the mixture between the plates. In Fig. 2, *a*, *b* and *c* refer to Relations 1, 2, and 3, respectively.

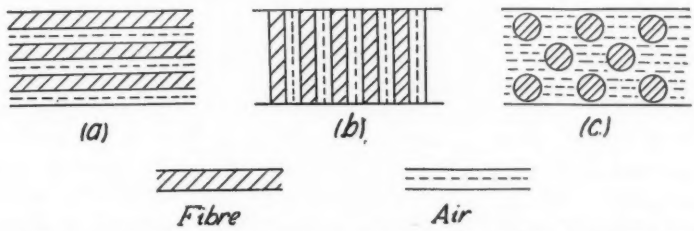

FIG. 2. *Diagrammatic representation of typical distributions of dielectric and air in condenser.*

For the measurement of the dielectric constant of cellulose from the capacity measurements of a condenser filled with cellulose fibre, it is obvious that the first relation cannot be applied. It might appear that the relation between ϵ_m and ϵ given in Equation (3), would be the correct one. However, cellulose consists of fibres, the average length of which is 2.5 cm., while the distance between the plates of the experimental condenser used in this work was 0.265 cm. Also, from the manner in which the cellulose was packed into the condenser, it is probable that the second relation is the one most closely approximated.

From the dielectric constant of the mixture of dry cellulose and air in the condenser (as calculated above), it is possible to determine the dielectric constant of cellulose by means of Equation (2). The volume percentages of dry cellulose and air are 7.87 and 92.13%. Hence, the dielectric constant of cellulose, ϵ, is

$$1.24 = 0.921 + 0.079\epsilon$$
$$\epsilon = 4.11$$

Similarly, from Equation (3)

$$\log 1.24 = 0.079 \log \epsilon$$
$$\epsilon = 13.21$$

There is no generally accepted value for the dielectric constant of cellulose. It is pointed out in The International Critical Tables (2) that the value of ϵ is between 3.9 and 7.5. It is improbable that the dielectric constant of cellulose is 13, as given by Equation (3). That of a carbohydrate such as sugar is 4. Hence, it would appear that Equation (2) gives for the dielectric constant of bone-dry cellulose a value that is of the right order of magnitude. As the main interest in the subsequent work lies in the relative values to be

assigned to the dielectric constant of the adsorbed water, and as the experiments were carried out in such a way that the position of the cellulose fibres was not altered by the adsorption of the water vapor, whatever arrangement of the cellulose fibres holds for the calculation of the dielectric constant of dry cellulose also holds for the subsequent calculation of the dielectric constant of the adsorbed water. Since Equation (2) gives a reasonable value for the dielectric constant of cellulose, this relation will be used in the calculation in connection with the adsorbed water. It can be expected that the relation of any one value of the dielectric constant of adsorbed water to another is correct.

In the use of Equation (2), extended to include the system cellulose–air–water, it was assumed that during adsorption the volume of the water remained unchanged. It has been shown that a contraction in volume of the adsorbed water takes place. Even if this contraction is as large as that found by Filby and Maass, it was not assumed by them that the water alone suffered this contraction. Part of the decrease in volume will undoubtedly be participated in by the cellulose. Thus, the true volume of the water is an unknown quantity, and was not taken into account. Later on, this will be referred to again, as the values for the dielectric constant of adsorbed water show that some such contraction in the system does take place when adsorption begins.

Results

The experimental data and the calculated values of the dielectric constant are given in Table I. The true weight of water sorbed on the sample, corrected for the amount of water vapor in the total evacuated volume of the

TABLE I

CALCULATED DIELECTRIC CONSTANTS

Weight of water sorbed, gm.	Gm., H_2O/gm. cellulose	True capacity, cm.-units	Dielectric constant of mixture	Dielectric constant of adsorbed water
Run 1				
0.0	0.0	74.73	1.241	—
0.096	0.0189	77.01	1.279	15.73
0.438	0.0862	90.60	1.504	25.48
0.792	0.156	119.0	1.976	39.22
Run 2				
0.0	0.0	74.96	1.245	—
0.037	0.0073	75.58	1.255	12.81
0.117	0.0230	77.63	1.289	16.70
0.230	0.0452	81.61	1.355	20.84
0.343	0.0675	86.28	1.433	23.63
0.453	0.089	90.74	1.507	24.91
0.611	0.120	103.85	1.724	33.46
0.840	0.165	122.0	2.026	39.51
0.0	0.0	75.10	1.247	—

apparatus, is shown in the first column. Knowing the weight of the sample, 5.084 gm., it was possible to calculate the weight of water adsorbed per gram of dry cellulose. The third column shows the true capacity of the condenser and its contents, in units of the scale divisions of the measuring condenser, when the water concentrations are those shown in the preceding columns. The dielectric constants of the heterogeneous system cellulose–air–water are shown in Column 4. These data, shown in Fig. 3, were calculated as

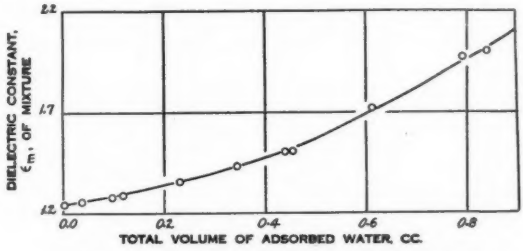

FIG. 3. *Relation between dielectric constant of mixture cellulose–water and air and water content of cellulose.*

mentioned previously. The dielectric constant of the mixture, ϵ_m, increases as the volume of water adsorbed becomes larger. In the last column the dielectric constant of the adsorbed water, calculated from an extended relation similar to that given by Equation (2), is shown. A typical example follows:—

Total volume of the condenser, 41.4 cc.; weight of cellulose, 5.084 gm.; volume of cellulose = $5.084 \times 0.62 = 3.26$ cc.; volume of water, 0.23 cc.; volume of air = $41.4 - 3.26 - 0.23 = 37.91$ cc.; dielectric constant of air, 1; dielectric constant of cellulose, 4.11; dielectric constant of the mixture, 1.35. Hence,

$$1.35 \times 1 = 1 \times \frac{37.91}{41.4} + 4.11 \times \frac{3.26}{41.4} + \epsilon_{H_2O} \times \frac{0.23}{41.4}$$

$$\epsilon_{H_2O} = 20.84.$$

The dielectric constant of 0.23 gm. of adsorbed water is 20.84. The data in Column 5 are shown graphically in Fig. 4. An inflection in the curve occurs at a point corresponding to a water content of approximately 0.09 gm. of water per gram of dry cellulose. This apparent discontinuity may be explained in the following manner.

If the water first adsorbed on the cellulose surface occupies a smaller volume than is accounted for if a density of 1 gram per cc. is assigned to it, then the dielectric constant of the adsorbed water as calculated is too small. In the range of small water contents, the curve might well take the form shown by the dotted line, if the volume contraction of the adsorbed water could be taken into account.

The values of the dielectric constant shown in the last column of Table I are the mean dielectric constants of the adsorbed water over the concentration range from the concentration corresponding to zero adsorption to that at which the measurement was made. It is possible to calculate the dielectric

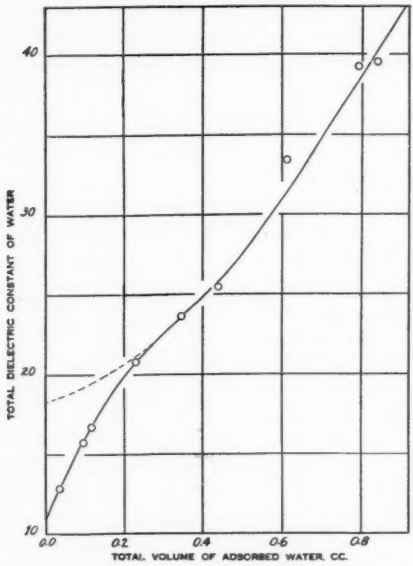

FIG. 4. *Relation between dielectric constant of all water adsorbed on cellulose and amount of water adsorbed.*

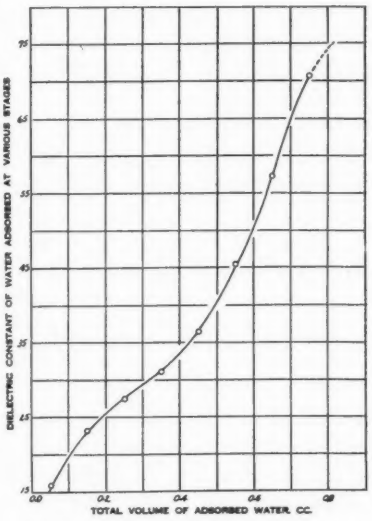

FIG. 5. *Relation between dielectric constant of water adsorbed at various stages and volume of adsorbed water.*

constant of a small volume of water that would increase the water content concentration over a small range. The additive relation expressed by Equation (2) may be given in the form—

$$\epsilon_{v_2} \times v_2 - \epsilon_{v_1} \times v_1 = \epsilon_{(v_2 - v_1)},$$

where ϵ_{v_1} and ϵ_{v_2} are the dielectric constants when the volumes of sorbed water are v_1 and v_2 respectively, and ϵ is the dielectric constant of the small increment of water. In Table II the value of ϵ for each increment of water is given.

TABLE II

AVERAGE DIELECTRIC CONSTANT OF WATER ADSORBED OVER A SMALL CONCENTRATION RANGE

Range of water content, $V_2 - V_1$, (cc.)	Dielectric constant of water added	Range of water content, $V_2 - V_1$, (cc.)	Dielectric constant of water added
0.0–0.1	15.8	0.4–0.5	36.5
0.1–0.2	23.6	0.5–0.6	45.5
0.2–0.3	27.5	0.6–0.7	57.3
0.3–0.4	31.1	0.7–0.8	70.7

In Fig. 5 the average dielectric constant for each definite volume of water, 0.1 cc., adsorbed by the cellulose over the concentration ranges shown in Table II, is plotted against the mean volume of water present on the cellulose between these concentration limits.

When the concentration is 0.8 cc. of adsorbed water, 16% adsorption, the cellulose sample has sorbed an amount of water that is just 4% lower than that found at the fibre saturation point. The last portion of water adsorbed might be expected to be mainly in capillary tubes. Such adsorbed water would have a dielectric constant of 79, so that the dielectric constant of the adsorbed water apparently approaches that of liquid water.

Discussion of Results

Since the value for the dielectric constant of cellulose is a reasonable one and that of the adsorbed water near the fibre saturation point agrees with the accepted value for the dielectric constant of water, all the indicated values of the dielectric constants of water probably do not differ much from the true values. The relation used in the calculation would give too small a value, since only a part of the cellulose fibres are in pillar formation. However, the lines of force would be drawn in to a certain extent if the dielectric is spread in pillar formation, and the relation in Equation (2) would give too high a value for the dielectric constant of the mixture. It may be that the cellulose spread laterally just compensates for this effect and that the results found are, therefore, very nearly the absolute ones.

However, no emphasis is laid on the foregoing fact, as it may be entirely fortuitous, and the value of the dielectric constant of cellulose may well be higher than that given by Equation (2), namely, 4.11.

The main object of this investigation has been achieved independently of the accuracy of the absolute values. It has been shown that the dielectric constant of the adsorbed water becomes larger with increased adsorption, gradually reaching the value for liquid water.

Von Tausz and Rumm (5) found that the dielectric constant of water adsorbed on tobacco decreased from 90 to 25, when the water content was reduced from 19 to 15%. A change of this magnitude is improbable. The dielectric constant of water at 25° C. is actually less than 90 (4). The 4% change that occurs in water concentration in the vicinity of the fibre saturation point will not change the nature of the adsorbed water to so appreciable an extent. The relation that these experimenters used, Equation (3), while probably legitimate for their measurements with powders, is not so when applied to a fibrous material, which on packing spreads, to some extent, from one electrode to the other.

Conclusion

The large value of the dielectric constant of a polar liquid is due mainly to the orientation that the liquid molecules, which are free to rotate, assume in an electric field. Adsorbed molecules will not have the freedom that those in the liquid have. The water molecules that form the first adsorbed layer

on the cellulose micelle will be strongly held to the surface and will rotate through only a very limited range. The dielectric constant of these adsorbed water molecules would be low. The molecules in a second adsorbed layer would not be as securely anchored, and would be free to rotate through a larger range under the influence of an electric field. Hence, the dielectric constant of the adsorbed water increases with further additions. At a point in the water adsorption where the adsorbed molecules are no longer under the influence of the surface, the dielectric constant of the adsorbed water would reach a maximum value equal to that of liquid water. That the dielectric constant does not increase abruptly to its limiting value as soon as the initial free surface has been saturated is to be expected. New surface for water adsorption is created continuously as further amounts of water are adsorbed. This fact is shown clearly in Fig. 5. The experimental results are, therefore, an excellent confirmation of the hypothesis regarding the physical structure of cellulose, and the mechanism of adsorption that was given in the introduction.

From the forms of the various graphs, one is tempted to draw quantitative conclusions regarding the amount of water which is adsorbed, the amount held as liquid water, and the amount of new cellulose surface created in the various stages of adsorption. However, it will be well to postpone these estimates until the absolute value of the dielectric constant of cellulose has been definitely established. Further, the experimental apparatus in its present form is not such as to permit of the estimation of the dielectric constant of water left by desorption. It can be predicted, however, that when this investigation is continued, information of even greater interest than that from the heat of wetting measurements will be obtained (1).

References

1. ARGUE, G. H. and MAASS, O. Can. J. Research, 12 : 564-574. 1935.
2. INTERNATIONAL CRITICAL TABLES, Vol. 2, p. 310, McGraw-Hill Book Co., New York. 1927.
3. LICHTENECKER, K. Physik. Z. 27 : 115-158. 1926.
4. LINTON, E. P. and MAASS, O. J. Am. Chem. Soc. 53 : 957-964. 1931.
5. TAUSZ, J. and RUMM, H. Kolloidchem. Beihefte, 39 : 58-104. 1933.
6. URQUHART, A. R. and WILLIAMS, A. M. Shirley Inst. Mem. 3 : 307-320. 1924.

A NOTE ON THE SPECIFIC HEATS OF LIQUID DEUTERIUM OXIDE[1]

By R. S. Brown[2], W. H. Barnes[3] and O. Maass[4]

Abstract

Preliminary determinations of the specific heats of liquid deuterium oxide from 4° to 65° C. are described. The average specific heats over the temperature ranges 4° to 26° C., 26° to 45° C., and 26° to 65° C., are 1.018, 1.003 and 1.008 respectively, while the average specific heat between 4° and 65° C. is 1.01 cal. per gm. per degree.

In a previous investigation of the specific heats and latent heat of fusion of solid deuterium oxide (3) it was found that the average specific heat of liquid D_2O is higher than that of water between 3.8° and 25° C. In the present note some preliminary determinations of the specific heats of liquid deuterium oxide over the temperature range 4° to 65° C. are described.

The adiabatic calorimeter (1) previously employed (3) was modified for the present study by replacing the inner calorimeter vessel with one of smaller capacity, and by extending the supports for the radiation thermocouple junctions in order to ensure the optimum distance (about 1 mm.) between the junctions and the wall of the inner vessel.

The 12 gm. sample of 98% deuterium oxide (3) was transferred from the platinum container to a Pyrex bulb of about 14 cc. capacity by the method outlined in the previous paper (3), and was sealed therein. The same weight of distilled water was sealed in a second Pyrex bulb of the same shape and virtually the same capacity.

The total heats of the bulbs plus D_2O and H_2O, respectively, were measured from known initial temperatures to a final temperature of 26.0° C. Oil thermostats, automatically controlled to within ± 0.05°C., were employed to bring the containers and contents to the initial temperatures desired.

It was found that appreciable heat losses from the bulbs occurred during their transference from the thermostat to the calorimeter. This disadvantage in the present procedure, when results of a very high degree of accuracy are desired, has already been pointed out (2). In the present determinations these heat losses were estimated in the following manner. A series of total heat measurements of the bulb containing ordinary water for different periods of transfer was made from each initial temperature. The times of transfer were determined to within 0.1 sec. The heat losses were calculated by means of the equation.

$$h_x = (C_{H_2O}\, w_{H_2O} + C_{Pv}\, w_{Pv})\,(t_i - t_e) - H,$$

where h_x is the heat loss during transfer for time x.

[1] *Manuscript received June 14, 1935.*
Contribution from the Chemistry Department, McGill University, Montreal, Quebec, Canada.
[2] *Graduate Student, Chemistry Department, McGill University.*
[3] *Assistant Professor of Chemistry, McGill University.*
[4] *Macdonald Professor of Physical Chemistry, McGill University.*

C_{H_2O} and C_{Py} are the specific heats of water and Pyrex, respectively, for the temperature range $(t_i - t_e)$, where t_i is the initial, and t_e the final, temperature.

w_{H_2O} and w_{Py} are the weights of water and Pyrex, respectively,

H is the total heat of the Pyrex bulb and water from t_i to t_e as measured in the calorimeter.

A curve of the heat losses plotted against times of transfer was drawn for each initial temperature. The time required to transfer the bulb containing deuterium oxide was observed for each determination, and the heat loss during the transfer was obtained from the curve for the initial temperature involved. About five experiments were made on the deuterium oxide from each initial temperature.

The total heats per gram (h_{D_2O}) of liquid deuterium oxide from the initial to the final temperature were calculated by means of the equation,

$$h_{D_2O} = \frac{H + h_x - C_{Py} w_{Py} (t_i - t_e)}{w_{D_2O}}$$

where H is now the total heat of the Pyrex container and deuterium oxide from the initial temperature, t_i, to the final temperature, t_e, as measured in the calorimeter.

It should be noted that since the weights of Pyrex and the surface areas of both bulbs were virtually the same, any error in assuming the values for C_{Py} disappears in the above expression since h_x contains C_{Py}.

Since the final temperature in the calorimeter was always within about 0.5° of 26.0° C., the total heats were corrected to this latter figure in the usual way (2).

The total heats taken up or given up by one gram of liquid deuterium oxide when warmed or cooled from various initial temperatures to 26.0° C. are given in Table I.

TABLE I

TOTAL HEATS OF LIQUID D_2O

Initial temp., °C.	4.0	26.0	45.0	65.0
Total heat, cal./gm.	−22.4	0.0	19.05	39.25

The maximum difference between the total heats observed in the different experiments from each initial temperature was less than 1%, so that the probable accuracy of the values in Table I is of the order of 0.5%. From these figures the average specific heats of liquid deuterium oxide over the temperature ranges 4° to 26° C., 26° to 45° C., and 26° to 65° C., are 1.018, 1.003 and 1.008, respectively, while the average specific heat between 4° and 65° C. is 1.01 cal. per gm. per degree.

The accuracy of the results shown above does not warrant other conclusions than that the specific heat of heavy water is slightly higher than that of ordinary water, although there appears to be a trend towards decreasing values with rise in temperature, and the minimum in the specific heat curve probably is at a higher temperature than is that for ordinary water. It is also of considerable interest to note that the molecular heat of heavy water is greater than that of ordinary water by an amount almost proportional to their differences in molecular weight.

As mentioned in the previous paper (3), certain improvements in the adiabatic calorimeter are under discussion at the present time. As these will permit the determination of the thermal constants of deuterium oxide to be made to at least one part in a thousand, it has been deemed advisable to discontinue the present investigation until the new calorimeter is completed. On account of the unavoidable delay which this will entail, it was considered to be of interest in the meantime to present the data contained in this note.

Acknowledgment

Acknowledgment is again made to the anonymous donors of a grant of $1,000.00 for calorimetric research in this laboratory which has made possible the present investigation.

References

1. Barnes, W. H. and Maass, O. Can. J. Research, 3 : 70-79. 1930.
2. Barnes, W. H. and Maass, O. Can. J. Research, 3 : 205-213. 1930.
3. Brown, R. S., Barnes, W. H. and Maass, O. Can. J. Research, 12 : 699-701. 1935.

THE REACTION PRODUCTS OF INDOLS WITH DIAZOESTERS[1]

By Richard W. Jackson[2] and Richard H. Manske[3]

Abstract

In conformity with findings of previous work on indols and in contradistinction to more recent work on pyrrols, the action of diazoesters on indol leads to 3-substituted as well as a small amount of 1 : 3-disubstituted derivatives. The formation of 2-substituted derivatives could not be demonstrated. The reaction discussed is a convenient one for the synthesis of a wide diversity of indol compounds.

Those natural derivatives of indol whose constitution has been elucidated in whole or in part, have invariably been found to carry substituents in the 3-position although the 2- and possibly the 1-position may also be occupied. Synthetically too, those derivatives with the substituents in the 3-position are in general more readily available, and this is particularly true when the substituents carry reactive groups which lend themselves to further syntheses.

The direct introduction of substituents into the pyrrol or alkyl-pyrrol nucleus leads to 2-substituted derivatives when this position is available. As examples, the synthesis of pyrryl-2-acetic acid by the action of ethyl diazoacetate on pyrrol (5), and the synthesis of 2-methylpyrryl-5-succinic acid (1) by the reaction between 2-methylpyrrol and maleic anhydride, may be cited. The latter of these reactions when applied to indol yields unexpected products (2). The action of ethyl diazoacetate on 1-methylindol, however, was found by Piccinini (6) to yield 1-methylindolyl-3-acetic acid, and 2-methylindol yields the corresponding 3-acetic acid. Nevertheless it seemed desirable to reinvestigate this reaction with indol to ascertain whether indolyl-2-acetic acid was one of the reaction products. The isolation of indolyl-3-acetic acid proved to be facile enough and in some respects this synthesis is the most satisfactory yet recorded (3). The presence of indolyl-2-acetic acid could not be demonstrated.

When an excess of the diazoester was employed there was obtained a moderate yield of indylene-1 : 3-diacetic acid*. This substance is of some interest in that heating or distilling it *in vacuo* eliminates only one carboxyl group, and this observation is pertinent in connection with its constitution. In view of the ready loss of carbon dioxide from indolyl-3- and from 1-methylindolyl-2-acetic acid (3), the decarboxylated product is formulated as 3-methylindolyl-1-acetic acid. The highly purified dibasic acid gives a coloration with Ehrlich's reagent only with difficulty, and in this respect resembles 1-methyl-

[1] *Manuscript received June 10, 1935.*
Contribution from the Department of Physiological Chemistry, Yale University, New Haven, Connecticut, U.S.A., and from the National Research Laboratories, Ottawa, Canada.

[2] *Formerly Assistant Professor of Physiological Chemistry, Yale University, New Haven, Conn., U.S.A.; at present Assistant Professor of Biochemistry, Department of Biochemistry, Cornell University Medical College, New York City.*

[3] *Chemist, National Research Laboratories, Ottawa.*

**It is proposed to use the term indylene for the disubstituted derivatives of indol in analogy with the term phenylene.*

tryptophane (7). The decarboxylated product reacts normally to the test. No tri-substituted product could be isolated even when a large excess of the diazoester was employed, and the attempted condensation of 2 : 3-dimethylindol yielded only the unchanged starting material together with the decomposition products of the diazoester.

While it is improbable that 2-substituted indols will become available by this method, an extension of the reaction to another diazoester, namely, diethyl diazosuccinate, has indicated a route by which a great diversity of indol-3-substituted derivatives may be prepared. The reaction product in the case cited is indolyl-3-succinic acid, which on gentle heating loses one carboxyl group and yields the known β-3-indolylpropionic acid.

Incidentally, another synthesis of indolyl-3-acetic acid is recorded. While of no particular merit for obtaining the unsubstituted acid, because of mediocre yields, the method, it is felt, may offer distinct advantages in connection with some derivatives of the acid. Diethyl β-cyanopropionacetal (4) was hydrolyzed to the corresponding acid, which was then hydrolyzed by means of hydrochloric acid to the semi-aldehyde of succinic acid, and the latter without being isolated was condensed with phenylhydrazine. The product, subjected to the Fischer indol synthesis, yielded the required acid.

In conclusion it is pertinent to note that the attempted condensation of 2 : 5-dimethylfuran* yielded no acidic products other than those derived from the decomposition of the ester.

Experimental

Indolyl-3-acetic Acid and Indylene-1 : 3-diacetic Acid

A dried ethereal solution of ethyl diazoacetate prepared from 50 gm. of glycine ester hydrochloride was slowly run into a Claisen flask (fitted with a long fractionating column) in which had been placed 19 gm. of indol and a trace of copper powder. The ether was rapidly distilled off as the solution was run in, so that the reaction was thus made to proceed smoothly. Finally, the product was heated to 100° C. in the vacuum of a water pump, transferred to a Claisen flask and distilled at 2 to 3 mm. There was frequently a second evolution of gas at this stage, and this was particularly pronounced in the experiment in which the proportionate quantity of diazoester was greatly increased.

The almost colorless distillate was hydrolyzed with an excess of methanolic potassium hydroxide, the solution diluted with water and the methanol distilled off. Thorough extraction of this solution with ether yielded 2 gm. of indol. The alkaline solution was then acidified with hydrochloric acid and again exhaustively extracted with ether. The combined extracts were dried with sodium sulphate and the ether distilled off. The solid, reddish residue was transferred to a suction funnel and washed with cold ether.

*We are indebted to Mr. A. F. G. Cadenhead of Shawinigan Chemicals Ltd. for a gift of this furan.

The indolyl-3-acetic acid readily dissolved in the ether and was recovered from the filtrate by removal of the solvent. It was recrystallized from a concentrated solution in ethyl acetate by the addition of benzene, or from hot water. The latter solvent is preferable when the acid is already of a good grade. In either case, the adequately purified product melted at 167 to 168° C.*, with the evolution of carbon dioxide, and this melting point was not lowered when the material was admixed with a specimen prepared from indolyl acetonitrile or one synthesized by the method to be detailed later.

The residue from the ether extraction was washed cautiously with cold ethyl acetate and then dissolved in the same solvent at the boiling point. The solution was treated with charcoal, filtered and evaporated to a small volume and, when cooled somewhat, treated with dry ether. This induced almost immediate crystallization. The product, filtered off, washed and dried, melted at 238° C. with evolution of carbon dioxide. Repetition of the purification raised the melting point to 242°. The diacetic acid is moderately soluble in warm water and methanol, but sparingly soluble in cold ethyl acetate or ether. The purest specimen gave no immediate color with Ehrlich's reagent. Calcd. for $C_{12}H_{11}O_4N$: N, 6.03%. Found: N, 5.93%. (Kjeldahl.) Neutralization equivalent: calcd., 116.5; found, 115. The yield of indolyl acetic acid was 12 gm. and that of the diacetic acid was 1.2 gm.

In a second experiment 35 gm. of indol and the diazoester ester from 150 gm. of glycine ester hydrochloride were employed, and the product, worked up as described above, yielded a small amount of indol, 10 gm. of indolyl-3-acetic acid and about four grams of indolyene-1 : 3-diacetic acid. The mother liquors of the acid fraction were submitted to further exhaustive fractionation. Small amounts of both the acids mentioned above were isolated but no new acid was discovered at any stage of the work.

3-Methylindolyl-1-acetic Acid

The diacetic acid described above was heated in an oil bath to 240° C. under slightly reduced pressure until the evolution of carbon dioxide ceased, and then distilled at 3-4 mm. The distillate was extracted with aqueous sodium bicarbonate and then the filtered solution was extracted several times with ether, acidified and again extracted with ether. The last extract was dried with sodium sulphate and the solvent largely removed. Cautious addition of benzene induced rapid crystallization. The acid, filtered off and washed with benzene and then recrystallized from ether-benzene, melted sharply at 178° C. It gave an intense pink color with Ehrlich's reagent. The acid is moderately soluble in hot water and crystallizes in slender needles. Calcd. for $C_{11}H_{11}O_2N$: N, 7.41%. Found: N, 7.49%. (Dumas.)

Indolyl-3-succinic Acid

A dried ether solution of diethyl diazosuccinate prepared from 112 gm. of aspartic acid ester hydrochloride was slowly added to 58 gm. of indol and a trace of copper powder in a Claisen flask equipped with a condenser for

*All melting points are corrected.

distillation. The reaction mixture was kept hot by means of the steam bath. Nitrogen was copiously evolved but the reaction never became violent. When the reaction had ceased the mixture was freed of readily volatile products by heating the reaction mixture to 100° C. under the vacuum created by a water pump. The oily residue was then distilled at 5 mm. At first indol distilled and as the temperature rose a gas was evolved. The gas evolution ceased in a short time and the main fraction distilled at about 250° C. The distillate was hydrolyzed with an excess of methanolic potassium hydroxide. A considerable quantity of water was added, the methanol boiled off and the cooled solution repeatedly extracted with ether; 35 gm. of indol was thus recovered. The alkaline solution was acidified with dilute sulphuric acid. No precipitate was obtained. The solution was extracted repeatedly with ether, the combined extracts washed once with a little water and dried over sodium sulphate, and the solvent removed. The dark oily residue rapidly crystallized, and in this condition was only moderately soluble in ether. A dark tarry impurity was removed by two successive charcoal treatments in the minimum volume of hot water. On cooling, a copious yield of almost colorless indolyl-3-succinic acid was obtained. This melted at 198° C. with evolution of carbon dioxide. The total yield of acid including that recovered from the mother liquors was 21 gm.

The bulk of the indol succinic acid was esterified with absolute ethanol and hydrogen chloride and subsequently distilled at about 200° C. at 3 mm. A specimen of the ester, twice recrystallized from benzene and petroleum ether and then once from benzene, melted at 79–80° C. The pure white crystals were apparently solvated because upon standing they lost both weight and lustre. Calcd. for $C_{16}H_{19}O_4N$: N, 4.85%. Found: N, 5.16%. (Dumas.)

The remainder of the ester was hydrolyzed with ethanolic potassium hydroxide and the indolyl succinic acid recovered. The purest material was secured from the potassium salt which separated from the cooled alcohol solution. The acid, after crystallization from hot water (charcoal), was beautifully crystalline and melted at 199° C. However during the purification, the substance assumed a slight pinkish cast. This property recalls the similar behavior of the related indolyl-3-acetic acid. The recoveries of the ester and acid were virtually quantitative. Calcd. for $C_{12}H_{11}O_4N$: N, 6.01; C, 61.8; H, 4.76%. Found: N, 5.90, and 6.19 (Dumas); C, 62.2; H, 4.70%.

One gram of the dibasic acid was cautiously heated over a free flame until the evolution of carbon dioxide ceased. The residue was recrystallized once from hot water, then dissolved in aqueous sodium carbonate, regenerated from the solution after treating with charcoal and filtering, and recrystallized from hot water. Colorless plates of β-3-indolyl-propionic acid, melting at 131° C. either alone or admixed with an authentic specimen, were thus obtained.

Indolyl-3-acetic Acid

A solution of 47 gm. of β-cyano-propionacetal (4) in 75 cc. of methanol was treated with 17 gm. of potassium hydroxide in 25 cc. of water. The mixture was slowly evaporated on a steam bath. It was then treated with 400 cc. of water in two portions and evaporated after each addition. The residue was dissolved in 400 cc. of water, and the solution clarified by filtration (charcoal). The filtrate was heated on a steam bath for an hour with 40 cc. of concentrated hydrochloric acid and then treated with an excess of sodium acetate. A clarified solution of 33 gm. of phenylhydrazine in dilute acetic acid was added. The oily phenylhydrazone, which was at once precipitated, was extracted with ether. The solvent was removed and the residue freed of moisture by heating at 100° C. with suction. The residue was then heated under reflux with a solution of 30 gm. of sulphuric acid in 140 cc. of absolute ethanol for four hours. Much water was added and the oily product extracted with ether, washed with aqueous sodium bicarbonate, and dried over sodium sulphate. The residue obtained on removal of the ether was distilled *in vacuo*. The fraction boiling at 172 to 178° C. at 2 mm. was hydrolyzed with methanolic potassium hydroxide. The solution was diluted with water, freed of methanol, and filtered after treatment with charcoal. Cautious addition of dilute hydrochloric acid to the filtrate yielded a crystalline acid which was filtered off, washed with water, dried, and washed with benzene. This product when recrystallized from hot water, or from ether-benzene, yielded flat colorless plates melting at 167° C. with the elimination of carbon dioxide and the production of 3-methylindol. Admixture with an authentic specimen of indolyl-3-acetic acid prepared from indolyl-3-acetonitrile or with a specimen prepared from indol and ethyl diazoacetate caused no depression in the melting point.

Acknowledgment

The authors are grateful to Mr. H. Laidlaw for preparing a pure specimen of 2 : 3-dimethylindol and for assistance in some of the experiments with the ethyl diazoacetate.

References

1. Diels, O. and Alder, K. Ann. 490 : 277-294. 1931.
2. Diels, O. and Alder, K. Ann. 498 : 1-15. 1932.
3. King, F. E. and L'Ecuyer, P. J. Chem. Soc. 1901-1905. 1934.
4. Manske, R. H. Can. J. Research, 5 : 592-600. 1931.
5. Nenitzescu, C. D. and Solomonica, E. Ber. 64 : 1924-1931. 1931.
6. Piccinini, A. Gazetta, 29 : 363-371. 1899.
7. Wieland, H., Konz, W. and Mittasch, H. Ann. 513 : 1-25. 1934.

RECHERCHES SUR LA MATIÈRE AROMATIQUE DES PRODUITS DE L'ÉRABLE À SUCRE[1]

PAR J. RISI[2] ET A. LABRIE[3]

Résumé

La matière aromatique du sirop et du sucre d'érable est un produit complexe, très instable, formé d'une partie solide et d'une partie liquide résineuse. La partie solide contient de la vanilline et de l'acide vanillique. La partie résineuse fournit, après dédoublement par l'émulsine, du gaïacol. Les extraits de la sève d'érable ne contiennent pas la matière aromatique du sirop et du sucre; celle-ci se développe seulement durant la cuisson. La sève contient de la vanilline, de l'acide vanillique et du gaïacol. La concentration de ces dérivées phénoliques dans la sève est de 0.5 parties par million. Il se forme une quantité additionnelle de substances phénoliques au cours de la cuisson. La substance aromatique donne en milieu alcalin des phénolates inodores et de couleur brun foncé. Un sirop aromatique et peu coloré doit donc être préparé à un pH inférieur à 7. La coloration jaune ou brune du sirop n'est pas due essentiellement à la formation de caramel.

L'écorce de l'érable contient une glucosidase qui hydrolyse la coniférine et l'amygdaline; elle est semblable à l'émulsine, nous l'appelons "Acérase". La sève d'érable contient un ferment du type de l'amylase qui dédouble l'amidon de l'arbre en un disaccharide de nature non déterminée, et qui est actif même à des températures relativement basses.

Le bois d'érable contient très peu de coniférine, laquelle se transforme, vers le 1er septembre, en substances résineuses de nature ligneuse. Les graines d'érable ne contiennent pas de coniférine, mais la même substance aromatique que le sirop. La coniférine peut être la substance-mère de la vanilline dans le bois et la sève d'érable. Dans l'extrait aromatique du sirop il n'y a pas de coniférine, d'alcool et d'aldéhyde coniférylique et de "Sulfitlaugenlakton".

L'arome des produits de l'érable est principalement dû à la formation d'hadromal au cours de la cuisson de la sève. A côté de l'hadromal, il peut y avoir de très faibles quantités d'autres matières aromatiques. La sublimation destructive de l'hadromal donne de la vanilline, du gaïacol et de l'acide vanillique, tout comme les extraits aromatiques du sirop d'érable. La synthèse de l'hadromal peut se réaliser à partir du sucrose (furfural), de la vanilline et du gaïacol. Il est probable que l'hadromal ne se trouve pas à l'état libre dans les bois; l'hadromal de Czapek et de Combes est plutôt formée par synthèse catalytique à partir des dits fragments de la lignine.

Introduction

Les trois espèces d'érables, *Acer saccharum*, *Acer saccharinum* et *Acer rubrum* fournissent au printemps une sève sucrée qui donne par évaporation à grande surface du sirop et du sucre à arome caractéristique. Nelson (12), qui voulait identifier la nature chimique de cette substance aromatique, arrive à la conclusion: "Investigation of the flavor of maple syrup showed that it depends to a great extent on an unstable phenolic substance which is associated with a crystalline aldehyde melting at 74–76° and similar in odor and properties to vanillin. Maple syrup may contain minute quantities of other aldehydic substances which influence the flavor". Snell (16) dit que le principe aromatique est identique ou semblable à la vanilline, par suite de l'odeur et des propriétés des extraits. L'un de nous (14) a établi des méthodes

[1] *Manuscrit reçu le 11 janvier, 1935.*
Contribution de l'Ecole Supérieure de Chimie, Université Laval, Québec, Canada, basée sur une thèse présentée par A. Labrie pour l'obtention du degré de D. Sc. de l'Université Laval. Une partie du travail a été exécutée avec l'assistance financière du National Research Council of Canada.
[2] *Professeur de chimie organique, Université Laval.*
[3] *Etudiant gradué de l'Université Laval et boursier du National Research Council of Canada.*

de dosage des fonctions phénoliques et aldéhydiques dans les produits de l'érable, permettant de distinguer des nombreux produits falsifiés les produits authentiques de l'érable. Le but du présent travail était de préciser nos connaissances sur l'origine et la nature chimique du principe aromatique des produits de l'érable.

Partie théorique

1. Extraction et propriétés des extraits du sirop et de la sève

Par extraction à l'éther d'un sirop dilué, traité par l'émulsine à 25–35° C. pendant 2 semaines, on obtient un résidu brun, résineux, très aromatique. Une partie du résidu est soluble dans l'éther de pétrole et abandonne une substance solide blanche, associée à un produit collant. Le solide recristallisé (très faibles quantités) démontre les réactions de la vanilline.

Par extraction à l'éther de la sève d'érable fraîche, on obtient quelques aiguilles incolores disséminées dans une huile jaune. Les cristaux ont été identifiés comme acide vanillique. La purification de la partie huileuse était impossible.

Dans la sève fraîche traitée par l'émulsine, on a pu constater, après extraction à l'éther, la présence de gaïacol, qui doit donc se former par hydrolyse d'une substance plus complexe contenue dans la partie résineuse des extraits de sirop et de sève.

La concentration en substances phénoliques (vanilline et gaïacol) de la sève est de 1/2,000,000 dosées comme vanilline. Vu que l'on concentre la sève à 1/20 de son volume dans la fabrication du sirop et que les sirops contiennent de 20 à 70 parties de phénols par million (14), on doit conclure qu'une quantité additionnelle de phénols libres se forme par hydrolyse durant la cuisson.

La partie phénolique de la substance aromatique donne, par extraction de la solution étherée à la soude, un phénolate inodore et coloré en brun. En acidulant prudemment on obtient après une autre extraction un résidu à odeur voisine de celle de la vanilline. Elle explique aussi la raison pour laquelle un bon sirop peu coloré et très aromatique doit être préparé à un pH inférieur à 7.

En soumettant, à titre de comparaison, une solution diluée de caramel à une extraction analogue, on constate que le pigment est insoluble dans l'éther et que l'agitation avec de la soude ne produit aucune coloration. Le pigment brunâtre du sirop n'est donc pas dû essentiellement à la formation de caramel pendant la cuisson, contrairement à ce que prétend Balch (1); au contraire, la coloration du sirop dépend en majeure partie de la substance aromatique elle-même colorée.

2. Les agents hydrolytiques de l'érable

Dans le but d'étudier certains dédoublements hydrolytiques, nous avons recherché des ferments dans l'arbre vivant.

L'extraction de l'écorce d'érable fournit une glucosidase du type de l'émulsine, que nous voudrions appeler "Acérase"; elle hydrolyse la coniférine et l'amygdaline.

La sève d'érable contient un autre ferment du type de l'amylase et qui dédouble rapidement l'amidon, contenu en grandes quantités, au printemps, dans les cellules des racines, des jeunes tiges et de l'assise de croissance de l'érable. La sève ne donne pas la réaction de l'amidon, mais le ferment qu'elle contient doit être une amylase de saccharification, qui est active, d'après Müller-Thurgau, déjà à des températures voisines de 0°. Il nous a cependant été impossible de trouver du maltose dans la sève, quoique la présence d'un disaccharide autre que le sucrose soit probable.

*3. La substance aromatique en rapport avec la coniférine, l'alcool et l'aldéhyde conifér*ylique

La présence de vanilline dans la sève et dans les extraits de sirop d'érable, ainsi que d'une glucosidase dans l'écorce nous a conduit à rechercher l'origine de la matière aromatique dans la coniférine très répandue dans le règne végétal.

En appliquant la méthode de Tiemann et Haarmann (18) au bois d'érable, il nous a été possible d'extraire du cambium un peu de coniférine, mais avec un rendement beaucoup plus faible que dans le cas des conifères. Après le 1er septembre, l'érable n'a presque plus de sève et le cambium du jeune bois ne contient plus de coniférine; l'extraction donne seulement un résidu résineux à odeur de vanilline et démontrant les réactions de la lignine.

Par extraction des graines d'érable on obtient une substance résineuse qui ne contient pas de coniférine, mais qui est aussi aromatique que les extraits de sirop d'érable.

La présence de coniférine dans le bois d'érable établie, nous avons voulu examiner si la matière aromatique contenait son produit d'hydrolyse, l'alcool conifér*ylique*, ou son produit d'oxydation, l'aldéhyde conifér*ylique*, ou un dérivé de polymérisation, appelé "Sulfitlaugenlakton". Nous avons préparé ces corps à titre de comparaison; ils ont des propriétés nettement différentes de la vanilline et des extraits de sirop et ne se trouvent pas à l'état libre dans la matière aromatique de l'érable.

4. La substance aromatique en rapport avec l'hadromal

L'hadromal a été isolée du bois par Czapek (4), et plus tard par Combes (3) et par Hoffmeister (7). Grafe (5) prétend qu'elle est composée de vanilline, méthylfurfural et pyrocatéchine. A cause de sa composition et à cause des propriétés aromatiques fort intéressantes que ces auteurs donnent, nous avons entrepris l'étude de l'hadromal.

Dans les produits de l'érable, nous avons isolé la vanilline et l'acide vanillique, mais nous n'avons pu déceler le furfural et le méthylfurfural, quoique la cuisson du sucrose en solution faiblement acide doive entraîner la formation de ces produits. Voici la raison: En concentrant une solution de sucrose faiblement acide, on constate après peu de temps la présence de furfural (papier d'acétate d'aniline); mais si on ajoute de la vanilline, la réaction du furfural n'apparaît que beaucoup plus tard. Il semble donc que la vanilline

entre immédiatement en réaction avec le furfural naissant, ce qui se produirait aussi dans la concentration de la sève d'érable dont le pH est ordinairement en bas de 7.

Nous n'avons jamais pu isoler la pyrocatéchine dans toutes nos extractions de sirop et de sève, mais nous y avons trouvé son éther monométhylique, le gaïacol. L'hadromal devrait donc contenir un reste gaïacolique et non un reste pyrocatéchique, ce qui est d'autant plus probable si on considère les propriétés de l'hadromal qui ressemblent beaucoup à celles de la lignine, et le fait que Lüde (11) a obtenu du gaïacol et de l'acide vanillique comme principaux produits de dédoublement dans la sublimation de la lignine du bambou.

En soumettant l'hadromal, préparée d'après Czapek (4), à une sublimation destructive dans l'appareil décrit par Lüde, nous avons aussi obtenu du gaïacol et de l'acide vanillique. Les conditions et les résultats sont indiqués dans le tableau No. 3. En opérant dans les mêmes conditions sur un extrait aromatique de sirop d'érable, on obtient les mêmes produits, mais avec un rendement plus faible.

Afin de prouver davantage que l'hadromal est un des principaux constituants aromatiques des produits de l'érable, nous avons essayé de faire sa synthèse. En effet, il nous a été possible de prouver de cette façon, que l'hadromal est composée de furfural, de vanilline et de gaïacol, et non de méthylfurfural, vanilline et pyrocatéchine, comme le prétend Grafe. En chauffant une solution de sucrose avec de la vanilline et du gaïacol dans des conditions déterminées, on obtient une très faible quantité d'une substance identique à l'hadromal dans ses propriétés, et ayant l'arome des extraits de sirop d'érable. En omettant le sucrose, il ne se forme pas de trace d'hadromal, ce qui prouve qu'il y a, dans le premier cas, formation intermédiaire de furfural ou de oxyméthylfurfural. En répétant l'expérience avec de l'*a*-oxyméthylfurfural, préparé d'après Kiermayer (10), à la place du sucrose, le résultat est encore négatif. Il faut donc admettre la formation de furfural, lequel se combine immédiatement avec la vanilline, tel que déjà mentionné.

L'hadromal se forme encore mieux en chauffant les dits ingrédients d'abord en milieu acide, ensuite en milieu alcalin de pH convenable. L'extrait étheré du produit de réaction possède un arome très développé et identique à celui des produits de l'érable.

Nous avons enfin étudié l'action de certains catalyseurs autres que l'acétate de manganèse, en particulier l'acétate de plomb et le chlorure stanneux. Ces deux sels catalysent la synthèse de l'hadromal positivement. Cette observation est importante au point de vue théorique, si on considère que Czapek et Combes, ont isolé l'hadromal du bois en présence d'un excès de l'un ou de l'autre des deux sels. Nous sommes portés à croire que l'hadromal, aldéhyde instable, n'existe pas à l'état libre dans les bois et que ces auteurs l'ont involontairement synthétisé au cours de leurs opérations, à partir du suc cambial qui contient, à côté de sucrose, plusieurs produits de métabolisme de la lignine, tels que la vanilline et le gaïacol. Déjà Keppeler (9) avait mis l'existence de l'hadromal dans la nature en doute, et nos expériences devraient le prouver définitivement.

Cette idée est d'ailleurs appuyée par l'histoire génétique du principe aromatique des produits de l'érable. La sève ne contient pas de trace d'hadromal ou autre matière aromatique caractéristique pour le sirop et le sucre. L'arome se forme entièrement au cours de l'évaporation de la sève à grande surface et en présence d'air. Cette synthèse se fait à partir du sucrose, de la vanilline et du gaïacol présents dans la sève. Nous avons réalisé la combinaison en hadromal en dehors des évaporateurs de la cabane à sucre. La synthèse de l'arome doit être une oxydation lente, car elle ne se produit pas par concentration de la sève dans le vide ou en présence d'un gaz inerte.

L'arome caractéristique du sirop et du sucre d'érable est donc principalement dû à la formation d'hadromal au cours de l'évaporation de la sève. Vu que la finesse de l'arome varie souvent selon l'origine des produits et les soins apportés à leur fabrication, il peut y avoir, à côté de l'hadromal, des traces d'autres matières aromatiques, par exemple des glucides phénol-aldéhydiques ou des résines formées par polymérisation de l'hadromal instable.

Nous continuons nos travaux dans le but d'isoler d'autres matières aromatiques, d'étudier le mécanisme exacte de la formation de l'hadromal et d'élucider sa constitution dont la connaissance avancerait sans doute la chimie de la lignine.

Partie expérimentale

1. Extraction et propriétés des extraits du sirop et de la sève

a. Extraction du sirop

A 18 litres de sirop d'érable à 30% de sucre, nous avons ajouté de l'émulsine extraite d'amandes amères (2), et comme préservatif, une solution de fluorure de sodium formant 1% dans le mélange. Le tout est demeuré pendant 14 jours à une température variant entre 25–35°. Nous avons ensuite extrait ce sirop deux fois avec 200 et 100 cc. d'éther par litre; l'excès du solvant distillé dans le vide, nous avons obtenu un résidu amorphe, brun et résineux, d'arome d'érable très prononcé. En traitant cette substance par l'éther de pétrole, une partie se dissout, et le résidu, repris par l'acétate d'éthyle, ne démontre aucune tendance à la cristallisation. La partie soluble dans l'éther de pétrole dépose des aiguilles groupées en rosettes, très aromatiques. Après une autre cristallisation de l'éther de pétrole, il se forme un peu de résine, qui, absorbée par une plaque poreuse, laisse une substance solide blanche en très faible quantité. Recristallisée de l'éther de pétrole, elle se présente en aiguilles incolores groupées en rosettes et semble être très pure et uniforme. Très instable, elle devient collante après quelques heures seulement passées dans un desiccateur à vide; elle se ramollit alors vers 60° et donne, sans passer par un point de fusion déterminé, une résine jaune qui ne se solidifie plus après refroidissement.

Cet extrait donne les réactions de coloration suivantes:— acide sulfurique concentré–jaune, puis brun chocolat; chlorure de fer–bleu verdâtre; aniline–jaune pâle; phloroglucine et acide chlorhydrique–rose clair; benzidine et acide acétique–jaune pâle.

L'extrait contient sans doute de la vanilline, laquelle donne les mêmes réactions, excepté avec l'acide sulfurique, qui provoque une coloration jaune seulement, mais tous deux précipitent des flocons blancs par addition d'eau. Cette différence est probablement due à la présence d'une autre substance que nous étudierons plus loin.

b. Extraction de la sève d'érable

Dix-neuf litres de sève fraîche ont été extraits à l'éther, et celui-ci, desséché sur du chlorure de calcium, a été distillé dans le vide. Le résidu a formé une huile jaune, contenant plusieurs cristaux en forme d'aiguilles. Par un lavage rapide à l'éther de pétrole et par une recristallisation de l'éther ordinaire, il s'est déposé une substance blanche, cristallisée en aiguilles groupées en étoile, que nous avons identifiée comme étant de l'acide vanillique: P.F. 207°; P.F. mixte, 207° C.

Il y a toujours à côté de cette substance cristalline une forte proportion d'une huile résineuse jaune, d'odeur forte de vanilline, mais il nous a été impossible de la purifier pour isoler cette dernière.

c. Présence du gaïacol dans la sève

On abandonne 9 litres de sève pendant deux semaines avec de l'émulsine et on extrait à l'éther. Dans le résidu huileux, on peut déceler le gaïacol par l'odeur et les réactions de coloration.

d. Dosage des corps à fonction phénolique dans la sève

Nous avons employé la méthode de Folin et Denis (19). Comme solution témoin, on s'est servi d'une solution de vanilline 1/500,000; 5 cc. de la solution témoin ont donné la même coloration que 20 cc. de sève d'érable. La concentration en substances phénoliques de la sève d'érable est donc de 1/2,000,000, calculée comme vanilline.

e. Formation de phénolates

Nous avons extrait un gallon de sirop authentique avec de l'éther, et agité la solution éthérée avec une solution aqueuse de 5% de soude. La dernière s'est colorée en brun, tandis que la solution éthérée s'est décolorée et cela après une seule extraction à la soude. La partie aqueuse neutralisée avec prudence par une solution de 5% d'acide chlorhydrique tourne au jaune clair au point de neutralité. Extrait de nouveau à l'éther, le résidu, après évaporation du solvant, possède une odeur très voisine de la vanilline, sans être absolument identique.

2. Les agents hydrolytiques de l'érable

a. Extraction de l'"Acérase" de l'écorce d'après la méthode de Bertrand et Thomas (2)

Les écorces d'érable broyées en poudre ont été traitées par l'eau pendant trois jours en présence de fluorure de sodium, comme préservatif. La solution filtrée a été traitée par deux fois son volume d'alcool à 95%, et une substance

blanche floconneuse s'est précipitée, qui, redissoute dans l'eau, a été essayée sur une solution de coniférine de la façon suivante:

I. Solution de 1% de coniférine plus 1% de fluorure de sodium.
II. Solution de ferments extraits des écorces plus 1% de fluorure de sodium.
III. Solution de 1% de coniférine plus ferments extraits des écorces plus 1% de fluorure de sodium.

Ces trois solutions ont été placées dans l'étuve maintenue à 37° C. pendant sept jours. Après ce temps, le glucose formé a été dosé de la façon ordinaire par la liqueur de Fehling, le précipité d'oxyde cuivreux a été redissout dans le mélange d'acide sulfurique et de sulfate ferrique, et le sulfate ferreux formé a été dosé par une solution de permanganate de potassium $N/100$. Les résultats sont indiqués dans le tableau No. 1.

TABLEAU No. I.

		$KMnO_4$ (N/100), cc.
I	20 cc. de sol. Fehling (3 min. d'ébullition)	0.4
II	20 cc. de solution de ferment plus 20 cc. de sol. Fehling	0.4
III	20 cc. de sol. de coniférine plus 20 cc. de sol. Fehling	0.4
IV	20 cc. de sol. de coniférine plus 2 cc. de sol. de ferment plus 20 cc. de sol. Fehling.	1.2

La quantité indiquée de permanganate employé correspond à la quantité de glucose formée.

La consommation de quantités constantes de permanganate dans les trois premiers cas, considérés comme essais à blanc, est due exclusivement à l'autoréduction de la liqueur de Fehling à la température d'ébullition. Dans le quatrième cas, on constate nettement que la coniférine a été hydrolysée par l'extrait des écorces, la quantité de glucose formé étant même appréciable.

b. Extraction de l'"Acérase" de l'écorce d'après la méthode de Schneegans (15)

Les écorces pulvérisées ont été traitées par quatre fois leur poids de glycérine, et abandonnées pendant trois semaines à la température du laboratoire. La glycérine a ensuite été filtrée, centrifugée, et les ferments ont été précipités par l'alcool et redissouts dans l'eau. Les essais d'hydrolyse effectués avec cet extrait sur de l'amygdaline ont été exécutés comme ceux que nous avons faits sur la coniférine.

TABLEAU No. 2

		$KMnO_4$ ($N/100$), cc.
I	20 cc. de sol. Fehling (3 min. d'ébullition)	0.4
II	15 cc. de sol. de ferments plus 20 cc. de sol. Fehling	0.4
III	15 cc. de sol. d'amygdaline plus 20 cc. de sol. Fehling	0.8
IV	15 cc. de sol. d'amygdaline plus 2 cc. de sol. de ferments plus 20 cc. de sol. Fehling.	1.9

On remarque que l'amygdaline en solution aqueuse est déjà un peu dédoublée par la chaleur. L'écart entre III et IV est assez grand cependant pour constater sans aucun doute que, dans le quatrième cas, un ferment est entré en action.

c. Preuve pour la présence dans la sève d'un ferment du type de l'amylase

Nous avons préparé une suspension aqueuse de 0.5% d'amidon, additionnée de 1% de fluorure de sodium, et avons laissé couler la sève d'érable dans cette solution contenue dans un récipient stérilisé, attaché au "chalumeau". Après trois heures, nous avons obtenu la réaction des dextrines, et après six heures, tout l'amidon a été transformé en disaccharide. Nous avons réussi à faire dédoubler de cette façon jusqu'à 20 cc. d'une suspension de 1% d'amidon, durant une journée. Ce ferment travaille encore vite à des températures relativement basses, de 0 à 15° C., température de la coulée printanière.

3. La substance aromatique en rapport avec la coniférine, l'alcool et l'aldéhyde coniférylique

a. Extraction de la coniférine du bois d'érable

Au cours de l'été, nous avons appliqué la méthode de Tiemann et Haarmann (18), en grattant le cambium d'érable avec des morceaux de verre, mais la solution filtrée et concentrée n'a pas déposé de cristaux de coniférine après concentration au cinquième. Nous avons poussé la concentration plus loin; il s'est formé une solution résineuse qui empêchait toute cristallisation, mais qui donnait les réactions de la coniférine.

Nous avons cependant réussi à démontrer sa présence plus nettement par extraction d'une petite quantité de cambium frais d'érable, par l'alcool amylique; après la distillation de l'excès du solvant, nous avons obtenu une faible quantité de dépôt, cristallisé en feuillets, semblables à ceux que l'on obtient par cristallisation de la coniférine du cyclohexanone. Ce produit donne une coloration violette avec de l'acide sulfurique concentré, et toutes les autres réactions de la coniférine. Après une nouvelle recristallisation de l'eau chaude, on obtient des feuillets uniformes qui dégagent, après quelque temps, l'odeur de la vanilline.

Après le 1er septembre, nous avons enlevé des copeaux de jeune bois d'érable (cambium), et les avons fait bouillir avec de l'eau. Cet extrait aqueux a été repris par l'éther, qui a entraîné des résines à forte odeur de vanilline, ensuite extrait par l'alcool amylique. Le résidu, après évaporation du solvant, possède l'odeur caractéristique de la vanilline et ne donne pas les réactions de la coniférine, mais bien des réactions semblables à la lignine.

b. Extraction des graines d'érable

Nous avons pris 40 g. de graines, dont l'écorce avait été enlevée, et nous les avons extraits par l'alcool dans un Soxhlet, pendant six heures. La solution alcoolique se colore fortement en jaune verdâtre, et le résidu laissé après distillation de l'alcool est résineux et brun. Cette résine dissoute dans l'eau et de nouveau extraite par l'éther a donné un résidu toujours résineux, et aussi

aromatique que les extraits provenant du sirop d'érable. Toutes les tentatives de faire cristalliser cette résine ont échoué, et nous n'avons pu déceler la coniférine dans cet extrait de graines d'érable.

c. Préparations comparatives

L'alcool coniférylique a été préparé par hydrolyse de la coniférine d'après F. Tiemann (17), l'aldéhyde coniférylique par la méthode de Pauly et Feuerstein (13) modifiée par Hillmer et Hellriegel (6), et la "Sulfitlaugenlakton" d'après B. Holmberg (8).

4. La substance aromatique en rapport avec l'hadromal

a. Préparation de l'hadromal

Nous avons "isolé" l'hadromal du bois de chêne en suivant les méthodes de Czapek (4), de Combes (3) et de Hoffmeister (7). Dans tous les cas nous n'avons obtenu que des traces d'hadromal.

b. Sublimation destructive de l'hadromal

Nous avons soumis l'hadromal obtenu selon la méthode de Czapek à une sublimation dans l'appareil imaginé par Lüde (11); le tableau No. 3 résume les résultats:

TABLEAU No. 3

Temps, min.	Température, °C.	Produits obtenus
10	40	Gouttelettes d'eau, odeur de vanilline
20	60	
30	80	
40	100	
50	120	Substance huileuse jaune, odeur de gaïacol
60	130	
70	140	
80	150	
90	160	Aiguilles blanches dispersées dans la partie huileuse (acide vanillique).
100	170	
110	180	
120	190	

Par sublimation d'un extrait aromatique de sirop d'érable dans les mêmes conditions on obtient les mêmes produits, mais avec un rendement plus faible.

c. Synthèse de l'hadromal

A une solution contenant 5% de sucrose, on ajoute une quantité égale de vanilline et de gaïacol, un peu de malate de calcium, et de l'acétate de manganèse, afin d'être à peu près dans les conditions de milieu de la sève d'érable; on chauffe pendant une heure en solution faiblement acide, on rend le mélange alcalin par du carbonate de sodium, et on maintient l'ébullition pendant quatre ou cinq heures. La solution devient brune, mais elle se décolore

beaucoup en la neutralisant par l'acide chlorhydrique; on extrait ensuite par l'éther. Le résidu d'évaporation de l'éther est une poudre amorphe jaune (trace), qui ne possède plus l'odeur de la vanilline et du gaïacol, mais bien une odeur caractéristique, ressemblant beaucoup à l'odeur des extraits faits sur les produits de l'érable. Cette substance fond vers 73° C.; elle donne les réactions des aldéhydes et des phénols ainsi qu'une coloration rose avec la phloroglucine, et bleu verdâtre avec le chlorure ferrique. Elle se conserve assez bien à l'air, son arome s'y développe de plus en plus; un sirop préparé avec cet extrait synthétique est identique au sirop d'érable authentique par l'arome et la saveur.

En chauffant les mêmes ingrédients d'abord en milieu acide, puis en milieu alcalin, en présence de catalyseurs, tels que l'acétate de manganèse ou le chlorure stanneux, le rendement en hadromal est meilleur, quoique l'on n'obtienne que des traces.

Remerciements

Nous adressons à M. l'abbé Alexandre Vachon, directeur de l'Ecole Supérieure de Chimie, Université Laval, nos remerciements les plus sincères pour l'encouragement précieux qu'il a bien voulu nous témoigner au cours de l'éxécution de ce travail.

Bibliographie

1. Balch, R. T. Ind. Eng. Chem. 22 : 255-257. 1930.
2. Bertrand, G. et Thomas, P. Guide pour les manipulations de chimie biologique. H. Dunod et E. Pinat, Paris. 1920.
3. Combes, R. Chem. Zentr. 78, I : 132-133. 1907.
4. Czapek, F. Z. physiol. Chem. 27 : 141-166. 1899.
5. Grafe, V. Monatsh. 25 : 987-1029. 1904.
6. Hillmer, A. et Hellriegel, E. Ber. 62 : 725-727. 1929.
7. Hoffmeister, C. Ber. 60 : 2062-2068. 1927.
8. Holmberg, B. Ber. 54 : 2389-2406. 1921.
9. Keppeler, G. Z. angew. Chem. 34 : 374-375. 1921.
10. Kiermayer, J. Chem. Zentr. 66, II : 214. 1895.
11. Lüde, R. Beiträge zur Kenntnis des Bambus-Lignins. Diss. Leipzig, 1931.
12. Nelson, E. K. J. Am. Chem. Soc. 50 : 2006-2012. 1928.
13. Pauly, H. et Feuerstein, K. Ber. 62 : 297-311. 1929.
14. Risi, J. et Bois, E. Recherches analytiques sur la matière aromatique des produits de l'érable à sucre. Contribution de l'Ecole Supérieure de Chimie, Université Laval, No. 1. 1933.
15. Schneegans. Chem. Zentr. 68, I : 326. 1897.
16. Snell, J. F. National Research Council, Report of the President for 1928-1929, p. 56.
17. Tiemann, F. Ber. 8 : 1127-1136. 1875.
18. Tiemannn, F. et Haarmann, W. Ber. 6 : 608-623. 1874.
19. Woodman, A. G. Food analysis. 2nd. ed. McGraw-Hill Book Co., New York. 1924.